Investigations of Synaptic Alterations in Models of Parkinson's Disease

Dissertation

for the award of the degree

"Doctor rerum naturalium"

of the Georg-August-Universität Göttingen

within the doctoral program *Cellular and Molecular Physiology of the Brain*

of the Georg-August University School of Science (GAUSS)

submitted by

Mohammed Al-Azzani

from IBB/Yemen

Göttingen, 2023

Thesis Advisory Committee:

Prof. Dr. Tiago Fleming Outeiro

Department of Experimental Neurodegeneration, University Medical Center Göttingen

Prof. Dr. Silvio Rizzoli

Department of Neuro- and Sensory Physiology, University Medical Center Göttingen

Prof. Dr. Henning Urlaub

Bioanalytical Mass Spectrometry Group, Max Planck Institute for Multidisciplinary Sciences

Members of the Examination Board:

Reviewer: Prof. Dr. Tiago Fleming Outeiro

Department of Experimental Neurodegeneration, University Medical Center Göttingen

Second Reviewer: Prof. Dr. Silvio Rizzoli

Department of Neuro- and Sensory Physiology, University Medical Center Göttingen

Further members of the Examination Board:

Prof. Dr. Henning Urlaub

Bioanalytical Mass Spectrometry Group, Max Planck Institute for Multidisciplinary Sciences

Prof. Dr. Nils Brose

Department of Molecular Neurobiology, Max Planck Institute for Multidisciplinary Sciences

Prof. Dr. med. Christine Stadelmann-Nessler

Department of Neurology, University Medical Center Göttingen

Prof. Dr. Rubén Fernández-Busnadiego

Institute for Neuropathology, University Medical Center Göttingen

Date of oral examination: 03/08/2022

Affirmation

I hereby declare that I have written this thesis entitled "Investigation of synaptic alterations in models of PD" independently and with no other sources and aids other than those quoted. This thesis has not been submitted elsewhere for any academic degree.

Göttingen, June 2023 Mohammed Al-Azzani

Acknowledgements

First and foremost, I would like to express my heartfelt gratitude to Prof. Dr. Tiago Fleming Outeiro for his invaluable guidance and support during my Ph.D. His profound expertise, remarkable feedback, and continuous encouragement helped me a lot to move forward and to overcome various obstacles encountered in my research. I am very grateful for his belief in my abilities and for the opportunity to be a member of his research group.

My sincere thanks also go to Prof. Dr. Silvio Rizzoli and Prof. Dr. Henning Urlaub for being part of my thesis advisory committee. Their valuable input, suggestions, and discussions during thesis committee meetings contributed to enhancing the quality of my research.

To Prof. Dr. Nils Brose, Prof. Dr. Med. Christine Stadelmann-Nessler, and Prof. Dr. Rubén Fernández-Busnadiego, I am very thankful for accepting to be on my thesis examination board. Your willingness to evaluate my work is much appreciated.

My deepest thanks to DAAD organization, whose belief in my scientific potential made it possible for me to come to Germany and pursue my Ph.D. Their financial assistance enabled me to focus on my research project and contribute to the scientific community.

I want to extend my thanks to the GGNB office for their consistent assistance and support over my study period, especially during the hard times when I faced health issues.

To our postdoc, Dr. Annekatrin König, thanks a lot for your guidance and for teaching me the recombinant alpha-synuclein preparation work, and HPLC methods. Your engaging discussions and support were pivotal to my work.

Special thanks also go to our postdoc, Dr. Ellen Gerhardt, who helped a lot in the preparation of the plasmids that I needed in my study. Thank you also for the discussions and suggestions that were meaningful to my research.

Heartfelt thanks go to Mrs. Christiane Fahlbusch, our 'Lab Lifesaver', who helped me in the preparation of lentiviral preparations and was supportive all the time.

To my former colleague, Dr. Evi Vasili, who helped me a lot in the preparation and characterization of different alpha-synuclein species, and for her insightful discussions, which greatly contributed to my research.

Many thanks to Dr. Christof Lenz and Dr. Dietmar Riedel for their collaborative efforts and expertise in mass spectrometry analysis and electron microscopy, respectively. These contributions greatly enriched my research.

To Dr. Maria-Patapia Zafeiriou, who kindly allowed me to use her lab for MEA experiments, and Dr. Guobin Bao, who assisted me with MEA plating and recordings, my deep appreciation.

To all my former and current doctoral colleagues, it is your companionship that has added color to this journey, where we shared ideas, worries, and happy moments. Special thanks go to my colleague Patricia Santos, with whom I did collaborative work that has substantially contributed to the overall success of our research. Many thanks also go to my former doctoral colleague, Dr. Inês Brás, for assistance with animal work and for teaching me to prepare hippocampal cultures.

To all colleagues in the Department of Experimental Neurodegeneration, heartfelt thanks for your scientific contributions and personal support throughout my Ph.D. Your personal support, especially during challenging times, has been a significant source of strength for me.

Lastly, I would like to thank my friends and family for always being there for me. To my dear wife, I cannot thank you enough for your unwavering support, understanding, and patience throughout this challenging journey. Your belief in me, love, and encouragement have been my driving force. To my two incredible children, Mohsen and Mira, you are my inspiration. Your innocent smiles and boundless joy have brought light into my life, even during the most demanding times.

Table of Contents

List of figures

List of tables

List of Abbreviations

AD	Alzheimer's disease
AEX	Anion exchange chromatography
AGEs	Advanced glycation endproducts
AK	Adenylate kinase
ANOVA	One-way analysis of variance
aSyn	Alpha synuclein
aSyn M	aSyn monomers
aSyn O	aSyn oligomers
Aβ	Amyloid-beta
BCA	Bicinchoninic acid
BSA	Bovine serum albumin
CEL	Nε-carboxy-ethyl-lysine
CML	Nε-carboxy-methyl-lysine
Co-IP	Co-immunoprecipitation
CSF	Cerebrospinal fluid
CSPα	Cysteine-string protein-α
DAT	Dopamine active transporter
DIV	Days in vitro
DLB	Dementia with Lewy bodies
DMEM	Dulbecco's modified eagle medium
DMSO	Dimethyl sulfoxide
dPBS	Dulbecco's phosphate-buffered saline
EDTA	Ethylenediaminetetraacetic acid
EM	Electron microscopy
ER	Endoplasmic reticulum
FBS	Fetal bovine serum
GC	Golgi complex

GCIs	Glial cytoplasmic inclusions
HBSS	Hank's balanced salt solution
HEK	Human embryonic kidney
HEPES	4-(2-hydroxyethyl)-1-piperazineethanesulfonic acid
HIC	Hydrophobic interaction chromatography
HPLC	High-performance liquid chromatography
HSP27	Heat shock protein 27
IEX	Ion exchange chromatography
IPTG	Isopropyl β-D-1-thiogalactopyranoside
LBs	Lewy bodies
LNs	Lewy neurites
MAP2	Microtubule-associated protein 2
MEA	Multielectrode array
MGO	Methylglyoxal
MSA	Multiple system atrophy
MWCO	Molecular weight cut-off
NAC	Non-amyloid component
OD	Optical density
ON	Overnight
PBS	Phosphate buffered saline
PD	Parkinson's disease
PFA	Paraformaldehyde
PFFs	Pre-formed fibrils
PMSF	Phenylmethylsulfonylfluoride
pS129	Phosphorylation at S129
PSD95	Postsynaptic density protein 95
PTMs	Post-translational modifications
RIPA	Radioimmunoprecipitation assay

RP-HPLC	Reversed-phase high-performance liquid chromatography
rpm	Revolutions per minute
SDS	Sodium-dodecyl-sulphate
SDS-PAGE	Sodium dodecyl sulfate-polyacrylamide gel electrophoresis.
SEC	Size exclusion chromatography
SILAC	Stable Isotope Labeling by Amino acids in Cell Culture
SIRT2	Sirtuin 2
SNAP-25	Synaptosomal-associated protein 25
SNARE	Soluble NSF attachment protein receptor
SNc	*Substantia nigra pars compacta*
SYTG1	Synaptotagmin 1
TBS	Tris-buffered saline
TBST	Tris-Buffered Saline with Tween 20
VAMP2	Vesicle-associated membrane protein 2
WT	Wild type

Abstract

Alpha-synuclein (aSyn) is a presynaptic protein implicated in physiological synaptic roles, though its precise function is largely unknown. In Parkinson's disease (PD), the initial pathological events often involve synaptic impairments and aSyn aggregation, even before evident neurodegeneration. Abnormal aSyn forms can cause synaptic dysfunctions, but the toxicity of different aSyn species in along aSyn aggregation pathway is still a matter of ongoing debate.

In the first part of our study, we performed a comprehensive comparison of different exogenous aSyn (monomers, oligomers, and preformed fibrils (PFFs)) on primary hippocampal neurons. PFFs exposure at days in vitro (DIV) 7 mainly induced aggregation of endogenous aSyn associated with more neurotoxicity, and a decline in some synaptic protein levels at DIV 26. At DIV 21, the activity of recycling synaptic vesicle was impacted upon treatments with both oligomers and PFFs. Additionally, PFFs exposure at DIV 14 decreased neurons mean firing rate one-week post treatment.

In the second part of our study, we investigated how differences in recombinant aSyn purification protocols could affect its aggregation properties, potentially affecting downstream applications. We found that aSyn extracted under “High salt“ conditions showed a faster and higher aggregation profile compared to “No salt“ extracted aSyn using in vitro Thioflavin T based aggregation assays.

In the third part of our study, we studied aSyn interactions, particularly at synaptic vesicles isolated from adult mice brains, and performed aSyn pulldown assays. Proteomics data revealed many potential aSyn interactors. Gene ontology analysis linked these candidates to synaptic vesicle cycling, neurotransmitter release, and, interestingly, pathways associated with neurons and neuronal projections developments, suggesting aSyn has roles beyond traditional synaptic function roles. Using Stable Isotope Labeling by Amino acids in Cell culture (SILAC) proteomics in HEK cells, we discovered potential interactors for endogenous aSyn in control cell

lines. Many of these candidates have nuclear localization and are implicated in RNA and DNA processes, supporting aSyn roles in the nucleus.

Finally, we explored the effects of aSyn glycation, a posttranslational modification involved in neurodegeneration. We exposed mouse hippocampal neurons to glycated and unglycated aSyn at DIV 07. The glycated aSyn showed more neurotoxicity at DIV 26, but the capacity to induce aggregation of endogenous aSyn was unchanged regardless of glycation. Furthermore, glycated aSyn exhibited comparable effects on the levels of synaptic proteins compared to unglycated aSyn and did not significantly affect spontaneous neuronal activity in our assays.

In conclusion, our study revealed that aSyn PFFs induced more neurotoxicity and seeding potential than oligomeric species. Both forms, however, showed comparable synaptic vesicle recycling disruption, suggesting seeding-dependent and independent toxic mechanisms. We also found that different aSyn purification methods can affect its aggregation behavior, suggesting a need for standardized production protocols. Furthermore, we identified potential new aSyn interacting partners that could point towards novel physiological roles for aSyn. Lastly, while we did not observe synaptic effects for glycated aSyn, it did exhibit cytotoxicity, suggesting functional impacts may require higher concentrations.

1. Introduction

1.1 Exploring synucleinopathies: A focus on Parkinson's disease

A diverse group of neurodegenerative disorders shares the pathological hallmark of the accumulation of intracellular inclusions that are made primarily of fibrillar alpha synuclein (aSyn) aggregates or deposits. These diseases are, therefore, collectively referred to as synucleinopathies, and include dementia with Lewy bodies (DLB), multiple system atrophy (MSA), and Parkinson's disease (PD), the most common form of synucleinopathies. These cytoplasmic inclusions are called Lewy bodies (LBs) when they are localized to the cell bodies of neurons, or Lewy neuritis (LNs) when are formed in the neuronal processes (Grazia Spillantini et al., 1998; Spillantini et al., 1998; Wakabayashi et al., 1998; Wales, Pinho, et al., 2013). In MSA, aSyn deposits are called glial cytoplasmic inclusions (GCIs). Although these conditions share the presence of pathological aSyn aggregates and cell death, each condition has its own clinical features and main brain regions and cells affected .

1.1.1 Parkinson's disease

PD is the most common neurodegenerative movement disorder. Presenting mainly later in life, PD affects 1-2% of the general population over the age of 60 (Simon et al., 2020a; Tysnes & Storstein, 2017). Furthermore, it is expected that the prevalence of PD will increase dramatically in the future due to the aging of the general population, associated with the increased societal and economic burden (Simon et al., 2020b). Symptomatically, PD is characterized by motor symptoms including resting tremors, stiffness, and bradykinesia. These symptoms are due to the loss of dopaminergic neurons in *substantia nigra pars compacta* (SNc) (Figure 1A). In PD, neurodegeneration is progressive in nature, and a clinical diagnosis of the disease is usually made when there is already more than a 30% loss of dopamine-producing neurons, which is associated with the appearance of motor symptoms (Bohnen et al., 2006; Cheng et al., 2010; Fearnley & Lees, 1991).

Despite the fact that the disease is progressive in nature, current treatment options are limited to managing dopamine loss but not modifying the course of the disease. Motor symptoms are the classical symptoms that usually define PD diagnostic criteria; however, the course of the disease starts too early, up to 20 years before the appearance of motor symptoms. The period that precedes the onset of motor symptoms comprises the prodromal phase or stage of PD and is characterized by the start of neurodegeneration and presence of nonspecific symptoms, or the so-called non-motor symptoms, such as constipation, sleep disturbances, hyposmia, and cognitive impairment (Aarsland et al., 2010; Roos et al., 2022). The second neuropathological feature of PD is the accumulation of neuronal protein aggregates in the form of LBs (Figure 1A), and LNs, which have been reported to start forming in the early or prodromal stage of the disease (Poewe et al., 2017b).

1.1.2 Etiology of PD

Despite extensive research efforts to understand PD pathology, the exact etiology is still largely unknown. Most cases of PD are idiopathic or sporadic and are associated with aging and environmental factors as the main risk factors. 5–10% of PD cases have a genetic background causing familial forms of the disease (Kline et al., 2021; Poewe et al., 2017a). The SNCA gene, which encodes for aSyn, exhibits several missense mutations that are associated with familial PD. To date, 8 single point mutations have been identified in the SNCA gene, and they include A30P, A30G, E46K, H50Q, G51D, A53E, A53T, and E83Q (Figure 2A) (Kapasi et al., 2020; Krüger et al., 1998; Lesage et al., 2013; Pasanen et al., 2014; Polymeropoulos et al., 1997; Proukakis et al., 2013; Yoshino et al., 2017; Zarranz et al., 2004). Interestingly, all these mutations, except E83Q, occur in the N-terminal domain of aSyn, and most of these mutations result in early-onset PD or DLB. These aSyn mutations are associated with alterations of aSyn structure, affecting its oligomerization and aggregation properties, and the overall toxicity profile (Flagmeier et al., 2016; Lázaro et al., 2014a). Furthermore, multiplications or triplications of the SNCA gene have been documented to cause PD with an increase in aggregation of aSyn and LB pathology (Chartier-Harlin et al., 2004;

Ibáñez et al., 2004; Singleton et al., 2003). In addition to the SNCA gene, other mutations, including genes encoding leucine-rich repeat kinase 2 (LRRK2), Parkin, glucocerebrosidase (GBA), DJ-1, and PINK1 are known to cause familial PD cases (Bonifati et al., 2003; Lücking et al., 2000; Valente et al., 2004; Zimprich et al., 2004).

1.1.3 PD and Lewy body pathology

LBs appear as spherical packed structures and are primarily composed of insoluble aggregates of aSyn protein. aSyn, a natively disordered protein, tends to aggregate into fibrillar and filamentous insoluble structures under pathological conditions (Osterhaus et al., 1997). Along with aSyn, other proteinaceous elements, lipids, and membranous organelles and fragments are also present in LBs (Ikenaka et al., 2019; Shahmoradian et al., 2019). Although LBs and LNs have been extensively studied, the underlying mechanisms behind their formation and propagation, as well as the involvement of other associated structures, remain largely ununderstood. Furthermore, LBs pathology is not confined to any specific brain region but has been observed throughout different brain regions and even in the periphery (Dickson et al., 2010; Wakabayashi, 2020).

The distribution and spreading of LBs have been linked to the progression and severity of PD. Braak et al. proposed a staging system for describing the spread of LB pathology and disease severity in PD patients, although this system was initially used for Alzheimer's disease (AD) (Figure. 1B) (Braak, Del Tredici, et al., 2003; Braak, Rüb, et al., 2003). In the early stages of PD, LBs are present mainly in the olfactory bulb and the dorsal motor nucleus of the vagus nerve in the medulla oblongata as well as the peripheral autonomic nervous system (Rey et al., 2018a). The pathology spread later to the locus coeruleus and the raphe nuclei of the lower brain stem. Non-motor symptoms such as olfactory dysfunction, constipation, and sleep disturbances may appear during this period of the disease. Motor symptoms (bradykinesia, rigidity, and tremors) characterizing PD start manifesting in the mid-stage of the disease as LBs lesions extend to higher brain structures, including SN which is essential for motor

control. In the advanced stage of PD, there is a widespread pathology throughout all cortical regions, and the involvement of other circuits, such as those in the hippocampus associated with other clinical symptoms such as neuropsychiatric symptoms and more cognitive decline, and eventually severe dementia. (Koga et al., 2021; Spillantini & Goedert, 2000).

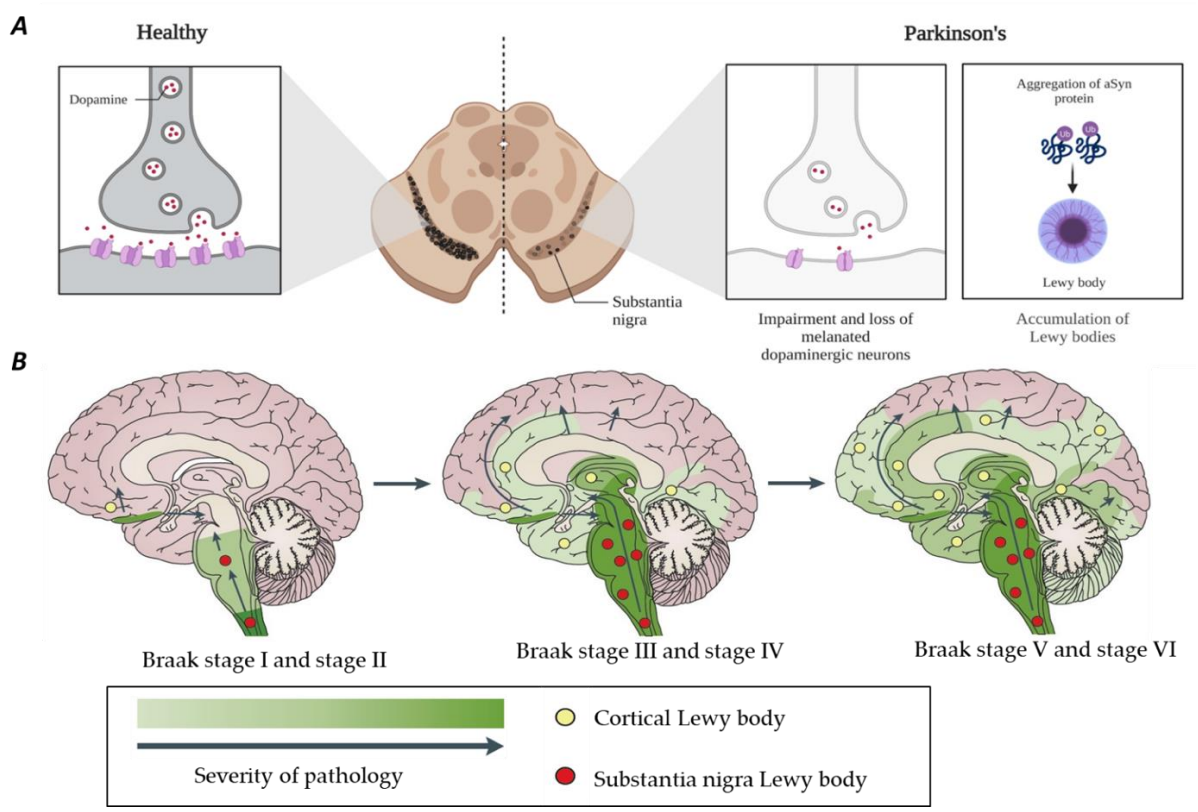

Figure. 1 Pathological features of PD. A. Compared to healthy individuals, PD patients have a significant loss of dopamine-producing neurons in the *substantia nigra* (SN), and the accumulation of intracellular misfolded aggregates of aSyn (LBs). **B.** LB pathology progression based on Break staging model. In the early stages (I, II), LB pathology occurs in the neurons of the lower brain stem. More brain regions are infiltrated including SNc, that is important for motor control, in the middle stages (III, IV), and finally, LBs spread throughout the brain including neocortical regions with disease progression (V, VI). Figure. **1A** was created with Biorender.com. Figure **1B** was adapted from (Poewe et al., 2017a).

1.1.4 Other synucleinopathies

In addition to PD, Synucleinopathies include DLB and MSA. While in PD, LBs are present in the SNc and are associated with the degeneration of dopaminergic neurons and, consequently, motor symptoms, LBs exist mainly in the cortical regions of DLB patients, where cognitive impairment is the main clinical feature although parkinsonism can present later (Mayo & Bordelon, 2014; Outeiro et al., 2019; Spillantini et al., 1998). On the other hand, MSA affects multiple systems of the body and is characterized by misfolding and aggregation of aSyn inside glial cells, forming inclusions called glial cytoplasmic inclusions (GCIs) (Goedert, 2001; Tu et al., 1998; Wakabayashi et al., 1998).

1.2 Structural aspects and synaptic localization of aSyn

aSyn is small protein that is expressed primarily in the central nervous system. Before its association with PD and other neurodegenerative diseases, aSyn was first extracted by Maroteaux et al. from the organ of the electric ray species *Torpedo californica* (Maroteaux et al., 1988b). In this study, they found aSyn to be localized in the synaptic vesicles and in proximity to the nuclear envelope of neurons, and therefore they proposed the name alpha synuclein based on its localization observations, where the ´´syn´´ is coming from its presence in the synapse and the ´´nuclein´´ part from the nuclear localization. Within the brain, high levels of aSyn are found mainly in the neocortex, hippocampus, striatum, cerebellum, and thalamus (Iwai et al., 1995; Maroteaux & Scheller, 1991). Although aSyn is mainly enriched in brain cells, it is ubiquitously expressed in other body regions such as red blood cells, the peripheral nervous system, and the gastrointestinal system (Baltic et al., 2004; Gelpi et al., 2014; Uéda et al., 1994).

1.2.1 aSyn structural properties

aSyn is a 140-amino acid protein with a size of 14.5 kDa. Structurally, aSyn is an intrinsically disordered protein consisting essentially of three regions (Figure. 2A)

(Emamzadeh, 2016). The first region, the N-terminal region, comprises the first 60 amino acids. It is amphipathic in nature and forms an alpha-helix when bound to lipid membranes (Eliezer et al., 2001a; Ulmer et al., 2005). The central region is the non-amyloid component (NAC) and consists of amino acids 61–95. The NAC domain is highly hydrophobic and plays an important role in the aggregation and fibrilization properties of aSyn (El-Agnaf et al., 1998; Giasson et al., 2001; Ueda et al., 1993). The C-terminal region is highly acidic, remains unstructured, and contributes to the overall unfolded state of aSyn (Eliezer et al., 2001b; Murray et al., 2003). This motif is involved in many aSyn interactions with other proteins and metals and has been documented to protect against aSyn aggregation (Burré et al., 2010a; Murray et al., 2003).

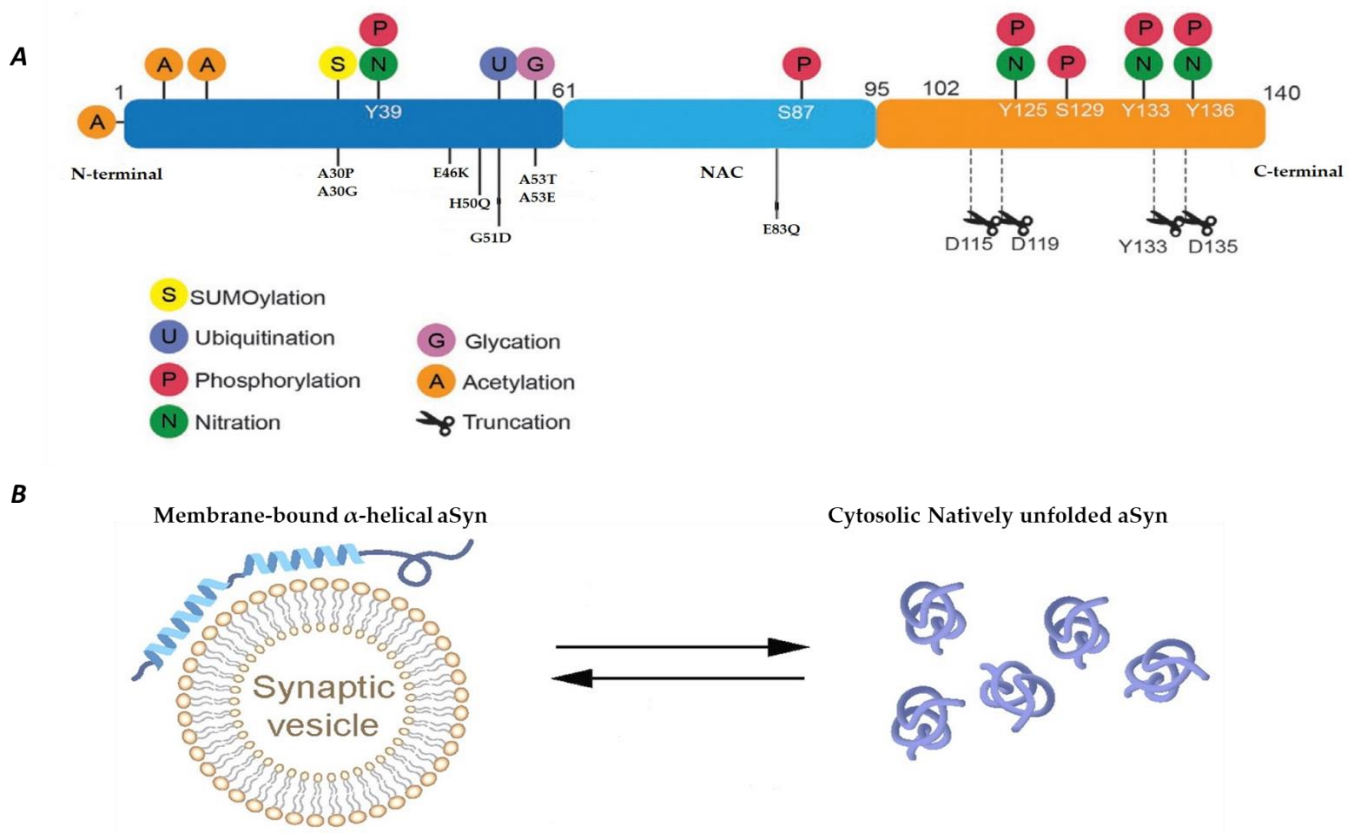

Figure 2. aSyn structural properties. A. Schematic depiction of aSyn structure. aSyn is composed of three regions. The N-terminus region (blue) spans the first 60 amino acids, has an important role in binding to lipid membranes, and contains most of aSyn mutations (A30P, A30G, E46K, H50Q, G51D, A53E, and A53T) associated with familial cases of PD. Represented in light blue, the NAC region (residues 61–95) is hydrophobic , implicated in aSyn aggregation, and contains the mutation E83Q discovered recently.

The amino acid residues 95–140 comprise the C-terminus domain (orange) that is rich in acidic amino acids and is important for aSyn interaction with metals and proteins. In this region, aSyn undergoes several posttranslational modifications (PTMs), including phosphorylation (P) and nitration (N) of tyrosine residues, and phosphorylation of S129, the most commonly encountered PTM in LB. aSyn truncations in this domain are also present and are associated with augmenting aSyn aggregation. The N-terminus region is also subjected to acetylation (A). Other PTMs, including SUMOylation (S), ubiquitination (U), and glycation (G), are more commonly occurring in the N-terminus region but can occur in other regions too. **B**. Inside cells, aSyn is found in two forms: freely soluble unfolded protein in the cytosol, which exists in equilibrium with the membrane-bound aSyn that adopts helical conformations. Figure. 2A was adapted with modifications from (Brás et al., 2020). Figure. 2B was adapted from (Gao et al., 2023).

Overall, aSyn is considered a largely natively unfolded or unstructured protein. There is no well-defined tertiary structure. However, membrane-bound aSyn adopts helical structures, while free cytosolic protein exists as disordered (Figure. 2B) (Eliezer et al., 2001a; Rovere et al., 2018). In addition, some studies also showed a physiologically relevant helical tetramer of aSyn which could exist in an equilibrium with the natively unfolded monomer (Bartels et al., 2011; Trexler & Rhoades, 2012). Nevertheless, the C-terminal region is highly flexible and stays unfolded under all conditions, whether aSyn binds to membranes, is freely soluble, or after aggregation (Farzadfard, Pedersen, et al., 2022; Murray et al., 2003).

1.2.2 Functional roles of aSyn at the synapse

Neuronal cells communicate with each other primarily through synapses. A synapse is essentially a structure involving two key components: a presynaptic bouton from one neuron, filled with vesicles containing neurotransmitters, and a postsynaptic neuron, carrying receptors for neurotransmitters. These two elements are separated by a region referred to as the synaptic cleft. Exocytosis is the process by which neurotransmitters from synapse vesicles are released to the extracellular space (synaptic cleft), leading to neuronal communication. For this process to happen, a collection of synaptic proteins from both the synaptic vesicle membrane and plasma

membrane needs to rearrange, assemble together, and form a complex to facilitate the fusion of synaptic vesicles with the target plasma membrane. This complex is called Soluble N-ethylmaleimide Attachment protein REceptor (SNARE) complex and includes syntaxin-1 and SNAP-25 on the presynaptic plasma membrane and VAMP2/synaptobrevin-2 on the synaptic vesicle (Figure. 3) (Lang et al., 2001). Furthermore, SNARE complex assembly is vital for all cellular processes involving the fusion of two membranes. However, many other proteins are implicated in neurotransmitter release and SNARE complex control. These include synaptotagmin and Munc18 (syntaxin-binding protein) (Zucker et al., 2014). Synaptotagmin is a transmembrane synaptic vesicle protein and consists of two domains: a luminal or intravascular domain and a large cytoplasmic domain that works as a Ca^{+2} sensor. Upon the arrival of the action potential at the presynaptic sites, voltage-gated Ca^{+2} channels open, leading to the influx of Ca^{+2} and binding to synaptotagmin, which triggers neurotransmitter release (Südhof & Rothman, 2009). Furthermore, the fusion of synaptic vesicles to the target plasma membrane is also facilitated by Munc18 which binds syntaxin, regulating SNARE complex assembly (Rizo & Südhof, 2002, 2012).

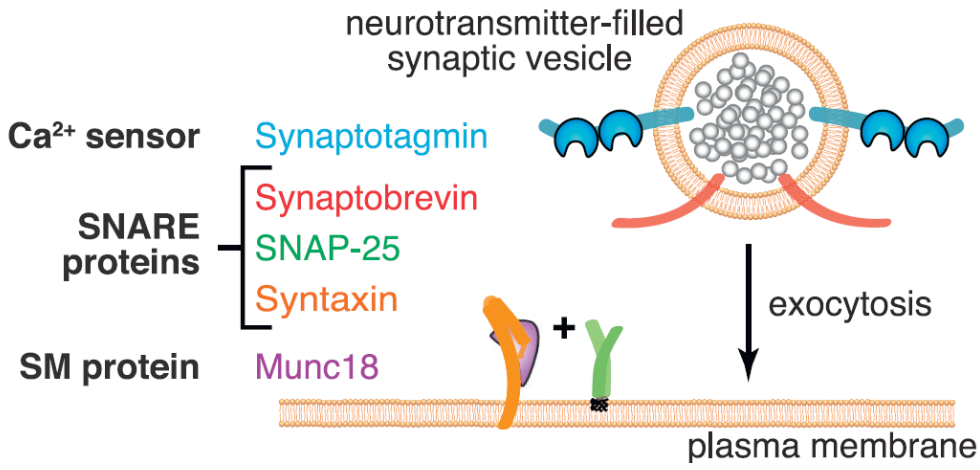

Figure 3. Basic elements of the synaptic fusion machinery. The SNARE complex includes three components: the vesicular SNARE synaptobrevin, and the plasma membrane SNAREs, syntaxin and SNAP-25. The SM-protein Munc18 and the vesicular protein synaptotagmin also play important roles in the exocytosis process. The figure was adapted from (Zucker et al., 2014).

aSyn is frequently described as a presynaptic protein due to its enrichment at the presynaptic sites. At the early stages of neurons development, aSyn is distributed throughout the neuron, but its concentration at the presynaptic locations increases with the maturation of neurons associated with synapse formation (Bayer et al., 1999; Galvin et al., 2001; Hsu et al., 1998; Withers et al., 1997). As there is no evidence for aSyn in synaptogenesis, this redistribution has been linked more to the affinity of aSyn to bind curved membranes of synaptic vesicles and interaction with synaptic proteins, suggesting regulatory functional roles at the synapse (Brás et al., 2020).

The exact physiological function of aSyn is still not fully understood, but the accumulated body of evidence supports roles related to synaptic vesicle docking and recycling, and neurotransmitter release. Several studies reported important roles for aSyn in these processes (Gao et al., 2023). aSyn, in its membrane-bound conformation, promotes SNARE complex assembly by its interactions with VAMP2. Studies suggest a chaperoning activity for aSyn for the formation of the SNARE complex and clustering of synaptic vesicles (Figure. 4) (Burré et al., 2010b; Diao et al., 2013; Sun et al., 2019). Reduced SNARE-complex assembly has been observed in aSyn null mice, affecting the exocytosis process (Burré et al., 2010b). Furthermore, aSyn compensated for the loss of chaperon cysteine-string protein-α (CSPα) in mice by assisting in the assembly of the SNARE complex at the synapse (Chandra et al., 2005). On the other hand, overexpression of aSyn potentially reduces synaptic vesicles release by perhaps interfering with the integration of vesicles into the synaptic vesicle cluster (Nemani et al., 2010), by reducing the proportion of vesicles that recycle, or by inhibiting their mobility (Scott et al., 2010). These findings show that aSyn concentration needs to be at optimal levels for the preservation of SNARE complex assembly.

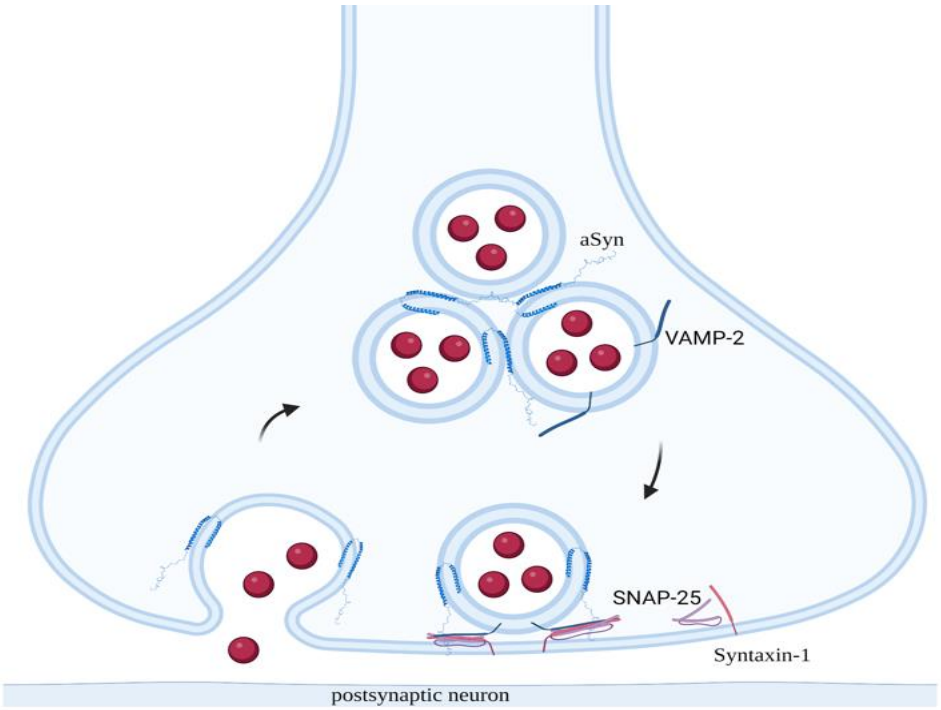

Figure 4. Function of aSyn at the synapse. aSyn plays important roles in the presynapse. Through binding to synaptic vesicles membranes and interaction with VAMP2, aSyn regulates synaptic vesicles clustering. aSyn chaperones SNARE complex assembly by binding to VAMP-2, facilitating exocytosis. Figure was created with Biorender.com.

1.3 aSyn – a key player in PD and other synucleinopathies

LBs were discovered for the first time in 1912 by the German neurologist Friedrich Heinrich Lewy. He described them as eosinophilic inclusions in the SN from the post-mortem brain of PD patients (Lewy FH, 1912). From that time, intensive research and several studies were conducted to check their composition and association with PD. In 1997, the protein aSyn was identified as the primary component of these structures, existing in aggregated and fibrillar forms (Spillantini et al., 1997). This major breakthrough marked the beginning of a new era in aSyn research and raised a lot of related questions about how aSyn could contribute to the pathology of PD.

1.3.1 aSyn link to PD

aSyn has been implicated in the pathogenesis of PD upon misfolding and aggregation, ultimately leading to LBs. Several lines of evidence associate aSyn toxicity

with PD. First, aggregated aSyn is the primary constituent of LB, which is the main pathological hallmark in most cases of PD (Grazia Spillantini et al., 1998; Spillantini, 1999). Second, several mutations or multiplications in the SNCA gene, which encodes aSyn, have been known to cause familial PD at an early age and to increase LB formation (Gasser et al., 2011; Klein & Westenberger, 2012). Furthermore, many cellular and animal models of aSyn overexpression have resulted in LB-like pathology, such as the presence of aggregated aSyn, neuronal loss, and motor function impairments. Finally, the levels of LBs and their distribution throughout the brain have been suggested to correlate with PD severity and progression (Braak, Del Tredici, et al., 2003; Dickson et al., 2010). Although the collected evidence strongly supports an association between LBs and PD, the exact role of LBs and their formation in the pathogenesis of PD remains a topic of ongoing debate and active research.

1.3.2 aSyn aggregation

Since aSyn aggregates are the main components of LBs and have been found in the brains of many PD, DLB, and MSA patients, there were several attempts to understand how the aggregation process of aSyn occurs. Although aSyn is largely unfolded or disordered in solution, it can, under certain conditions, misfold and aggregate. The process of aSyn aggregation is suggested to follow a nucleation-dependent polymerization pathway (Wood et al., 1999). According to this model, the process of aSyn aggregation can be segmented into three phases: the initial (lag or nucleation) phase, the log (growth) phase, and the steady (equilibrium) phase (Figure. 3). aSyn aggregation starts with the misfolding of aSyn monomers that self-associate, forming oligomeric intermediate species that have variable sizes and beta-sheet contents. This phase follows slow kinetics but represents the rate-limiting step in the aggregation pathway for aSyn. Once formed, these soluble oligomeric intermediate species serve as nuclei or seeds to rapidly recruit more monomers to be incorporated, giving rise to the generation of large oligomeric and protofibril species and finally,

mature fibrils that ultimately form LBs and LNs (H. T. Li et al., 2002; Qin et al., 2007). Unlike the initial phase, the growing of aggregates and formation of fibrils in the second phase is a rapid process. Once fibrils are not growing anymore, a plateau or equilibrium phase is reached where the rate of dissociation of monomeric proteins from fibrils is similar to the rate of monomers incorporation into fibrils (Harper & Lansbury, 1997). These formed fibrillar aggregates that form the main element of LBs are rich in beta sheet structures, insoluble, and resistant to cleavage by proteinase K, which is a broad-spectrum serine protease (Neumann et al., 2002).

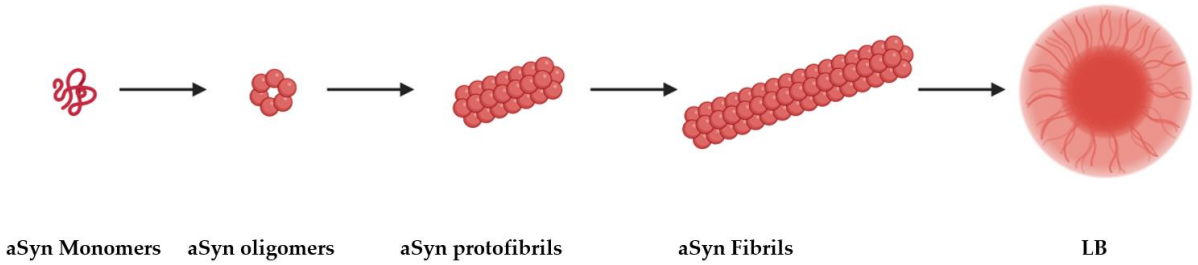

Figure 5. Aggregation pathway of aSyn. aSyn is a natively unfolded protein that, under not clearly understood conditions, starts misfolding into intermediate higher-order oligomers that incorporate more monomeric aSyn, resulting in the formation of large oligomeric and protofibrils under faster aggregation kinetics, leading finally to mature fibrils that form the core of LBs. The figure was created with Biorender.com.

1.3.3 aSyn LB pathology propagation

It is suggested that LB pathology might first start from non-dopaminergic regions of the brainstem or potentially even peripheral tissues and then spread in a somewhat standard pattern across neuroanatomically connected regions in the brain (Atik et al., 2016; Rey et al., 2018b). The first evidence of aSyn pathology spreading came out when it was observed, from two independent studies, that transplanted fetal neurons in the striatum of PD patients formed LB pathology, suggesting that pathological aSyn from the host brain can spread to the graft and the expansion of PD pathology to wide brain areas could occur via prion-like manner (Kordower et al., 2008; J. Y. Li et al., 2008). These observations were later supported by animal models

that showed direct evidence for the transmission of pathological aSyn from cell-to-cell. In these models, injection of preformed aSyn fibrils (aSyn assemblies) into the brains of non-transgenic mice resulted in cell-to-cell transmission of pathological aSyn and the formation of LB-like inclusions. All these data indicate that aSyn aggregates that are the primary LB component can be transmitted between neurons and serve as seeds to template the conversion of endogenous aSyn into other aggregates, leading to the propagation of LB-like pathology. These formed aSyn aggregates reproduce several main features of LB, such as fibrillar nature, insolubility, hyperphosphorylation at S129, and ubiquitination (Tarutani et al., 2016). Actually, this was the main rationale for using extracellular aSyn as a model of PD.

1.3.4 aSyn pathology at different cellular compartments

Mitochondrial compartment

Apart from the cytosol, many studies have demonstrated that aSyn can also localize to and get imported into the mitochondrial compartment, and it can happen under physiological conditions (W. W. Li et al., 2007; Nakamura et al., 2008; Zigoneanu et al., 2012). In addition, samples obtained from post-mortem PD brains revealed the presence of aSyn within the mitochondria (Devi et al., 2008). The buildup of aSyn within mitochondria has been linked to impairing mitochondrial membrane integrity, disrupting complex-I dependent respiration, and increasing reactive oxygen species (ROS) oxidative damage (Chinta et al., 2010; Devi et al., 2008; Loeb et al., 2010). All these factors lead to mitochondrial dysfunction and are implicated in the pathogenesis of PD (Hattori et al., 1991; Keeney et al., 2006; Parker et al., 1989). Mitochondria are also present in the synaptic compartment and play a crucial role in overall synaptic homeostasis (A. Lee et al., 2018). aSyn overexpression also seems to trigger mitochondrial fragmentation (Nakamura et al., 2011), which may, in turn, contribute to reduced synaptic performance (Exner et al., 2012). Moreover, aSyn-induced

dysfunction of synaptic mitochondria has been shown to manifest before impairments in overall mitochondrial function in neuronal cell bodies (Szegő et al., 2019).

Endoplasmic Reticulum and Golgi compartments

Several lines of evidence associate aSyn with endoplasmic reticulum (ER) and Golgi complex (GC) compartments. ER stress was evident in cellular models of PD, and elevated levels of aSyn oligomers have been observed within the ER of brain tissues of PD patients or animal models (Bellucci et al., 2011; Colla et al., 2012; Heman-Ackah et al., 2017; Holtz & O'Malley, 2003; Ryu et al., 2002). In addition, aSyn forms interactions with ER-resident chaperones and other proteins, ultimately disrupting ER signaling pathways (Bellucci et al., 2011; Lázaro et al., 2014b).

aSyn localized into the GC has been documented to impact its integrity. Once accumulated within GC, aSyn causes its fragmentation (Gosavi et al., 2002; Paiva et al., 2018a). Fragmented GC has been detected both in PD and MSA patients (Fujita et al., 2006; Sakurai et al., 2002). Data from cellular models indicate that GC fragmentation is an early pathological event prior to the formation of LB-like inclusions (Rendón et al., 2013). In the yeast model, it was shown that aSyn-related toxicity is due to the inhibition of ER-to-Golgi vesicular trafficking. This effect was reversed by overexpression of rab1, which is a key modulator of membrane trafficking (Cooper et al., 2006).

Nuclear compartment

When aSyn was discovered, its name was partially derived from its localization at the nucleus (Maroteaux et al., 1988b). However, aSyn presence and roles at the nucleus were a matter of debate at that time (Z. Huang et al., 2011; Wales, Lázaro, et al., 2013). Later, several studies confirmed that aSyn has a nuclear localization associated with modulating nuclear events (Garcia-Esparcia et al., 2015; Maroteaux et al., 1988a; Outeiro et al., 2008; Siddiqui et al., 2012; Zhong et al., 2010). Furthermore, the localization of aSyn at the nucleus was found to be enhanced by several aSyn mutations associated with PD (Fares et al., 2014; Kontopoulos et al., 2006). In addition,

previous research from our group found higher levels of phosphorylation of aSyn at S129 when aSyn has nuclear localization (Pinho et al., 2019). Although its exact function is still largely not resolved, aSyn has been reported to modulate gene expression and interact with many histones (Kontopoulos et al., 2006). In line with this, neurotoxicity for aSyn increased through inhibiting histone acetylation, and the use of histone deacetylase inhibitors was found to reverse this (Outeiro et al., 2007). Moreover, DNA fragmentation and repair mechanisms were also found to be affected when aSyn binds DNA (Pinho et al., 2019; Schaser et al., 2019a). Finally, a recently published study documented the presence of nuclear aSyn in the post-mortem brain tissue obtained from DLB cases, and was hyperphosphorylated at S129 (Koss et al., 2022). The presence of nuclear hyperphosphorylated aSyn that is usually associated with aSyn pathology supports nuclear aSyn pathological involvement.

1.4 aSyn PTM

Posttranslational modifications are chemical modifications of proteins amino acid residues that take place after their translations. PTMs occur physiologically and play a vital role in modulating the structural and functional properties of several proteins inside the cells. PTMs act as vital regulators of numerous biological processes and signaling pathways (Xu & Chou, 2015). Though PTMs are essential for normal physiological processes, some PTMs are pathological or associated with disease states (Santos & Lindner, 2017). aSyn undergoes several PTMs, some of which are associated with pathology (Manzanza et al., 2021). aSyn PTMs include but are not limited to, phosphorylation, ubiquitination, glycation, acetylation, nitration, SUMOylation, and truncation. Despite ongoing research, the specific contributions of these PTMs in the development of PD and other synucleinopathies remain largely unclear.

1.4.1 Phosphorylation

aSyn phosphorylation, a typical PTM, can happen in several amino acid residues, but the most studied and predominant form is phosphorylation of S129

(pS129). This modification is typically considered a pathological modification and is used as a marker of LB pathology and synucleinopathies. In PD and other synucleinopathies, around 90% of aSyn in LBs is phosphorylated at the serine 129 position (Anderson et al., 2006; Fujiwara et al., 2002a). It is often used in multiple studies when investigating endogenous aSyn aggregates and LB-like inclusions (Fayyad et al., 2020). The development of endogenous aSyn aggregates is often accompanied by an increase in the levels of pS129 in several cellular and animal models (Delic et al., 2018). However, whether this modification is pathogenic or neuroprotective is not clear, and is a matter of ongoing debate. Some studies have proposed pS129 to be cytotoxic (Karampetsou et al., 2017; Sugeno et al., 2008), while other studies did not observe any toxic effect and may instead have a neuroprotective effect (Azeredo da Silveira et al., 2008; Gorbatyuk et al., 2008; McFarland et al., 2009; Tenreiro et al., 2014). Furthermore, phosphorylation at S129 was reported to modulate gene expression and aSyn clearance. Although pS129 is used as a marker of LB pathology and endogenous aSyn aggregation, it is not known clearly whether phosphorylation occurs prior to aSyn aggregation or not. A recently published study found that phosphorylation of aSyn at serine 129 takes place following the initial aggregation of the aSyn (Ghanem et al., 2022).

While around 4% of aSyn is phosphorylated at S129 under physiological conditions (Anderson et al., 2006; Fujiwara et al., 2002b), the physiological role of pS129 has remained undefined, most likely due to its relatively low percentage. However, two recently published studies have shown a physiological role for pS129 for the first time. They reported that neuronal activity induces the phosphorylation at S129, mice living under environmentally enriched conditions have higher levels of pS129 and they exhibited synaptic plasticity, and pS129 aSyn binds presynaptic vesicle proteins, facilitating vesicle trafficking (Parra-rivas et al., 2022; Ramalingam et al., 2023). These new findings suggest dual roles for aSyn in health and disease states.

1.4.2 Glycation

Glycation is a PTM that is both age-associated and unavoidable. Glycation is a non-enzymatic series of reactions of reducing sugars with amino compounds, such as proteins, forming early glycation products. These early glycation products rearrange and break down, leading to the formation of carbonyl and dicarbonyl intermediates, including glyoxal and methylglyoxal (MGO), which are highly reactive. Finally, irreversible advanced glycation products (AGEs) are formed (Henning & Glomb, 2016). The main glycation sites in proteins are the N-terminal residue, and lysine and arginine residues (Paul J. Thornalley, 2008). Several byproducts of glucose metabolism are strong glycation agents, and the most prominent is MGO (P. J. Thornalley, 2005). MGO reacts with lysine and arginine residues of proteins, resulting in the formation of AGEs such as CML (Nε-carboxy-methyl-lysine), and CEL (Nε-carboxy-ethyl-lysine) (M. U. Ahmed et al., 1997; Brings et al., 2017). Glycation of proteins and the accumulation of AGEs are linked to diabetes-associated complications, including neuropathy (Singh et al., 2014). Higher glycation levels of proteins are observed in hyperglycemic conditions and diabetes due to increased production of MGO (Bierhaus et al., 2012; Uchiki et al., 2012; Yao & Brownlee, 2010).

AGE levels are high in the brains of patients with synucleinopathy and are detected in LBs (Castellani et al., 1996; Choi & Lim, 2010; Dalfo et al., 2005; Munch et al., 2000). These products are colocalized with aSyn in LBs in the SN (Munch et al., 2000).

Recently, our group has reported that aSyn is glycated in postmortem tissue from PD and DLB patients, and that aSyn glycation increases with aging in aSyn transgenic mice (Vicente Miranda et al., 2017). We also found aSyn can be glycated in vitro using dicarbonyl compounds, like MGO, preferably in the N-terminal region, likely due to the higher number of lysine (K) residues in this region of the protein. Interestingly, MGO glycation affects the aggregation of aSyn, promoting oligomerization but reducing fibrillization. Using in vitro and in vivo models, it was also found that glycation increases the aggregation and toxicity of aSyn, and increases

neuronal loss (Shaikh & Nicholson, 2008; Vicente Miranda et al., 2017). Furthermore, glycation reduces lipid binding in vitro, impairs synaptic transmission in hippocampal slice cultures, and impairs aSyn degradation pathways (Vicente Miranda et al., 2017). More recently, we found that the heat shock protein 27 (HSP27), an important protein in proteostasis that is also present in Lewy bodies, reduces MGO-mediated aSyn oligomerization in vitro, and reduces aSyn aggregation and toxicity in cells under glycation conditions (McLean et al., 2001; Outeiro et al., 2006; Vicente Miranda et al., 2020).

Glycation has also been implicated in other neurodegenerative disorders. In Alzheimer's Disease (AD), for example, amyloid-beta (Aβ) and tau have been found to be glycated (Vagelatos & Eslick, 2013; Vitek et al., 1994), and Aβ glycation aggravates its toxicity in neurons. Furthermore, aminoguanidine, a scavenger of reactive carbonyl groups, prevents early cognitive impairments in a mouse model of AD (Li et al., 2013). Importantly, higher amounts of glycated proteins were observed in the cerebrospinal fluid (CSF) of AD patients (N. Ahmed et al., 2005). We have also found that MGO-glycation potentiates neurodegeneration in cell and drosophila models of Huntington's disease (Vicente Miranda et al., 2016).

1.4.3 Acetylation

Acetylation, the covalent attachment of an acetyl group to the free amino group of amino acid residues in proteins, is one of the most abundant PTMs in eukaryotic and prokaryotic proteins. It can occur on the free a-amino group of the first N-terminal amino acid (N-terminal acetylation) or on the primary ε-amine group on the side-chain lysine residues (lysine acetylation). aSyn isolated from the brain of PD patients and healthy individuals (Anderson et al., 2006; Jakes et al., 1994; Ohrfelt et al., 2011), from rodent brains (Burre et al., 2013; de Oliveira et al., 2017), red blood cells (Bartels et al., 2011; Fauvet, Mbefo, et al., 2012), peripheral organs (appendix) and from a variety of mammalian cell systems have consistently shown that is N-terminally acetylated (Kellie et al., 2014; Theillet et al., 2016).

N-terminally acetylated aSyn presents primarily as an intrinsically disordered monomer (Fauvet, Fares, et al., 2012; Theillet et al., 2016). However, some studies also demonstrated a physiologically relevant helical tetramer of acetylated aSyn which could exist in equilibrium with the natively unfolded monomer (Fernandez & Lucas, 2018; Trexler & Rhoades, 2012). Notably, these acetylated forms tend to resist aggregation (Bartels et al., 2011), possibly by increasing the helical propensity of monomeric aSyn (Bartels et al., 2014; Iyer et al., 2016; Lijuan Kang et al., 2012).

Recently, the uptake and seeding capacity of acetylated aSyn fibrils were assessed in primary neuronal cells and cell lines (Birol et al., 2019). Strikingly, N-terminally acetylated aSyn preformed fibrils (PFFs) have increased seeding potential and induce the aggregation of endogenous aSyn earlier than unacetylated PFFs. Additionally, acetylated aSyn monomers and PFFs are internalized faster, which could explain the enhanced seeding competencies of acetylated PFFs. Interestingly, the uptake of acetylated aSyn fibrils is facilitated by neurexin1β, a glycoprotein that is abundant in the presynaptic terminals.

Finally, aSyn isolated from rodent brains from wild type animals was found to be acetylated in lysine (K) residues in the N-terminal region of the protein (K6 and K10) (de Oliveira et al., 2017; Lundby et al., 2012), suggesting lysine acetylation may be part of the normal biology of aSyn. While this modification has not been reported in human brain tissue, nor has it been associated with PD or other synucleinopathies, increasing evidence suggests lysine acetylation can impact the biophysical and biochemical properties of aSyn. Interestingly, Sirtuin 2 (SIRT2), a deacetylase that has been implicated in neurodegeneration (Outeiro et al., 2007), was found to interact with and modulate aSyn acetylation, aggregation, toxicity, and autophagy in vitro and in vivo (de Oliveira et al., 2017).

1.4.4 Other PTMs

aSyn is also subjected to ubiquitination. Studies have found that ubiquitin is found in LBs and colocalize with aSyn (Gómez-Tortosa et al., 2000; Oueslati et al., 2010). aSyn ubiquitination can occur in several lysine residues of aSyn and has been found to mark aSyn for degradation by the proteasomal system (Tofaris et al., 2011). Furthermore, mono-ubiquitination of aSyn is associated with increased oligomerization of aSyn (Rott et al., 2008). On the other hand, aSyn SUMOylation tends to have no effect on aSyn oligomerization and, but it inhibits its degradation by preventing aSyn poly-ubiquitination (Rott et al., 2017).

Nitration of aSyn is another PTM that has been reported, and it occurs in tyrosine residues Y39, Y125, Y133, and Y136 (Danielson et al., 2009; Takahashi et al., 2002). aSyn nitration reduces its ability to bind lipid membranes (Hodara et al., 2004). The effects of aSyn nitration on its aggregation are not clear, but some studies suggest reduced fibrilization of aSyn (Norris et al., 2003; Yamin et al., 2003).

Finally, although LBs are composed mostly of full-length aSyn, truncated forms of aSyn have been observed in LBs (Lewis et al., 2010; W. Li et al., 2005). aSyn truncations at the C terminus enhance aSyn aggregation and fibrilization (Hoyer et al., 2004). Several enzymes are involved in the cleavage process of aSyn, and it is thought that truncation of aSyn occurs under physiological and pathological conditions (Muntané et al., 2012).

1.5 Modeling PD and the use of exogenous aSyn species

Several models have been and are still in use for research regarding PD and other synucleinopathies. Since PD is typically characterized by two main pathological hallmarks, which are the degeneration of dopamine-producing neurons and the presence of aggregated aSyn in the form of LBs or LNs, the models used in PD usually aim to reproduce at least one of these pathological hallmarks. Being the classical and first-used model, toxins-based model usually leads to rapid and selective degeneration of dopaminergic neurons, recapitulating the first pathological hallmark with the associated motor deficits observed in PD (Schober, 2004). However, this model has two

main limitations. First, this model failed to reproduce the formation of aSyn and LB pathology (Jackson-Lewis et al., 2012). The second drawback is in the model itself, as it leads to acute neurodegeneration, opposing the progressive nature of neuronal loss in PD, and therefore is not suitable for studying disease-modifying therapies (Salat et al., 2016) .

Genetically based models are very important when studying familial forms of PD as they can express these mutations associated with PD mimicking many of the pathological features observed in these cases, and can help in understanding the mechanism of disease associated with such mutations (Barker & Björklund, 2020; Gonera et al., 1997; Y. Lee et al., 2012). However, many of these models can partially reproduce the significant loss of dopaminergic neurons, resulting in an incomplete motor phenotype, and the observed degeneration in the nigrostriatal pathway and motor symptoms are strongly influenced by the levels of the protein expressed and the specific promoter used to activate the expression of the transgene (Blesa & Przedborski, 2014; Pingale & Gupta, 2020).

Viral-based models are used to overexpress or knockdown the PD-associated protein aSyn in a selective and targeted manner, including certain cell types or brain areas (Lauwers et al., 2003; Van der Perren et al., 2014). These models are robust in inducing dopaminergic neurons loss and associated phenotypes (Löw & Aebischer, 2012). In addition, the feasibility of adjusting protein expression levels enables the researchers to adjust the toxic effects of the expressed protein, and to extend the time prior to neurodegeneration according to what they aim to study (Gombash et al., 2013; Visanji et al., 2016). However, these models have the limitations of using higher expression levels far away from physiological aSyn in order to induce pathology. This raises a question about their representation of the human condition. For example, aSyn levels are not found to be higher in idiopathic PD patients compared to healthy persons, and the level of aSyn in the brains of PD patients having the SNCA triplication mutation is only double that found in non-PD patients (Gombash et al., 2013; Miller et al., 2004). Additionally, aSyn aggregates observed were reported to not be filamentous

in nature, which may not reflect many features associated with LB inclusions (Volpicelli-Daley et al., 2016).

The fact that pathological aSyn present in LBs exists in aggregated forms and that idiopathic PD patients do not exhibit higher levels of aSyn protein compared to control individuals made researchers to focus recently on the aggregated aSyn, and to develop a model called preformed fibrils (PFFs) model (Polinski et al., 2018). This model is based on the use of recombinant aSyn to prepare PFFs. These fibrils tend to be amyloid in nature, having similar structural properties of aggregated aSyn found in LBs. Before the introduction to cells or injection to animals brains, these species are fragmented by sonication into shorter fibrils that can work as seeds or templates to induce formation of endogenous aSyn aggregates that recapitulates many pathological features observed in LBs, that is, they contain high levels of pS129 aSyn, they are ubiquitinated, they detergent insoluble, and they contain fibrillar structure that are very sensitive to Thioflavin S (Luk, Kehm, Carroll, et al., 2012a; Luk, Kehm, Zhang, et al., 2012; Volpicelli-Daley et al., 2014b). Unlike other models, they are able to induce endogenous aSyn aggregation under normal levels of aSyn expression, which is more representative of the idiopathic form of PD (Luk et al., 2009a).

aSyn PFFs have been documented to result in synaptic dysfunctions, alterations in the excitability of cells, and cytotoxicity in several cell line models (Luk et al., 2009a). When injected into the dorsal striatum, PFFs caused disturbances in dopamine release, neurotoxicity at SNc, and motor deficits from both transgenic and wild type (WT) animals (Abdelmotilib et al., 2017; Luk, Kehm, Zhang, et al., 2012; Paumier et al., 2015).

PFFs provide numerous benefits compared to other models. PFFs model is similar to viral vector- and toxins-based models in regard to the ability of researchers to trigger pathology, permitting spatiotemporal control of aSyn PFF introduction. Furthermore, the amount of PFFs introduced results in supra-physiological levels of aSyn, the model better reflects the human condition as the aSyn levels achieved are more in line with those observed in PD, unlike viral vector-based and specific transgenic models. In contrast to viral vector-based model, the observed pathology is

primarily due to pathological changes in the endogenous aSyn that are induced subsequent to the introduction of aSyn PFFs (Luk, Kehm, Carroll, et al., 2012a; Volpicelli-Daley et al., 2011). Furthermore, the progression of aggregation and pathological events in the aSyn PFF model is similar to those observed in humans, where synaptic dysfunction proceeds overt neurodegeneration and motor deficits (Abdelmotilib et al., 2017; Kordower et al., 2013).

Models based on using PFFs and oligomeric species are getting more popularity and are being used by several research groups in the field of PD. However, consistency in the production of PFFs has been considered a major challenge with variations across research labs. Acknowledging this, the Michael J Fox Foundation established a set of guidelines that should be taken into consideration when using the PFFs model (Polinski et al., 2018). Unexplained variations between experiments, batches, and laboratories, with regards to aggregation propensity of aSyn, remain a problem in the field.

aSyn used for the preparation of PFFs and oligomers is produced recombinantly from the bacteria *E.coli*. Several protocols are available in the literature for the production and purification of aSyn as shown in Table 1. By examining these protocols, it is very clear that there are a lot of variations across different purification methods and even within one method across different research groups. aSyn purified in these methods is frequently used to generate PFFs or oligomeric species, and variation in the production and purification procedures is expected to alter the aggregation propensity of aSyn affecting downstream applications. Furthermore, systematic studies that compare the effects of different protocols on the structural and aggregation properties of aSyn are very limited. Therefore, the issue of using different protocols, and the absence of efforts to develop a standard protocol for the production and purification of the starting monomeric material, similar to what is recommended for PFFs, will continue to be a major challenge making it more difficult to interpret study results among different labs about the effect of different aSyn species and impacting the usefulness of this valuable model.

Table 1. Overview of different protocols currently used for preparation and purification of recombinant aSyn protein.

aSyn Expression	aSyn Extraction	Purification	Storage	Reference
LB medium, 1 mM IPTG, 4 hours induction	40 mM Tris acetate buffer, sonication, and 10 min boiling	IEX, SEC	lyophilized	(Fauvet et al., 2012)
TB medium, No IPTG, ON incubation	High salt buffer, sonication, and 15 min boiling	SEC, IEX	Frozen	(Volpicelli-Daley et al., 2014a)
LB medium, 1 mM IPTG, 5 hours induction	periplasmic lysis by osmotic shock buffer	IEX	lyophilized	(C. Huang et al., 2005)
LB medium, 0,5 mM IPTG, ON induction at 25 °C	10 mM Tris lysis buffer, 30 min boiling, and ammonium sulfate precipitation	IEX, SEC	Frozen	(Strohäker et al., 2019)
IPTG, other details unstated	Cell lysate precipitated in ammonium sulfate	IEX, SEC	lyophilized	(Conway et al., 1998)
Details not stated	20 mM Tris and 100 mm NaCl, acid precipitation	IEX	Not stated	(Narhi et al., 1999)
LB medium, 1 mM IPTG, 4 hours induction	periplasmic lysis by osmotic shock buffer	IEX, HIC	lyophilized	(Campioni et al., 2014)
LB medium, 1 mM IPTG, 4 hours induction	20 mM Tris, sonication and 15 min boiling	IEX	lyophilized	(Kumar et al., 2020)

LB medium, IPTG concentration not stated, 4 hours induction	10 mM Tris, freeze-thaw, sonication, 20 min boiling, and ammonium sulfate precipitation	IEX	Not stated	(Hoyer et al., 2002)
LB medium, 0,5 mM IPTG, ON induction at 25 °C	500 mM NaCl and 100 mm Tris, 10 min boiling, and acid precipitation	IEX	Not stated	(Der-Sarkissiant et al., 2003)
LB medium, 0,44 mM IPTG, 2 hours induction at 37 °C	10 mM Tris, freeze-thaw, sonication, and ammonium sulfate precipitation	IEX, SEC	Not stated	(Ghee et al., 2005)
TB medium, 0.5 Mm IPTG induction for 16 hours at 37	100 Mm tris and 500 mm NaCl, freeze-thaw, 10 min boiling, and acid precipitation	RP-HPLC	lyophilized	(Galesic et al., 2021)
LB medium at 37 °C, 4 hours IPTG induction	Sonication, 5 min boiling	IEX, SEC, RP-HPLC	lyophilized	(Fares et al., 2016)

1.6 aSyn at the synapse: pathological implications

Synaptic dysfunction is an initial pathological event that has been documented in many neurogenerative diseases, including PD. Synaptic performance and alterations precede neurodegeneration or neuron cells loss (Janezic et al., 2013; Kordower et al., 2013; Milber et al., 2012). Prior to the formation of LBs, aSyn aggregates in the synapse have been observed in post-mortem tissue studies from DLB and PD (Kramer & Schulz-Schaeffer, 2007; Marui et al., 2002; Schulz-Schaeffer, 2010; Wu et al., 2019).

These studies suggest that aSyn pathology possibly starts at the synapse and then proceeds to the cell body. Given the important roles of aSyn interactions with the essential elements of synaptic function like SNARE complex proteins and synaptic vesicles, alterations disrupting these physiological interactions would ultimately lead to impaired synaptic function. In line with this, obstruction of synaptic vesicle docking has been reported upon binding of aSyn aggregates to VAMP2, disrupting SNARE complex assembly process (B. K. Choi et al., 2013). These aggregates have been suggested to form clusters with synaptic vesicles, inhibiting the trafficking process (L. Wang et al., 2014). Additionally, cellular and animal models overexpressing aSyn have shown a decrease in vesicle priming and neurotransmitter release as well as the redistribution of synaptic vesicles away from the active zone, along with a decline in the postsynaptic density (Garcia-Reitböck et al., 2010; Larsen et al., 2006). The mechanisms behind such synaptic impairments are largely unknown.

High aSyn levels have been shown to negatively impact dopaminergic neurotransmission, and it is believed that aSyn directly affects the activity of tyrosine hydroxylase, the enzyme that plays a key role in dopamine synthesis (Kirik et al., 2002; Perez et al., 2002). In addition, dopamine reuptake can be inhibited through the interaction of aSyn with dopamine active transporter (DAT), which can impair dopaminergic neurotransmission and lead to the accumulation of dopamine in the synaptic cleft (B.-K. Choi et al., 2013; Paxinou et al., 2001; Wersinger & Sidhu, 2003). Furthermore, recent research aiming to understand the particular susceptibility of dopaminergic neurons in PD has proposed that dopamine itself could induce the aggregation of alpha-synuclein, potentially exacerbating neuronal degeneration. Since dopamine itself has been reported to promote the oligomerization of aSyn (Mor et al., 2017; Outerio et al., 2009), the accumulation of both aSyn and dopamine can, therefore, lead to more neurotoxicity. Indeed, the interaction of aSyn oligomers with synaptic vesicles is associated with the creation of pores in their surface, potentially causing neurotransmitter leakage (Danzer et al., 2007a; Lashuel et al., 2002a; Volles et al., 2001). Dopamine leakage could potentially potentiate alpha-synuclein oligomerization, with

the possibility of further oxidative stress as a result of dopamine high reactivity (Mosharov et al., 2006).

Exploring the effects of different aSyn species at the synapse, various research groups have delved into the relative synaptotoxcity of aSyn oligomers and PFFs. Some studies have put forward evidence for the cytotoxic nature of aSyn oligomers (B.-K. Choi et al., 2013; Diógenes et al., 2012; Prots et al., 2018; Winner et al., 2011), positing that these soluble intermediates can disrupt membrane integrity and interfere with synaptic function. On the other hand, other research teams highlight the detrimental impact of PFFs, suggesting that these larger aggregates could impair various cellular processes, leading to neuronal loss (Mahul-Mellier et al., 2020; Volpicelli-Daley et al., 2011). Studies that did a comparative analysis of all aSyn species are very limited, however.

1.7 Objectives

Although the aggregation of endogenous aSyn has been implicated in PD pathology and the synaptic performance, it is still unknown what triggers the aggregation of endogenous aSyn leading to LB pathology. Furthermore, which toxic species along aSyn aggregation pathway is more toxic is a matter of ongoing debate. Many studies are using exogenous aSyn species to study the effects of different species on synaptic function. Some studies are in favor of the oligomer toxicity hypothesis, while other studies suggest fibrils as the culprit agents. Moreover, studies that perform comprehensive comparisons of all different species are very limited. Additionally, aSyn undergoes several posttranslational modifications, some of which are associated with PD and to be involved in impairing synaptic pathology. In our study, we aimed to produce different aSyn species, namely monomers, oligomers, PFFs, and glycated aSyn species, in order to do a comprehensive analysis of the synaptotoxcity profile of all tested species. We hypothesized that different forms/species of aSyn induce, for example, through aberrant direct or indirect effects on synaptic components, a series of synaptic injuries that disrupt normal synaptic biology, leading to cellular pathologies, neuronal dysfunction, and death, all of which are characteristic of PD. Thus, the characterization of the initial accumulation of small injuries will be instrumental for the design of future strategies to tackle the initial stages of PD.

Aims

1. **To determine the basic functional changes at the synapse induced by different forms of aSyn.**

   for this aim we produced different aSyn species (monomers, oligomers, and PFFs) and investigated their impact at the synapse using primary mouse hippocampal neurons. We analyzed the changes that could happen at the synapse on the biochemical and functional levels at different time points.

2. **To identify general and specific interacting partners of aSyn in HEK cells and isolated synaptic vesicles respectively**

For this aim, we were looking to check general interactors of aSyn using HEK cells and Stable Isotope Labeling by Amino acids in Cell Culture (SILAC) proteomics approaches.

We also investigated the potential interacting partners for aSyn at the synapses by isolating synaptic vesicles from adult mice brains and then running pulldown assays for aSyn to identify by proteomics analysis its potential interactome.

3. **To assess the effect of posttranslational modification aSyn glycation on synaptic activity**

   For this aim, we produced glycated aSyn species and treated mouse hippocampal neuronal cultures with these species studying biochemical and functional alterations that could be induced following exposure to these species.

2. Materials and Methods

2.1 Preparation and characterization of aSyn species

2.1.1 Expression and Purification of Recombinant WT Human aSyn

Escherichia coli strain BL-21 (DE3) cells transformed with the plasmid encoding WT human aSyn are grown overnight (ON) on an ampicillin agar plate. Next day, one colony from the agar plate is used to create a 200-400 ml preculture of LB medium supplemented with 200 μg/ml ampicillin incubated overnight at 37 °C with shaking at 180–200 rpm. The following day, the pre-culture is used to inoculate 2–4 liters of LB/ampicillin medium at 37 °C with shaking at 180–200 rpm. When the optical density (OD600) of the cultures is around 0.5–0.7, isopropyl-β-D-thiogalactopyranosid (IPTG, 1 mM) is added to induce the expression of the protein, and the cells are incubated further for 2 hours with agitation. After induction with IPTG, bacterial cells are collected by centrifugation (6600 g, 4 °C), and the bacterial pellet is frozen until further use. aSyn gets extracted by thawing the bacterial pellet on ice and resuspending it in high salt lysis buffer (750 mM NaCl, 10 mM Tris, pH 7.6, 1 mM Ethylenediaminetetraacetic acid (EDTA, Carl Roth, Germany)), with the fresh addition of one tablet of protease inhibitor cocktail (Roche, Basel, Switzerland) to the lysis buffer. After being ultrasonicated for a total of 5 min (30 sec ON, 30 sec OFF pulses, 60% power) each on ice, the lysed pellet extract sample is then boiled at 95 °C in a water bath for 15 min to precipitate unwanted proteins, which are removed later by centrifugation at maximum speed (around 16,000g, 4 °C, 20 min). The supernatant containing aSyn is collected and dialyzed at 4 °C with a dialysis membrane of 10 kDa molecular weight cut-off (MWCO) in 10 mM Tris, pH 7.6, 50 mM NaCl, 1mM EDTA.

Before purification with high-performance liquid chromatography (HPLC), aSyn protein sample is filtered through a 0.22 μm syringe filter to remove any insoluble particles that can clog the HPLC column and system. The protein sample is applied to the anion exchange chromatography (AEX) column Hiprep Q HP 16/10 (GE Healthcare Life Sciences) for purification. The anion exchange column was pre-equilibrated with a starting buffer (25 mM Tris, pH 7.6). The sample was injected

through a sample loop connected to the AKTA PURE HPLC system to the AEX column, and aSyn was eluted by running a linear gradient of 9 column volumes (CV) elution buffer up to 100% elution buffer (1 M NaCl in 25 mM Tris, pH 7.6). Fractions containing pure aSyn (as analyzed by SDS-PAGE and Coomassie staining) are collected and combined, and extensively dialyzed against deionized water. After being lyophilized (Zirbus), aSyn was frozen at -20 °C until further use.

2.1.2 Preparation of WT aSyn oligomers and monomers, and pre-formed fibrils (PFFs)

aSyn oligomers were produced according to previous protocols (Lashuel & Grillo-Bosch, 2005; Paslawski et al., 2016). aSyn was dissolved in phosphate buffered saline (PBS) to get a final protein concentration of 12 mg/ml. The concentration of aSyn was determined by measuring the absorbance of the protein at 280 nm and the molar extinction coefficient of 5960 M^{-1} cm^{-1} for aSyn. 60 mg of aSyn dissolved in 5 ml of PBS containing 5 µL of Benzonase (MERCK, 71,205–3) was passed through 0.22 µm syringe filters (MERCK, SLGP033RS) and transferred to 1.5 ml low-binding tubes. Protein samples were incubated for 5 hours with shaking at 900 rpm at 37 °C. The protein was centrifuged at 12000 g for 10 min at 4 °C to remove any aggregated aSyn material. The supernatant was collected and injected into a HiLoad® 26/600 Superdex® 200 preparation grade gel filtration column (GE Healthcare Lifesciences) previously equilibrated with PBS. aSyn protein was eluted at a flow rate of 2.6 ml/min and a fraction size of 2 ml. Oligomers containing fractions corresponding to the void volume peak were collected, combined, and concentrated to a concentration of 0.2–0.4 mg/ml. The fractions in the peak corresponding to the monomeric form of aSyn were also collected and concentrated to 5 mg/ml. Both protein forms were filtered through 0.22 µm spin filters to make them sterile for cellular studies, after which they were aliquoted under aseptic conditions, snap-frozen, and stored at −80 °C until further use.

To prepare PFFs, lyophilized aSyn was solubilized in sterile Dulbecco's phosphate-buffered saline (dPBS) to reach a concentration of 5 mg/ml. The protein solution was sterile filtered using 0.22 μm spin filters, incubated in low-binding tubes, and shaken for 7 days in a thermomixer set at 37 °C at 1000 rpm. At the end of the incubation time, a successful conversion of aSyn monomers to fibrils should produce a turbid or cloudy preparation. The fibrils were then centrifuged at 20,000 g for 30 minutes, and the fibrils pellet was initially resuspended in 300 ml sterile PBS to measure the protein concentration of converted monomers to fibrils. After protein concentration determination, an additional volume of PBS was added to get a final concentration of 5 mg/ml. PFFs were stored at −80 °C in small aliquots of 10–20 μL each.

2.1.3 Characterization of aSyn species

2.1.3.1 Sedimentation assay

To ensure aggregate formation in PFFs preparation, sedimentation analysis was conducted. 2 μL of 5 mg/mL PFFs preparation was diluted in 20 μL PBS and spun at 20,000 g for 30 minutes. The supernatant was collected carefully, and the pellet got resuspended in 20 μL PBS. 5X Laemmli buffer (250 mM Tris pH 6.8 (9090,3, Carl Roth, Germany), 10% SDS, 1.25% Bromophenol Blue (B0126, Sigma-Aldrich, MO, USA), 5% β-mercaptoethanol (63690, Fluka Analytical, Germany), 50% Glycerol (G5516, Sigma-Aldrich, MO, USA)) was added to both samples and the samples were boiled for 5 minutes at 95 °C. The same steps were followed also for monomeric and oligomeric species. the supernatant and pellet fractions were then run on a 15% sodium dodecyl sulfate polyacrylamide gel electrophoresis (SDS-PAGE) gel. After the end of the run, the gel was stained with Coomassie to visualize the bands. Unlike monomeric and oligomeric species, more aSyn should be observed in the pellet fraction than in the supernatant fraction of PFFs.

2.1.3.2 Thioflavin T Assay

25 μM of thioflavin T (ThT, Sigma-Aldrich, MO, USA) was mixed with aSyn species diluted in PBS to 7 μM in a total volume of 400 μL. 100 μL was pipetted to a 96-well black clear bottom plate in triplicate for each condition. The fluorescence intensity was read in a plate reader using 440 nm as the excitation wavelength and 480 nm for emission.

2.1.3.3 Electron Microscopy Analysis

Different aSyn species samples at a concentration of 0.1 mg/ml were bound to a glow discharged carbon foil covered 400 mesh copper grid. Samples were stained with uranyl acetate and evaluated at room temperature using an electron microscope (Talos L120C, Thermo Fisher Scientific).

2.1.3.4 Immunoblotting and dot blotting

Immunoblotting experiments were carried out to analyze different bands and or smears appearing on the blot when probed with an antibody against total aSyn. In summary, 200 ng of monomers, oligomers, and PFFs were mixed with 5X Laemmli sample buffer and loaded onto a 15% SDS-PAGE gel. After electrophoresis, separated proteins were transferred from the gel onto a nitrocellulose membrane using the iBlot 2 Gel Transfer device (IB21001, Thermo Fisher Scientific, MA, USA). The transfer process was carried out for 7 minutes at a constant voltage of 20 V. The membrane was then blocked with 5% skim milk in (TBS-T, 10 mM Tris-HCl, 150 mM NaCl (3957,2, Carl Roth, Germany), 0.1% Tween-20 (P2287, Sigma-Aldrich, MO, USA)) for a one-hour duration. The membrane was probed overnight with the primary antibody SYN-1 (BD; 1:1000 dilution) in blocking buffer against total aSyn levels in the blocking buffer at 4°C. On the following day, membranes were washed for 10 minutes 3 times in TBST and then incubated with a secondary antibody for one hour. After washing the membrane with TBST 3 times, the membrane was exposed shortly to the chemiluminescence HRP detection substrate, and protein bands on the membranes

were visualized using the Fusion FX chemiluminescence imaging system (Fusion FX, Vilber Lourmat, Marne-la-Vallée, France).

For dot blotting, a 96-well dot blot apparatus was assembled according to the manufacturer's instructions using a nitrocellulose membrane. 50 ng of monomers, oligomers, and PFFs diluted in a volume of 100 µL of each species were applied and subjected to vacuum filtration followed by immunoblotting. Dot blot membranes were incubated with anti-aSyn aggregate specific antibody MJFR-14 (ab209538, 2 ng/ml).

2.2 Preparation of glycated aSyn species

MGO glycated aSyn was prepared according to the protocol established in our lab. Briefly, 100 µM of sterile monomeric aSyn containing 5 mM MGO (Sigma-Aldrich, MO, USA) was incubated with shaking under constant agitation (300 rpm) for 5 days at 37 °C. Control preparations containing either aSyn or MGO alone were also produced simultaneously. After 5 days, preparations were aliquoted into small-size aliquots and kept at −80 °C until further use.

2.3 Neuronal cultures

2.3.1 Preparation of primary hippocampal cultures

Primary hippocampal neurons were prepared from C57BL6/J#00245 wild-type E15.5 embryos obtained from the animal facility of the University Medical Center Göttingen. All animal procedures were conducted in compliance with institutional and national German guidelines and received the necessary approvals from the University Medical Center Göttingen under license number 19/3213. In detail, pregnant mice were euthanized using CO2, and the embryos were removed from the uterus and placed in ice-cold HBSS containing 0.5% sodium bicarbonate solution (Sigma-Aldrich, MO, USA). Hippocampi were stereoscopically dissected from each embryo brain in ice-cold HBSS and transferred to a conical tube filled with HBSS to digest the tissue with 100µL of 0.25% trypsin (Gibco Invitrogen, CA, USA) at 37 °C. Trypsinization was inactivated by the addition of 100 µL DNase I (0.5 mg/mL, Roche,

Basel, Switzerland) and 100 µL fetal bovine serum (FBS) (Anprotec, Bruckberg, Germany). After dissociating the tissue using a glass pipette, the cells suspension was left for around 1 minute to allow the leftover debris to precipitate. The cells supernatant was collected, transferred to another tube, and centrifuged at 300 x g for 5 min. Finally, the cells pellet was resuspended in a neurobasal medium (Gibco Invitrogen, CA, USA) fortified with 2% B27 supplement (Gibco Invitrogen, CA, USA), 1% penicillin-streptomycin (PAN Biotech, Aidenbach, Germany), and 0.25% GlutaMAX (Gibco Invitrogen, CA, USA). Cells were counted using a Neubauer chamber and plated on previously treated glass coverslips with 0.1 mg/mL PLO (Poly-L-ornithine, Sigma-Aldrich, MO, USA) in a 24-well plates format with a seeding density of 130,000 cells per well. For immunochemistry work, cells were plated in previously coated 12-well plates at a seeding density of 400,000 cells per well. 750 µL of neurobasal medium was used for plating cells in 24-well plates and 1500 µL for 12-well plates. Cells were maintained in the same neurobasal medium until the day of treatment with aSyn species.

2.3.2 Primary hippocampal culture treatments with exogeneous aSyn species

Primary hippocampal neurons were maintained under standard growth conditions since the day of plating. Cells were kept in the original plating medium until the day of treatment. At days in vitro (DIV) 7, neuronal cells were treated by the addition of different aSyn species (monomers, oligomers, and PFFs) into the 24-well plates for immunocytochemistry work and to the 12-well plates for biochemistry work. PFFs were thawed at ambient temperature, diluted in PBS, and sonicated to make seeds. Half the volume of the old neurobasal plating medium was removed from each well and exchanged with a freshly prewarmed neurobasal medium. All the different species were diluted to a final concentration of 100 nM and added inside the newly added medium. Treated cells were grown until DIV 21 or DIV 26, and one-third of the medium was exchanged with fresh medium every 4-5 days. Glycated aSyn species were added to neuronal cells in the same manner and at the same concentration.

2.3.3 Multi-electrode array (MEA) experiments

Mouse hippocampal neurons were extracted and prepared from above and were used for these experiments. Cells were plated at a seeding density of 20,000 cells/μL in a total volume of 5 μL into CytoView MEA black 48-well plates (Axion Biosystems, USA) containing 16 microelectrodes in each well. The plates were previously coated with 0.1 mg/mL PLO. The cells were allowed to attach to the electrode area for approximately one hour before the addition of neurobasal plus (Gibco Invitrogen, CA, USA) medium used with B-27 Plus Supplement (Gibco, CA, USA), and 1% penicillin-streptomycin. 30% of media change was carried out every 2-3 days. Cells were treated with different aSyn species at DIV 14, and the basal spontaneous neuronal activity was recorded on the same day before the treatment using the Maestro Pro Platform (Axion Biosystems, USA) according to the manufacturer's instructions. MEA recordings were conducted again at DIV 20. Neuronal activity was recorded four times, with measurements taken every 15 minutes for a duration of 10 minutes each. Neuronal module AxlS Navigator software (Axion Biosystems, USA) was used to analyze recorded data. The data obtained were finally analyzed using GraphPad Prism 9 software (GraphPad, CA, USA).

2.3.4 Human embryonic kidney cells growth and infection

Human embryonic kidney (HEK) 293 cells (ATTC, VA, USA) were maintained under standard growth conditions at 37°C with 5% CO2 in DMEM medium (PAN Biotech, Aidenbach, Germany) with the addition of 10% FBS (Anprotec, Bruckberg), and 1% penicillin-streptomycin (PAN Biotech, Aidenbach, Germany) to the medium. Stable cell lines expressing pCDH-EF1 eGFP-IRES-eGFP, pCDH-EF1 aSyn WT IRES GFP, or pCDH-EF1 aSyn A30P IRES GFP were obtained by lentiviral infection of HEK 293 cells. After incubating cells for 4 days with lentivirus preparations, cells were passaged 4 times. More than 90% of cells were infected, as confirmed by microscopic

imaging. These cell lines were used for SILAC experiments. Lentivirus production was performed according to previously established protocols (Tiscornia et al., 2006).

2.3.5 Stable isotope labeling of amino acids in cell culture (SILAC)

For SILAC experiments, HEK293 cells stably overexpressing WT aSyn, A30P aSyn, or GFP (control cell line) produced as described above were used. Cells were switched to SILAC DMEM (PAN Biotech, Aidenbach, Germany) medium lacking L-glutamine, L-arginine (R), and L-lysine (K). SILAC medium was supplemented with 10% (v/v) dialyzed FBS (Sigma-Aldrich, MO, USA), 1% penicillin-streptomycin (PAN Biotech, Aidenbach, Germany), L-glutamine 584 mg/L (Gibco, UK), and light (L) isotopes (R0K0), medium (M) isotopes (R6K4) or heavy (H) isotopes (R10K8) amino acids. For SILAC medium, 0.5 ml aliquot stock solutions of R (Sigma-Aldrich, MO, USA) (84 mg/ml in PBS), and K (146 mg/ml in PBS) were added to a 500 ml SILAC medium bottle. To achieve sufficient incorporation of SILAC medium and heavy amino acids, cells were passaged at least 5-7 times. The labeling efficiency of all experiments was confirmed by mass spectrometry to be more than 95%. Cells were cultivated under standard growth conditions in a humidified chamber of 37 °C and 5% CO2. Cells were first grown in 75-cm flasks and later seeded to 10-cm dishes. For co-immunoprecipitation experiments, a total of five dishes were plated for each labeling state. When reaching confluency, the cells were harvested for the Co-IP, as will be explained later. By applying a switch to the specific labeling scheme, the 3 cell lines compared in the current study were labeled as explained below in the table below.

Table 2. SILAC experiment labeling scheme.

	L (R0K0) M (R6K4) H (R10K8)
Labeling State 1 (Forward Condition)	1. GFP(L) WT aSyn(M) A30P aSyn(H)
Labeling State 2 (Reverse Condition)	2. A30P(L) GFP(M) WT aSyn(H)

2.4 Molecular biology and biochemistry techniques

2.4.1 Isolation of synaptic vesicles

Synaptic vesicles were prepared from the whole brains of 8–12-week-old mice according to previously established protocols (Hell & Jahn, 2006). Briefly, animals were sacrificed by cervical dislocation followed by head decapitation. After dissection, brains were transferred to a 50-ml conical tube containing an ice-cold homogenization buffer of 0.32 M sucrose, 4 mM 4-(2-hydroxyethyl)-1-piperazineethanesulfonic acid (HEPES), pH 7.4, and the following preparation steps were done at 4 °C. 8 to 10 mouse brains were used for each individual experiment. The collected brains were homogenized in a 5-ml glass-Teflon homogenizer at 900 rpm for nine strokes in the presence of protease inhibitors: 200 mM phenylmethylsulfonyl fluoride (PMSF), 1 mg/mL pepstatin A in DMSO, both diluted 1/1000. After centrifuging brain homogenate (BH) at 1000 g for 10 minutes, the supernatant (S1) was collected, and the resulting pellet (P1) was left behind. The S1 fraction was spun at 12,000 g for 15 minutes to obtain the pellet (P2) that consists mainly of synaptosomes, while the supernatant (S2) was discarded. While avoiding the dark brown portion at the bottom part of the pellet, which is mainly made up of mitochondria, the whitish part of the P2 was gently resuspended in homogenization buffer and centrifuged again at 13,000 g to obtain the crude synaptosomes (P2') pelelt that was reconstituted in the homogenization buffer. The release of synaptic vesicles from intact synaptosomes was achieved by the addition of 9 volumes of ice-cold water to the resuspended P2', and 100 μL of 1M HEPES, pH 7.4. The synaptosomes were then transferred to a 5-ml glass-Teflon homogenizer and homogenized for 3 strokes at 900 rpm. The lysed P2' was centrifuged at 33,000 g for 20 minutes to obtain the supernatant (LS1) and the pellet (LP1). The LS1 fraction was transferred immediately to a capped ultracentrifuge tube without disturbing the LP1 fraction. The LS1 was subjected to ultracentrifugation for 2 hours at 260,000 g for pelleting the synaptic vesicles (LP2), and the supernatant (LS2) that contains synaptic cytosol was discarded. The LP2 was resuspended in PBS with the addition of protease inhibitors and homogenized in a 1 ml glass-Teflon homogenizer.

Using a 23- and 27-gauge hypodermic needle connected to a 2-ml syringe, the homogenized LP2 was consecutively sheared with gentle trituration. The final synaptic vesicles LP2 suspension was then aliquoted and stored at −80 °C until use for the next steps. For checking the enrichment of synaptic vesicles through all differential centrifugation steps, aliquots from each collected or discarded fraction were saved for the determination of protein concentration using the bicinchoninic acid (BCA) protein assay (Thermo Fisher Scientific, MA, USA).

2.4.2 Identification of aSyn interactome

2.4.2.1 Identification of aSyn general interacting partners using SILAC proteomics

To identify the general interactomes of WT aSyn and A30P aSyn, we conducted SILAC experiments in HEK293 cells. As mentioned before, for labeled cells, we conducted two biological replicates. In the first SILAC experiment, or forward condition, cells overexpressing GFP were grown in *light* SILAC medium, cells overexpressing WT aSyn were grown in *medium* SILAC medium, and cells overexpressing A30P aSyn were maintained in *heavy* SILAC medium. In the reverse condition, this labeling system was switched in the following order: A30P(L)-GFP(M)-WT(H).

For co-immunoprecipitation experiments, a total of five 10-cm dishes were plated for each cell line in both labeling states. When reaching confluency, the cells were prepared for Co-IP. The cell culture medium was aspirated from culture dishes, and the cells were rinsed once with ice-cold PBS. 2 ml of ice-cold PBS was added to each 10 cm dish, and the cells were then harvested on ice using a cell scraper. The cell suspension was then transferred to a 15-ml falcon tube and centrifuged at 220 g for 5 minutes. The cells pellet was resuspended in the lysis buffer 10 mM HEPES (Carl Roth, Germany), pH 7.4, 10 mM KCl, 100 mM NaCl, 0.05% (v/v) Nonidet P-40 (Fluka Analytical, Germany), 1x Protease and phosphatase inhibitors (cOmplete™ protease inhibitor and PhosSTOP™ phosphatase inhibitor; Roche, Basel, Switzerland), and incubated on ice for 30 min to ensure complete cell lysis. The cell lysate was then

centrifuged for 10 min at 17000g to pellet cellular fragments and debris. The supernatants were collected carefully and transferred to new tubes. Protein concentration for '*light* labeled', '*medium* labeled', and '*heavy* labeled' cell lysates for both forward and reverse labeling states was measured using the Bradford protein assay (Bio-Rad, CA, USA).

The Co-IP experiments were performed immediately using Dynabeads Co-Immunoprecipitation Kit (InvitrogenTM, Waltham, MA, USA) according to the manufacturer's recommendations and as previously described (Lagundžin et al., 2022). Kit components include 2.8 μm Dynabeads™ M-270 Epoxy beads, Buffers C1, C2, HB, LB, and SB. Briefly, the process of antibody-coupling to the beads was performed one day prior to harvesting cell lysates. For each sample, 5 mg of Dynabeads™ M-270 Epoxy was weighed out, transferred into a 1.5 ml Eppendorf tube and washed with 1 ml of C1 buffer by pipetting up and down. To separate the washed beads, the tubes were placed on a magnet rack (DynaMagTM-2 Magnet, Invitrogen™), where they get accumulated on the tube wall attaching the magnet side. The supernatant is discarded carefully without disturbing the beads, and the beads are then removed from the magnet. 120 μL (30 μg) of anti-human aSyn monoclonal antibody SYN211 (Santa Cruz Biotechnology, USA) was added to each 5 mg washed beads. The washed beads were mixed with SYN211 antibody after the addition of 130 μL of C1 to get a final volume of 250 μL. An equal volume (250 μL) of C2 buffer was added to the tube, and the beads were mixed by pipetting. The tubes containing the beads were left incubated on a mixing rotator (Stuart SB3, UK) overnight at 37 °C. The next day, the tubes were placed on the magnet for one minute to collect the conjugated beads, and the supernatant was removed. The beads were then subjected to one wash with buffer HB while pipetting up and down gently. After being placed on the magnet for one minute and discarding the supernatant, the beads were removed and washed with 800 μL of buffer LB. Following removal from the magnet, the beads were given two quick washes with 800 μL of buffer SB each, and then a long wash with the same buffer was performed by incubating the beads on a mixing rotator at ambient

temperature for 15 minutes. The tubes were placed on the magnetic rack for 1 minute and removed from the magnet after carefully discarding the supernatant. The antibody-coupled beads were then resuspended in 0.1% (w/v) bovine serum albumin (BSA) in PBS, and the mixture was incubated for 5 minutes at room temperature on the rotator. The tubes were again placed on the magnet for one minute and the supernatant was removed. The antibody-covalently coated beads were then redissolved in SB buffer and used immediately for the subsequent Co-IP steps. For pull-down assays of SIALC experiments, 5 mg of antibody-conjugated beads were transferred to a new tube with the addition of the appropriate volume of each cell lysate comparison group, corresponding to 2 mg of total proteins. The resulting mixtures were incubated overnight at 4 °C with an orbital rotator after taking aliquots as inputs. The next day, the tubes were placed on the magnetic rack for 1 minute, and the depleted (unbound) supernatant was carefully removed to avoid disturbing the Co-IP complex. The beads were removed from the magnet and resuspended gently with washing buffer A (10 mM HEPES, pH 7.4, 10 mM KCl, 50 mM NaCl, 1 mM $MgCl_2$, 0.05% (v/v) Nonidet P-40). The beads were collected again on the magnet, and two extra washing steps with washing buffer A were performed. Washing buffer B (10 mM HEPES pH 7.4, 10 mM KCl, 1 mM $MgCl_2$, 0.07% (v/v) Nonidet P-40) was then added, and the beads were incubated on a rotator for 5 min at ambient temperature. The beads were then collected on the tube wall using the magnet, and the supernatant was removed. To release the protein complex from the antibody-coupled beads, the beads were resuspended with 500 μL of high pH sample elution buffer (0.5 M NH40H, pH 11.0, 0.5 mM EDTA (Lonza AccuGENE, Basel, Switzerland)) and left incubated on the rotator for 15 minutes. The beads were placed on the magnet, and the supernatant containing the elute was collected and transferred to a new tube. The elution step was repeated to ensure the complete release of the protein complex from the antibody-conjugated beads. The second elute was combined with the previous one. Finally, the protein complex elutes from the different SILAC comparison groups were lyophilized and reconstituted later in 60 μL. 10 μL of each sample was used for protein

concentration determination, and the validation of Co-IP protocol. The remaining volumes were kept at −80 °C until sample preparation for mass spectrometric analysis.

2.4.2.2 Identification of aSyn-interacting partners in synaptic vesicles

Co-IP experiments were performed to identify aSyn interactors using synaptic vesicles from WT mice. Mouse monoclonal antibody SYN-1 (BD) was used to pull down aSyn and its potential interacting complex. We conducted in parallel mouse monoclonal IGg1 antibody as a negative control. To achieve this, 30 μg of each antibody was coupled to 5 mg Dynabeads™ M-270 Epoxy for each comparison state. The antibodies coupling process was conducted exactly as described before for SILAC Co-IP experiments. The following day, the SYN1-conjugated beads were incubated with a total of 600 μg of synaptic vesicles obtained from WT animals for pull-down experiments, and the same was true for the IGg1-coupled beads. The Co-IPs were done in a similar way to the SILAC ones described above, with some modifications. First, synaptic vesicles were directly coupled to the beads in their original buffer, PBS, without the addition of any lysis buffer. At the end of Co-IP, the protein complexes were eluted from the antibody-conjugated beads, lyophilized, and resuspended in 60 μL PBS. 10 μL aliquot was used for checking Co-IP with western blot, and the remaining volume was kept at −80 °C until used for mass spectrometric analysis.

2.4.2.3 Mass spectrometric analysis for SILAC

Collaborating with Dr. Christof Lenz and Prof. Dr. Henning Urlaub from the Core Facility Proteomics of University Medical Center Göttingen, mass spectrometry analysis work was conducted according to (Atanassov & Urlaub, 2013). Briefly, for running analysis, equal amounts of light, medium, and heavy protein complex elutes obtained from the Co-IP experiments were combined at a 1:1:1 ratio for each forward or reverse condition. The replicates of the two samples were then mixed with 4X NuPAGE LDS sample buffer (Invitrogen), boiled for 5 minutes at 95 °C, and separated

on 4–12% NuPAGE Novex Bis-Tris gels. After Coomassie staining, gel lanes were divided into 12 slices and subjected to in-gel trypsin digestion. The resulting peptides mixtures were prepared for nanoLC-MS/MS analysis after being extracted, dried, and reconstituted in 2% acetonitrile/0.1% formic acid. Reversed phase-C18 columns were used to enrich and separate samples. Using a Q Exactive mass spectrometer (ThermoFisher Scientific, Dreieich, Germany), the eluent was analyzed employing the data-dependent acquisition (DDA) approach. The top 12 peptide precursors were isolated, fragmented, and recorded. Two technical replicates were performed for each sample. The processing of raw data was performed using MaxQuant Software version 2.0.1 (Max Planck Institute for Biochemistry, Martinsried, Germany), and protein identification was run against UniProtKB human reference proteome v1.2021 with default parameters, aiming for a 1% false discovery rate (FDR). Using SILAC options, relative protein quantification was performed with the utilization of the "re-quantify" option. A minimum of 2 quantitation events was considered, and SILAC ratios were normalized. The relative protein quantitation data from the MaxQuant Software results were imported into Perseus software version 1.6.15.0 (Max Planck Institute for Biochemistry, Martinsried, Germany) for statistical analysis. Statistical evaluation included the removal of reverse/contaminant hits, log2 conversion and sign correction of SIALC ratios, and significance B testing (Cox & Mann, 2008).

2.4.2.4 Mass spectrometry analysis for Co-IP from SVs

Mass spectrometric analyses were performed by the Core Facility Proteomics at the University Medical Center Göttingen. Samples were mixed with 5x sample buffer and separated on NuPAGE 4–12% Bis-Tris gels (Invitrogen) by running them a distance of 1 cm. After being stained with Coomassie, each sample was cut into one intact piece. Samples were then digested in-gel with trypsin and prepared for nanoLC-MS/MS analysis as described before in SILAC proteomics (Atanassov & Urlaub, 2013). Unlike the SILAC samples, data-independent acquisition (DIA) was employed on the Q Exactive mass spectrometer (ThermoFisher Scientific, Dreieich, Germany) (Muntel et al., 2019). Three technical replicates were performed for every sample. For data

processing, Spectronaut Software v16 (Biognosys, Schlieren, Switzerland) was used for protein identification, the construction of a spectral library, and DIA peak integration (Bruderer et al., 2015). Using the default specifications of the built-in Pulsar algorithm, peptides and proteins were identified against the UniProtKB mouse reference proteome (revision 01-2021) with a 1% FDR. DIA peak integration was carried out following the default parameters of Spectronaut software, and the extraction of peak areas based on the spectral library was performed at 1% FDR. Finally, statistical evaluation was done for the summed peak areas at the peptide and protein levels per replicate.

2.4.3 Preparation of cells lysates from hippocampal neurons and immunoblotting

2.4.3.1 Preparation of cell lysates

After treatment with different aSyn species, the neuronal medium was aspirated, and the cells were rinsed twice with ice-cold PBS. After removing PBS, the cells were incubated on ice with either radioimmunoprecipitation assay (RIPA) buffer (50 mM Tris, pH 8.0, 0.15 M NaCl, 0.1% SDS, 1.0% NP-40, 0.5% Na-Deoxycholate, 2 mM EDTA) or 2% SDS in TBS (50 mM Tris, 150 mM NaCl, pH 7.5). Protease and phosphatase inhibitors (cOmplete™ protease inhibitor and PhosSTOP™ phosphatase inhibitors; Roche, Basel, Switzerland) were added freshly to both lysis buffers. For RIPA, the cells were detached from the plate surfaces by scraping them, and then transferring the harvested cells to an Eppendorf tube. The cell lysate was placed on ice for 30 minutes to ensure complete cell lysis. After centrifugation at 4 °C, the supernatant was collected carefully, while the pelleted part containing cellular debris was discarded. Cell lysed in 2% SDS were transferred to tubes and boiled for 10 minutes at 95 °C. The total protein concentration for cell lysate was determined using the Bradford protein assay (Bio-Rad, CA, USA).

2.4.3.2 Immunoblotting

SDS-PAGE was used to separate proteins loaded into the gels according to their size (Laemmli, 1970). Based on the molecular weight of interest, separating gels with 12 or 15% acrylamide and 7.5 % stacking gel were prepared and cast into the gel assembly apparatus to prepare self-made gels. Additionally, 4-15% precast gradient polyacrylamide gels were used in some experiments. To run samples in SDS-PAGE, 30 µg of total protein from different samples were denatured by getting mixed with 5X sample loading buffer and heated for 5 min at 95 °C. Then, a pre-stained protein ladder and samples were loaded into the gel. The gel was run initially at a constant low voltage of 80 V for 15 minutes and then at 120 V until the sample loading buffer migrated to the bottom of the gel.

After SDS-PAGE, protein bands were transferred onto nitrocellulose (IB23001X3, Thermo Fisher Scientific, MA, USA) membranes for western blotting. The transfer process was carried out for 7 min at constant 20 V using the iBlot2 Transfer system (IB21001, Thermo Fisher Scientific, MA, USA). Before proceeding with immunodetection, membranes were stained with the reversible stain Ponceau S (Carl Roth, Karlsruhe, Germany) for 1-2 minutes to quickly check the quality of protein transfer. The membranes were destained in distilled water.

For immunoblotting, the membranes were blocked for 1 hour at ambient temperature with blocking buffer (5 % skim milk (70166, Fluka Analytical, Germany) in TBST. The membranes were then left incubated in primary antibodies of interest overnight at 4°C (table) diluted in blocking buffer. The next morning, the membranes were subjected to 3 TBST washes for 10 min each, followed by incubation at room temperature for 1 hour with either HRP-conjugated or LICOR-specific secondary antibodies diluted in blocking buffers (Table 3). After 3 washes in TBST, proteins bands of interest were detected by either shortly incubating the membranes with Immobilon Western Chemiluminescent HRP Substrate (WBKLS0500, Millipore, MA, USA) followed by observation in the chemiluminescence imaging system (Fusion FX, Vilber Lourmat, Marne-la-Vallée, France) or Odyssey® Infrared Imaging System for LICOR

secondary antibodies. Variations in protein expression levels among different treatment groups were analyzed and quantified by performing densitometry calculations in Fiji software (Schindelin et al. 2012).

2.4.4 Labeling of live primary hippocampal neurons with Synaptotagmin 1 antibody

To check the amount of SV recycling, we incubated living hippocampal neurons exposed to different aSyn species as described above with the antibody directed against the luminal domain of synaptotagmin 1 SYTG1 (Synaptic Systems, Göttingen, Germany). The cells were incubated in the culture medium with the antibody at a dilution of 1:120 for 1 hour. The media was then aspirated from all the wells, and the cells were washed two times with PBS and fixed immediately with 4% paraformaldehyde (PFA) for the next immunocytochemistry steps in order to analyze the uptake of SYTG1 antibody, which is an indirect measure of synaptic vesicles recycling (Truckenbrodt et al., 2018).

2.4.5 Immunocytochemistry

At the end of treatment with different aSyn species, hippocampal neurons plated on coverslips were first washed two times with PBS and fixed for 20 minutes in 4% PFA at room temperature. Following washing the fixative with PBS three times, the cells were then got permeabilized for 10 minutes with 0.1% Triton X-100 (Sigma-Aldrich, MO, USA) in PBS. To prevent non-specific binding, cells were blocked with 3% bovine serum albumin (BSA) in 1x PBS at room temperature for one hour and then incubated overnight with primary antibodies (Table 3) diluted in the blocking buffer. The next day, the cells were incubated with secondary antibodies (Table 3) diluted in the blocking buffer for two hours after being washed three times with PBS. Cells were then washed once with PBS, and DAPI (Carl Roth, Karlsruhe, Germany) was used to counterstain nuclei. After three PBS washes, the coverslips were finally mounted on

glass slides using mowiol. Mounted coverslips were left overnight at room temperature to get dry for microscopic imaging.

Table 3. List of antibodies used in this study.

Primary Antibodies used in this study					
Antibody	Species	Company	Cat- Nr	WB dilution	ICC dilution
alpha Synuclein	mouse	BD	610787		1:1000
alpha Synuclein phospho S129	rabbit	Abcam	ab51253	1:1000	1:1000
alpha Synuclein	rabbit	Abcam	ab138501		1:1000
FluoTag-X2 anti-PSD95 Atto 656	mouse	NanoTag Biotechnologies	N3702-AT565-L		1:500
MAP2	rabbit	Proteintech	17490-1-AP		1:1000
MAP2	mouse	Abcam	ab92434		1:1000
PSD 95	mouse	Synaptic System	124 011	1:1000	
SNAP-25	rabbit	Synaptic System	111002	1:1000	
Synapsin I	rabbit	Abcam	ab254349	1:1000	
Synaptobrevin 2 (VAMP 2)	rabbit	Synaptic System	104 202	1:1000	
Synaptophysin	mouse	Sigma	S5768	1:1000	
Synaptotagmin 1 cytoplasmic tail	rabbit	Synaptic System	105 008	1:1000	
Synaptotagmin 1 lumenal domain	rabbit	Synaptic System	105103		1:120
β-actin	mouse	Sigma	A5441	1:5000	
Secondary antibodies Immunofluorescence					
Alexa Fluor 488 Anti-mouse IgG	Donkey	Invitrogen	A21202	1:1000	
Alexa Fluor 488 Anti-rabbit IgG HCA	Donkey	Invitrogen	A-21206		1:1000
Alexa Fluor 555 Anti-Mouse IgG	Donkey	Invitrogen	A31570		1:1000
Alexa Fluor 555 Anti-Rabbit IgG	Donkey	Invitrogen	A31572		1:1000
Atto 647 antibody Anti-Rabbit IgG	Goat	Sigma	40839		1:1000
Secondary antibodies for Western blot					

HRP conjugated anti-mouse IgG	sheep	Amersham	NXA931	1:10000	
HRP conjugated anti-rabbit IgG	donkey	Amersham	NA934V	1:10000	
IRDye 680LT Anti-Mouse IgG	Donkey	LI-COR	926-68022	1:20000	
IRDye 680LT Anti-Rabbit IgG	Donkey	LI-COR	926-68023	1:20000	
IRDye 800 CW Anti-Rabbit IgG	Donkey	LI-COR	926-32213	1:15000	
IRDye 800CW Anti-Mouse IgG	Donkey	LI-COR	926-32212	1:15000	

2.4.6 Microscopic imaging

Treated cells were imaged on a confocal laser scanning microscope (LSM 900, Carl Zeiss Microscopy, Germany) using a63x oil objective or a 20x objectiv and a pinhole of 1 Airy unit. Z-stacked images were acquired for some experiments. The same exposure time was applied to acquire images of different conditions. To obtain images of super-resolution quality for cells stained with synaptic proteins, the Airyscan detector equipped on the Carl Zeiss LSM 900 microscope was used. Images were analyzed with Zen blue software and Fiji software (Carl Zeiss Microscopy, Germany). Analysis of pre- and post-synaptic puncta was performed using the SynQuant plug-in in Fiji (Y. Wang et al., 2020).

2.4.7 Toxilight assay

To check cytotoxicity among different treatment groups, we employed the ToxiLight assay kit (Lonza, Basel, Switzerland) following the manufacturer's instructions. In this assay, the levels of adenylate kinase (AK) released from damaged cells into cells medium are measured. 20 μL in triplicates of cells medium collected at DIV 26 was pipetted into a luminescence 96-well plate, and incubated with 100 μL of

AK for 5 min. The luminescence intensity was then measured using TECAN plate reader (Infinite 200® PRO, TECAN, Switzerland).

2.5 Statistical analysis

Statistical analysis was performed from at least 3 independent biological replicates for all different experiments. We used GraphPad Prism 9 software (GraphPad, CA, USA) to analyze different data. A one-way analysis of variance (ANOVA) followed by Dunnet's post-hoc test was used to compare groups. Data were expressed as mean ± SEM and were deemed significant with a p value less than 0.05.

3. Results

3.1 Preparation and characterization of different exogenous aSyn species

In order to study the effect of different forms of aSyn on synaptic function, aSyn monomers (M), oligomers (O), and PFFs were produced and characterized using different techniques. The preparation of aSyn oligomers includes incubating monomeric protein for 5 hours with agitation at 37. During this period, 1-5% monomeric aSyn population will be converted to oligomers. The preparation was then applied to the size exclusion column to separate oligomers from monomers. Oligomers usually elute at the void volume peak around 120 ml elution volume. This retention volume corresponds to a molecular weight above 500 kDa using gel filtration standards (Figure. 6A and B). Results obtained from native gel further support this observation, as the oligomeric sample remained in the native gel pocket and did not migrate (Figure. 6C). The different aSyn species used in the current study were characterized by the sedimentation assay in order to make sure of the solubility status of each preparation. As expected, we observed more aSyn in the pellet than the supernatant fraction for PFFs preparation, and the opposite for monomeric and oligomer preparations that are soluble (Figure. 5D). Immunoblotting and dot blotting further confirmed the presence of higher molecular weight species in oligomers and PFFs (Figure. 6E and F). ThT is a fluorescent dye that has a higher affinity for β-sheet enriched structures, and therefore, the ThT assay is used as a quality control to check the successful conversion of monomeric aSyn into amyloid structures. As expected, higher ThT fluorescence was detected in PFFs species, with modest fluorescence in oligomeric preparation compared to monomeric aSyn (Figure. 6G). Finally, we performed EM to check the morphological and structural properties of the different species. EM analysis showed a heterogenous population of oligomers with regards to size and shape, while no detected species for aSyn monomeric preparation as expected. EM images of PFFs revealed twisted and straight fibrils identical to those described in the literature (Figure. 6H).

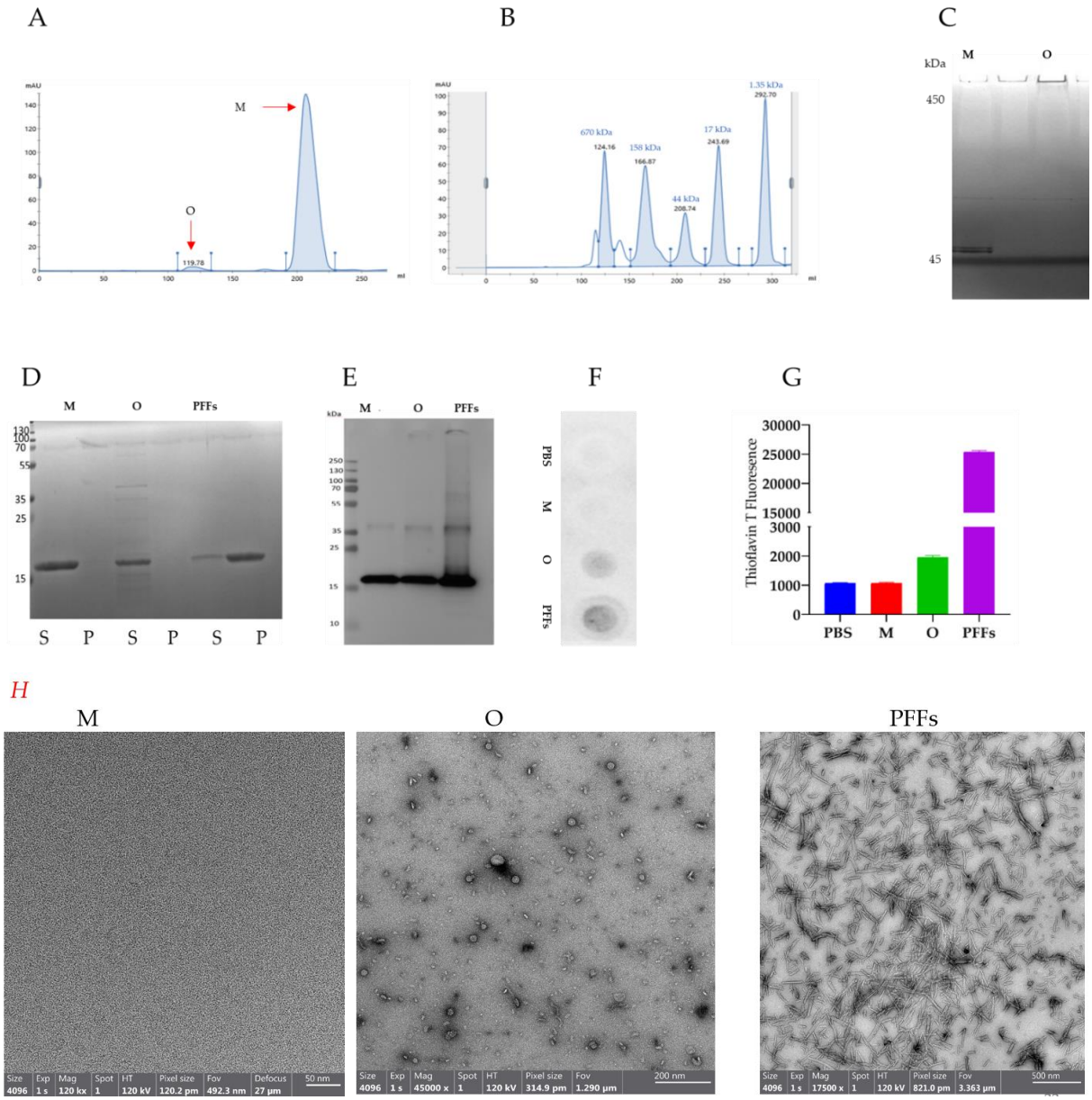

Figure 6. Characterization of different aSyn species. A. Gel filtration chromatogram for purification of aSyn oligomers (O). **B.** Gel filtration chromatogram for Calibration Kit proteins Thyroglobulin 670 kDa, gamma-globulin 158 kDa, Ovalbumin 44 kDa, Myoglobin 17 kDa, Vitamin B12 1.35 kDa. **C.** Native gel for aSyn monomers (M) and oligomers (O). **D.** Sedimentation assay for aSyn M, O, and PFFs. Images from Coomassie stained gel where S refers to the supernatant and P to the pellet fraction. **E.** immunoblot for aSyn M, O, and PFFs. **F.** Dot blot for aSyn M, O, and PFFs. ThT assay for PBS,M, O, and PFFs. **H.** EM images for aSyn M, O, and PFFs.

3.2 The effects of different aSyn at the synapse

To study if different aSyn species can impact synaptic function in different ways, I used the primary mouse hippocampal neurons model. Neuronal cultures were

left to grow until DIV 7, when the cells were treated with different aSyn species. The cultures were maintained until DIV 21 for certain tests or DIV 26 for other tests (Figure. 7). To gain comprehensive insights into the various synaptic alterations that could result from some species, I employed several assays to address these potential alterations.

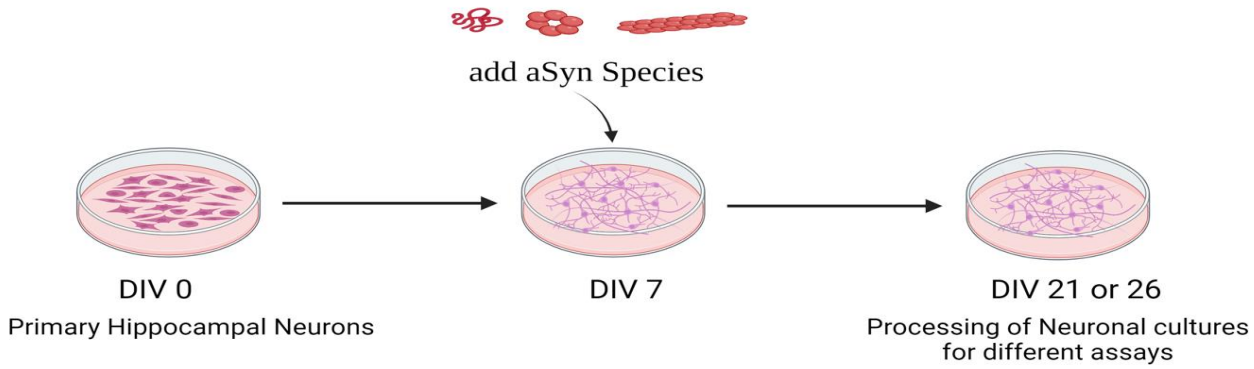

Figure 7. Schematic of experiments on the hippocampal primary neuronal culture treatments with different aSyn species. Neuronal cultures were plated, and the day of plating was considered DIV 0. Neurons were exposed to different aSyn species (aSyn monomers, oligomers, and PFFs) at DIV 07 for most assays. Different assays for neuronal cultures were conducted at DIV21 or DIV 26. Figure was created with Biorender.com

3.2.1 Cytotoxicity assays

To investigate which aSyn species have toxic effects on neuronal cells, the ToxiLight assay was conducted. This assay is based on checking cell membrane integrity by measuring the levels of adenylate kinase (AK) released from compromised cell membranes into the culture medium. Therefore, the cytotoxic effects of various aSyn species were tested on DIV 26, which corresponds to 20 days after the treatment. Cells exposed to aSyn PFFs exhibited significant toxicity, whereas monomeric and oligomeric species were similar to those observed in control cells treated with vehicle PBS (Figure. 8C). Furthermore, MAP2 immunostaining showed a notable decline in MAP2 fluorescence intensity, suggesting enhanced neuronal and synaptic toxicity as MAP2 is a neuronal protein that is a typical marker of dendrites (Figure. 8A and B).

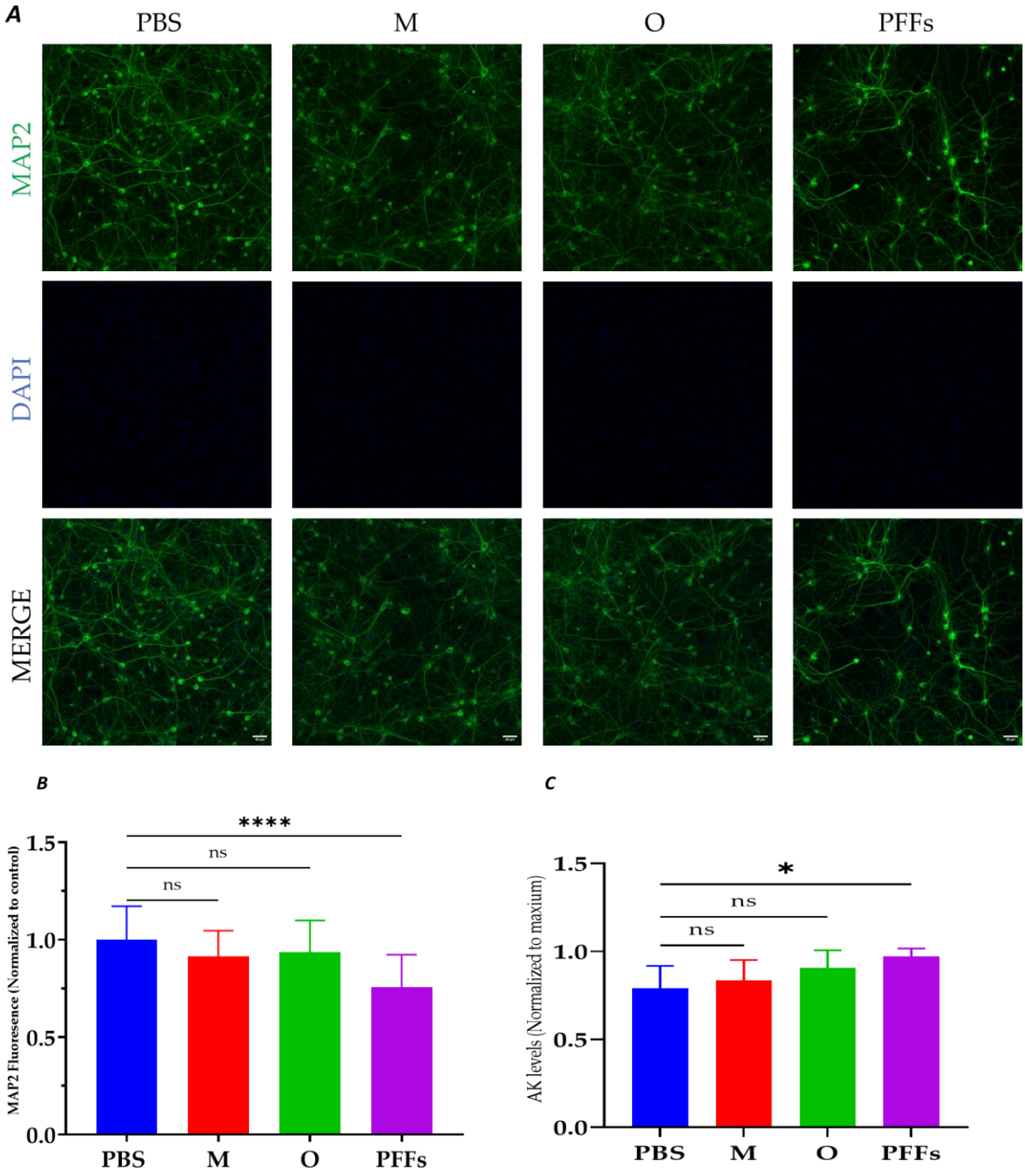

Figure 8. PFFs species are more cytotoxic to hippocampal neurons. A. Representatives confocal images for mouse hippocampal neurons exposed to different aSyn species at DIV 7 and immunostained with MAP2 at DIV 26. Cells were counterstained with DAPI. Scale bar equals 40 μm **B.** Quantification of MAP2 fluorescence intensity from **A** normalized to PBS mean value (n = 3). C. Toxlight cytotoxicity assay for treated cells with different species represented by the levels of adenylate kinase (AK). AK levels were normalized to maximum value. All data are expressed as mean ± SD. * p-value < 0.05, ** p-value < 0.01, *** p-value <0.001, **** p-value <0.0001.

3.2.2 Investigating the seeding efficiency of different species

The pathology and toxicity associated with aSyn have been largely linked to its aggregation and the potential of these aggregates to further enhance more incorporation of endogenous monomeric aSyn, a process that is called seeding. In my study, I am using aSyn PFFs, which are known for their seeding efficiency, and oligomers that contain a wide range of higher molecular weight species, some of which can have seeding potential. I am trying to investigate the differences in the seeding activity of the different species I prepared and to see if such differences can be associated with different effects on the synaptic function in mouse hippocampal neurons treated with these species. Hippocampal neuronal cultures were treated with aSyn monomers, oligomers, and PFFs as described before. The aggregation of endogenous aSyn as well as the phosphorylation of aSyn at serine 129, were checked. pS129 is the main PTM that is encountered in LB and is usually a pathological marker for endogenous aSyn aggregation. Aggregation of endogenous mouse aSyn and the appearance of pS129 were detected mainly in neurons exposed to PFFs, suggesting the more seeding capacity for PFFs compared with other species (Figure. 9A). Immunostaining of cultured cells revealed that PFFs induced the formation of aSyn inclusions with high levels of pS129 immunofluorescence within these inclusions compared with other treatment groups. Higher molecular weight bands of aSyn with the detection of pS129 were also detected in immunoblots, further confirming our observations (Figure. 9B). These data indicate PFFs species have higher seeding efficiency than oligomers.

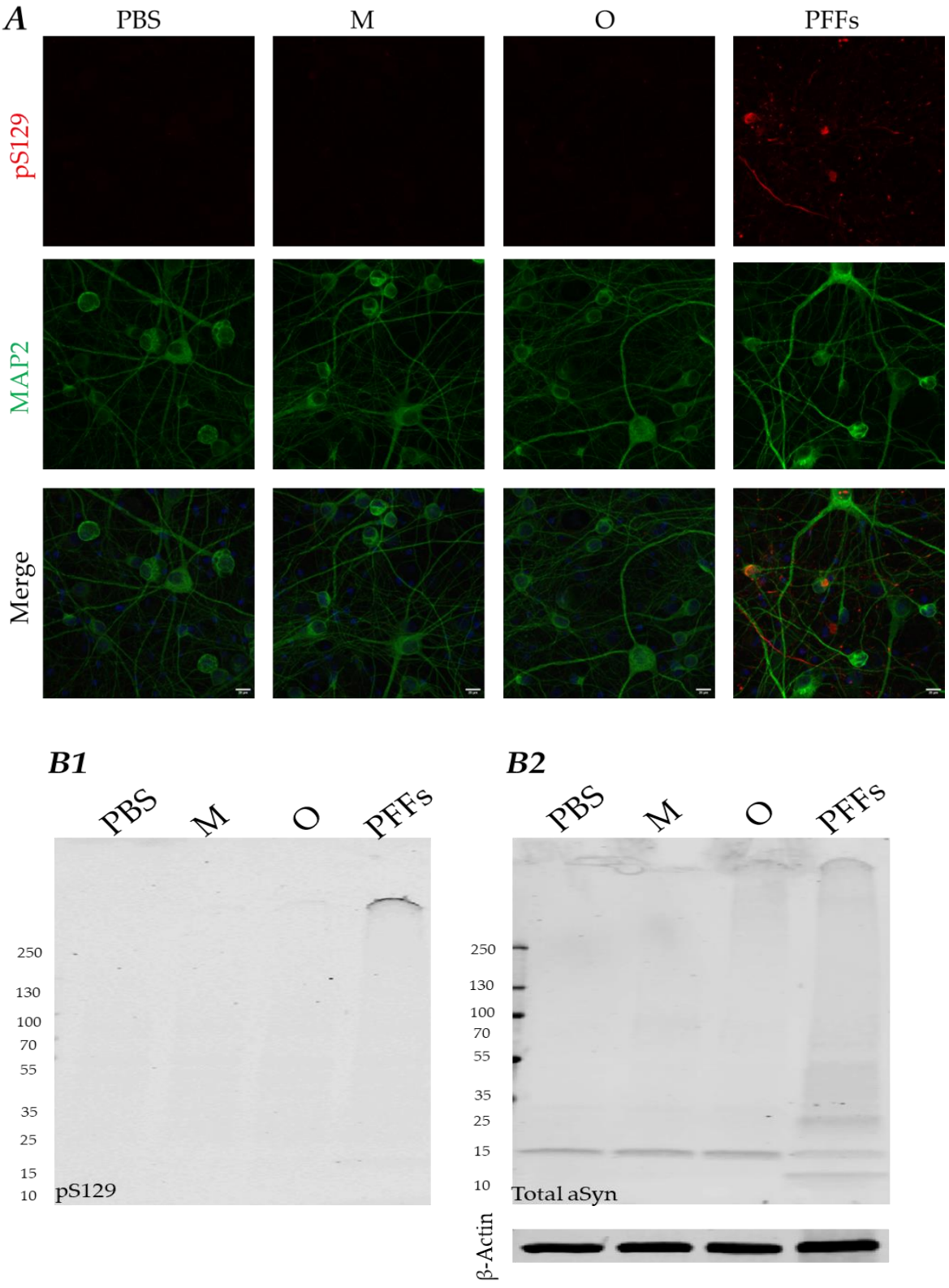

Figure 9. PFFs seed the aggregation of endogenous aSyn. A. Representative confocal images for mouse hippocampal neurons exposed to different aSyn species at DIV 7 and immunostained with MAP2, and pS129 at DIV 26. Cells were counterstained with DAPI. Scale bar equals 20 μm. **B.** Representative immunoblot probed with pS129 antibody (upper) and total aSy antibody (lower). β-actin was used as a loading control.

3.2.3 The impact of different aSyn species on synaptic proteins levels

After assessing the differences in seeding potential between aSyn monomers, oligomers, and PFFs, I aimed to study the effects of the different species on synaptic proteins at the biochemical level. Given that changes in synaptic protein levels are associated with modulating the synapse physiology and pathology, I measured the biochemical levels of some pre- and postsynaptic proteins at two time points, specifically DIV 21 and DIV 26. At DIV 21, no alterations in the levels of presynaptic proteins VAMP2, SNAP25, and synaptotagmin 1 (SYTG 1) or postsynaptic protein PSD95 were observed (Figure. 10A and B). Quantification of the levels of these proteins from immunoblots showed no significant reduction.

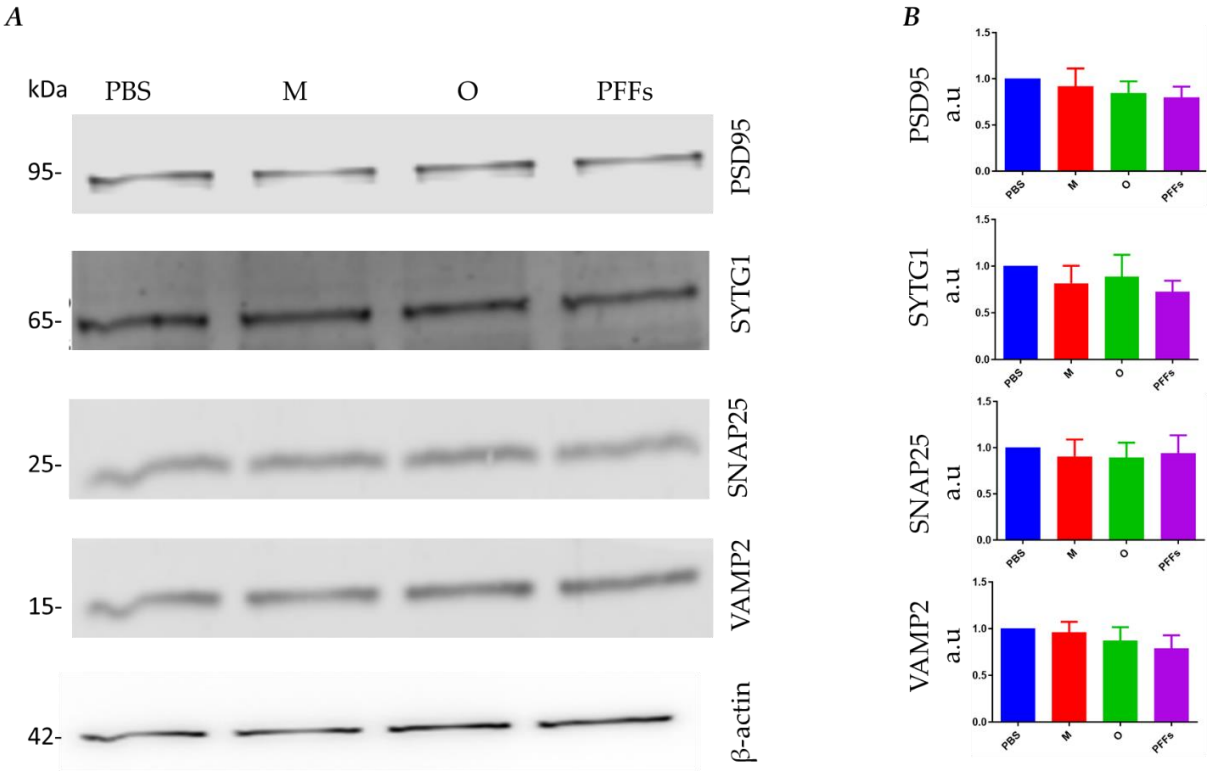

Figure 10. Different treatments at DIV 21 have no impact on the biochemical levels of different synaptic proteins. A. Representative immunoblots of different synaptic proteins. Mouse hippocampal neurons were treated at DIV 7. **B.** Quantification of the biochemical levels of the relevant proteins. β-actin was used as a loading control. a.u., arbitrary unit.

This means that at this time point, these different preparations have no effect, or the effect is not yet pronounced enough to be detected biochemically. In order to check

this, I checked the expression levels of the different tested synaptic neurons at a later time point when the neurons get older. Interestingly, a substantial reduction in levels of VAMP2 and PSD95 was noticed at DIV 26. When quantifying the levels from immunoblotting, this effect was mainly found in hippocampal cultures exposed to PFFs (Figure. 11A and B). In this study, the decrease in synaptic protein levels seems to be more pronounced with exposure to PFFs species, and PFFs effects are more harmful at the synapse in a time-dependent manner, where ultimately their toxic effect leads to synaptic dysfunction.

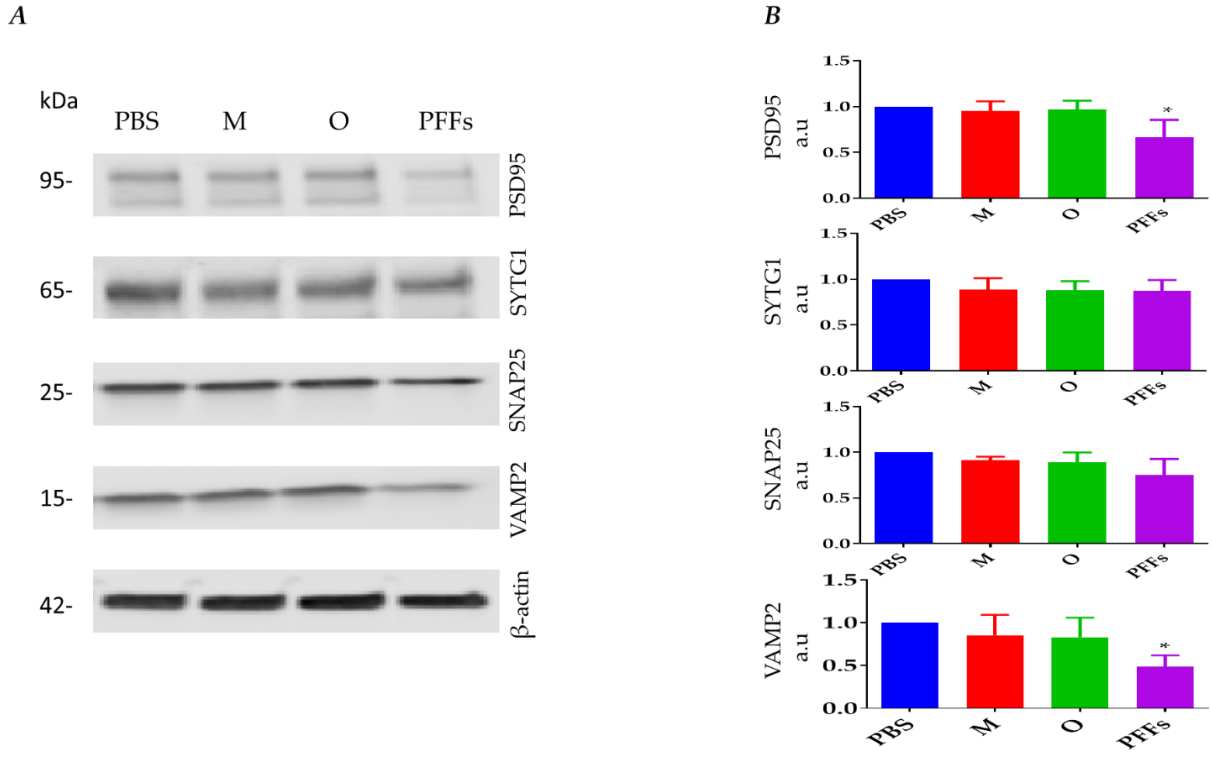

Figure 11. PFFs treated neurons show lower levels of PDD95 and VAMP2 at DIV26. **A.** Representative immunoblots different synaptic proteins. Mouse hippocampal neurons were treated as DIV 7. **B.** Quantification of the biochemical levels of the relevant proteins. β-actin was used as a loading control. a.u., arbitrary unit. All data are expressed as mean ± SD. * p-value < 0.05, ** p-value < 0.01, *** p-value <0.001, **** p-value <0.0001.

3.2.4 The role of different aSyn species in modulating neuronal activity

Changes in the levels of synaptic proteins in mouse hippocampal neurons were not readily observable post-treatment with different aSyn species at DIV 21 as shown

before. Consequently, we wanted to explore if we could detect any earlier functional changes at the synapse prior to the reduction in the synaptic protein pool. To examine this, we conducted MEA experiments to check the spontaneous neuronal activity. Hippocampal neurons were cultured in multi-well MEA plates equipped with electrodes for measuring neuronal firing. Basal neuronal activity was recorded before the cells were treated with the different aSyn species at DIV 14, and then DIV 20 posttreatment. We observed significant differences between different aSyn preparations on neurons spontaneous firing. A large drop in neuronal mean firing rate is already observed at DIV 20 for cells exposed to PFFs species (Figure. 12). However, busting activity of neurons was comparable among different groups. There was no significant difference in the frequency and duration of bursting. This data suggest that exposure to PFFs impact overall neuronal or spiking activity at this time point.

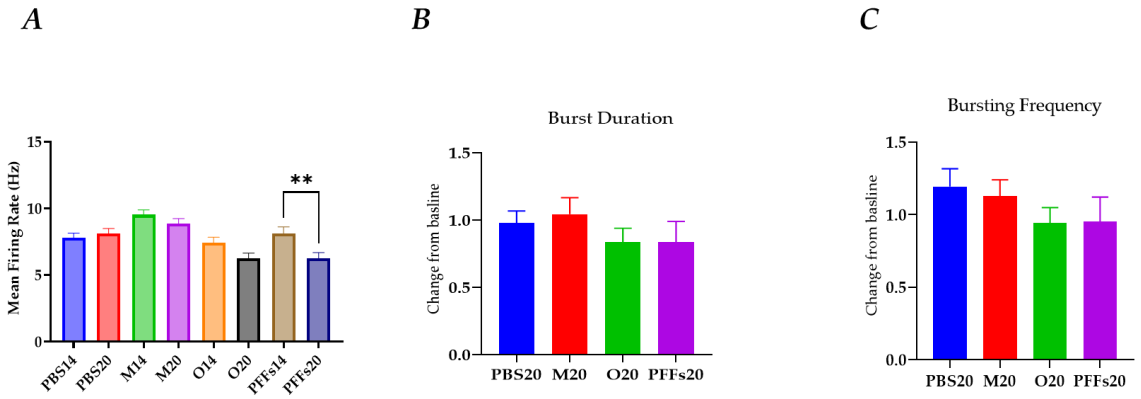

Figure 12. Exposure to PFFs leads to reduced overall neuronal activity. Data were obtained from recording spontaneous neuronal activity using MEA experiments. A. Mean firing rate in Hz for neuronal cultures exposed to different treatments. Recordings were done at DIV 14 prior to different treatments and then at DIV 20. **B.** Burst duration, and **C.** Bursting frequency for neuronal cultures at DIV 20. Bar graphs of values in B and C are represented by changes from baseline DIV 14 values. N=4. All data are expressed as mean ± SEM. * p-value < 0.05, ** p-value < 0.01, *** p-value <0.001, **** p-value <0.0001.

3.2.5 Synaptotagmin 1 antibody uptake assay

In my project, we also used the uptake of an antibody directed against the luminal domain of synaptic protein SYTG1 as an additional assay to test any possible synaptic alterations for different treatments on the functional level. At DIV 7, cultured cells were treated with different aSyn species, and two weeks later I performed a SYTG antibody uptake assay at DIV 21. SYTG1 antibody was added to living cells culture medium. During the exo-endocytotic cycle, the antibody will be uptaken by cells, and the amount of uptake is an indirect measure of recycling synaptic vesicles. After incubation with SYTG antibody, the cells were then immunostained to analyze the uptake of SYTG uptake antibody. Interestingly, lower SYTG fluorescence intensity was observed in cells exposed to PFFs and oligomers compared to monomer treated group, which represent lower SYTG uptake and disruption of synaptic vesicle recycling process (Figure. 13A and B).

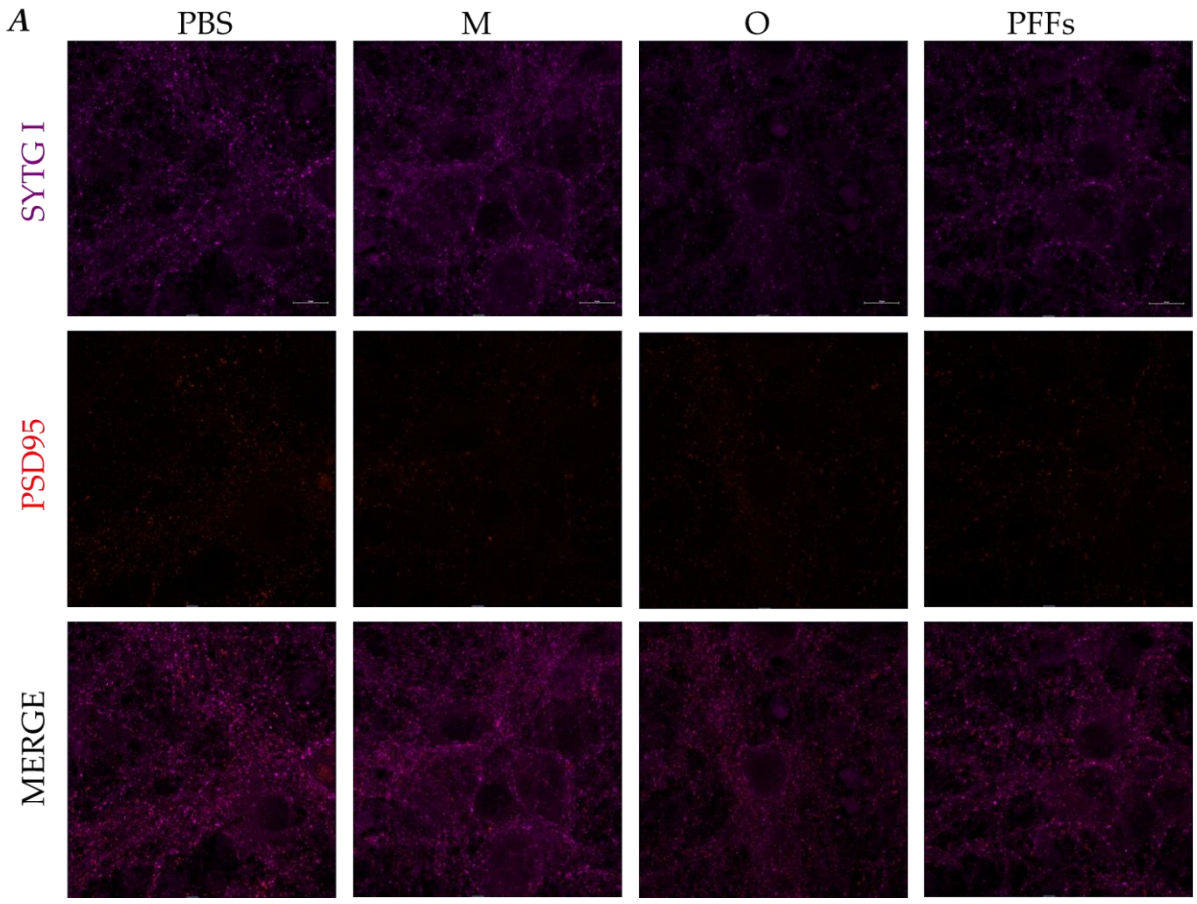

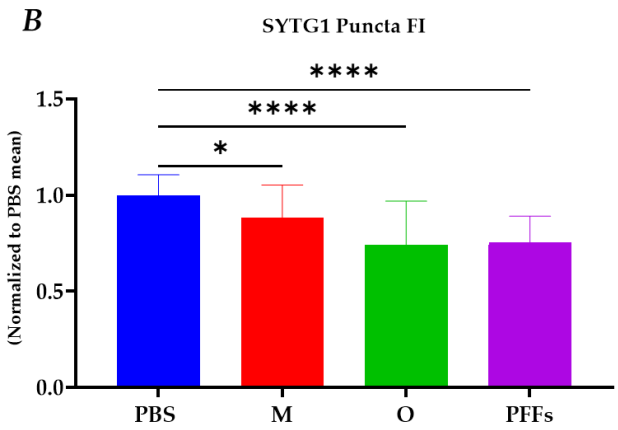

Figure 13. The effects on recycling synaptic vesicles are more pronounced in hippocampal neurons exposed to PFFs and oligomeric species. A. Representative confocal images for mouse hippocampal neurons exposed to different aSyn species at DIV 7. Neuronal cultures were incubated with luminal SYTG1 antibodies in their culture medium for one hour and then fixed, and immunostained with PSD95. Scale bar = 10 µm. **B.** Quantification of SYTG1 puncta mean fluorescence intensity FI, which is reflective of SYTG1 antibody uptake and synaptic vesicles recycling activity (N=3). Values were normalized to the PBS mean value for each replicate (N = 3). All data are expressed as mean ± SD. * p-value < 0.05, ** p-value < 0.01, *** p-value <0.001, **** p-value <0.0001.

3.3 Recombinant aSyn: Extensively used in PD research with no standard purification protocol.

Due to its aggregation and seeding properties, and the associated PD-like pathology, recombinantly generated aSyn is heavily used to produce in vitro oligomeric and fibrillar species that are employed in many cellular and in vivo PD models to recapitulate many pathological features associated with PD. Additionally, recombinant aSyn monomers are increasingly used for in vitro diagnostic seeding assays. Nevertheless, there is no standard protocol among different labs and between studies to produce and purify starting monomeric material, and various protocols are concurrently in use. In my study, I was interested in investigating how changes in aSyn purification protocol can impact its aggregation properties and potentially affect the downstream applications mentioned above. We aimed to explore how NaCl salt concentration in lysis extraction buffer can affect its aggregation propensity, as many production protocols use a variable range of NaCl concentrations. After the expression of aSyn in bacteria, I collected and lysed the bacterial pellet either using high salt (750 mM NaCl) or no salt extraction buffers. aSyn was purified with AEX followed by studying the aggregation properties of aSyn. We first tested aSyn purity before running aggregation assays using SDS-PAGE and Coomassie staining, and only a single band that is migrating just above 15 kDa was observed. This band corresponds to the presence of aSyn in its monomeric state (Figure 14A). Additionally, one aliquot of each condition was loaded to a size exclusion chromatography column prior to the lyophilization of protein, and I obtained mainly one peak in the gel filtration chromatogram, indicating that aSyn exists mainly in its monomeric form (Figure. 14B).

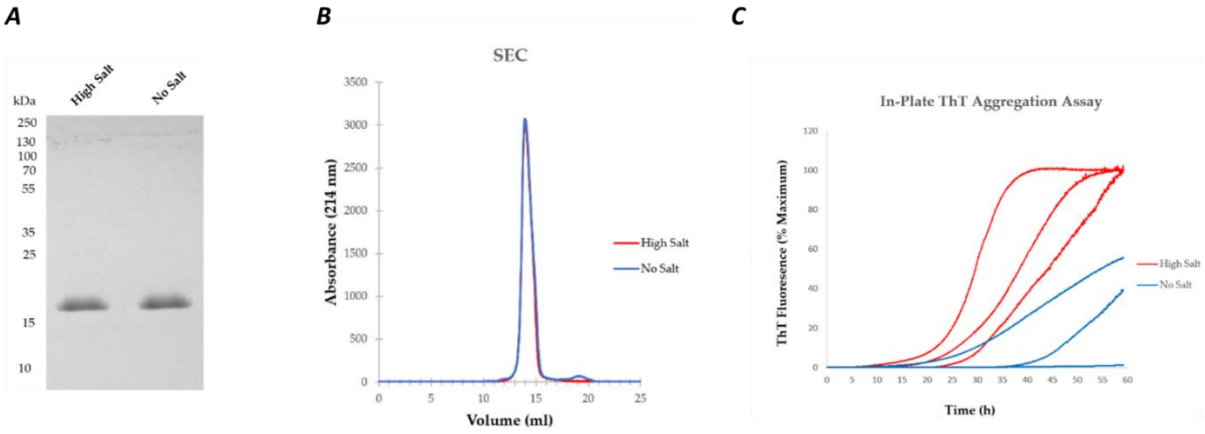

Figure 14. Effect of cell lysis buffer on the aSyn aggregation assays. A. aSyn purity after AEX was checked by SDS-PAGE and Coomassie staining. A total of 5 µg of AEX-purified aSyn from both extraction methods were loaded to the gel. **B.** SEC chromatogram of aSyn after AEX. **C.** Aggregation profiles of aSyn purified using differently extracted cell lysates monitored by changes in ThT fluorescence over time. N = 3 and each N represents an individually produced aSyn batch.

Looking deeply at the gel filtration chromatogram, we also analyzed the shoulders just eluting before the monomeric peak. These shoulders are usually indicative of the presence of aSyn multimers (Figure. 15A and B). Also, the chromatogram of "No salt" extracted aSyn showed a small peak at 19 mL of elution volume (Figure. 15A). However, SDS-PAGE did not show any protein bands in this peak (Figure. 15B). In an attempt to further investigate what this peak could be, the absorbance spectrum at 214 nm wavelength was also checked, as this wavelength is usually more suitable for detecting tiny amounts of proteins that are indistinguishable at 280 nm. We found that the absorbance for this peak is just slightly higher but not significant in the "No salt" condition (Figure. 15C). Furthermore, the absorbance spectrum at 260, a wavelength associated with maximum absorbance values for nucleic acids, was assessed to rule out nucleic acid contamination. Compared with the 280 nm chromatogram, a higher absorbance was obtained for this peak in "No salt" extracted aSyn (Figure. 15D). However, when examining an agarose gel stained with ethidium bromide, we found no evidence of nucleic acids, as we have seen nothing.

For ThT-based aggregation days, aSyn extracted from both purification methods was incubated with ThT in 96-well plates and changes in ThT fluorescence were monitored over time under agitation. Surprisingly, we found that extraction buffer composition affects the aggregation behavior of aSyn. aSyn extracted in the absence of salt displayed a delayed onset of aggregation and an overall lower ThT aggregation profile (Figure. 14C). In addition, the plateau phase was not reached for "No salt" purified aSyn within the timeframe analyzed. In conclusion, the observed influence of extraction buffer composition on the aggregation profile of aSyn highlights its potential effect on many downstream applications, as different purification protocols would ultimately result in variations in the starting purified monomer.

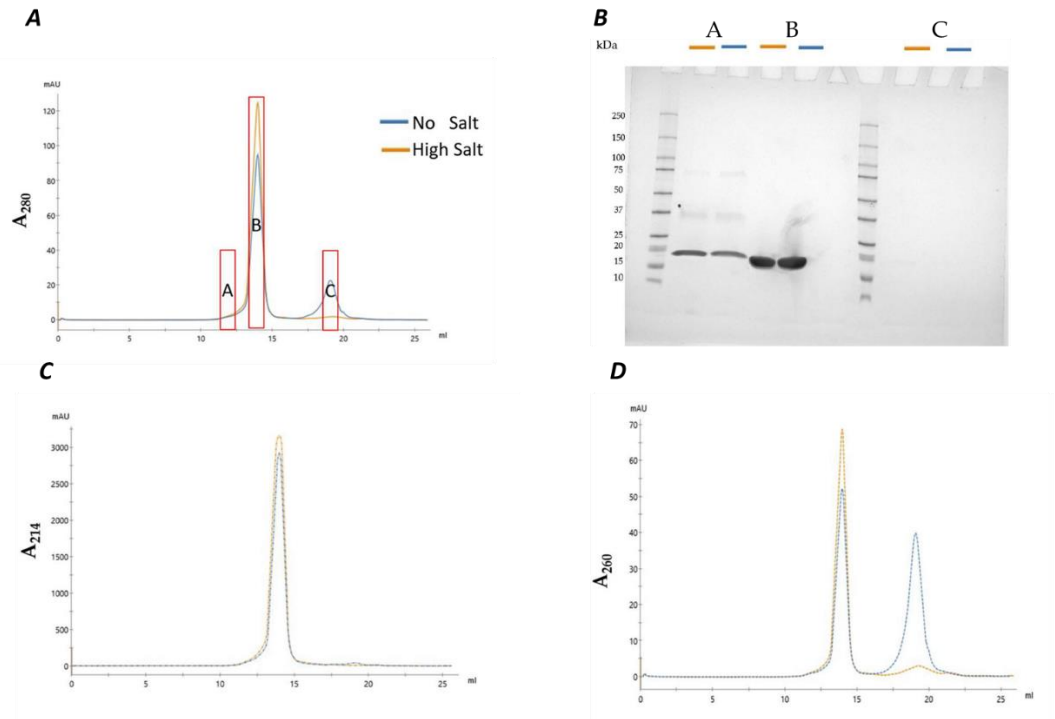

Figure 15. High salt extracted aSyn show mainly one peak corresponding to a monomeric state at different wavelengths spectra. A. SEC chromatograms of aSyn after AEX using absorbance at 280 nm. **B.** SDS-PAGE and Coomassie staining for samples loaded from monomeric peak shoulder (A) monomeric peak (B) and next eluting peak (C). High salt extracted aSyn chromatogram is represented in the color orange and No salt extracted aSyn is represented in blue. **C.** SEC chromatograms of aSyn after AEX using absorbance at 214 nm. **D.** SEC chromatograms of aSyn after AEX using absorbance at 260 nm.

3.4 Identification of aSyn interactome in isolated synaptic vesicles

Many of the putative roles of aSyn are primarily due to its interaction with other proteins. Given that aSyn is enriched in synaptic terminals and that it plays important physiological functions in synaptic vesicle exocytosis and neurotransmitter release, it is of high importance to study its interacting partners. Although aSyn has been studied for its physiological and pathological impacts on the synapse, the interactome of aSyn at the synapse is largely unknown. To further enhance our understanding of aSyn at the synapse, we isolated synaptic vesicles from WT mouse in order to identify unique aSyn interacting partners at these structures, employing proteomic techniques in collaboration with Prof. Urlaub's laboratory.

3.4.1 Isolation and validation of synaptic vesicles

To study aSyn interactors, I and my colleague Patricia Santos isolated the synaptic vesicles from the whole brains of wild-type (WT) mice. We followed the protocol developed by (Hell & Jahn, 2006), and the isolation of synaptic vesicles was included using differential centrifugation steps (Figure. 16A). To validate the successful isolation of synaptic vesicles, the enrichment of synaptic vesicles represented in the LP2 fraction was confirmed by using an antibody targeting the synaptic vesicle protein synaptophysin. As shown in the western blot, we found that synaptophysin band to be markedly enriched in the LP2 fraction from LS1 fraction, and apparently not detected in the LS2 fraction (Figure. 16B1). Furthermore, isolated synaptic vesicles were analyzed with electron microscopy imaging to check the quality of isolated SV. The typical shape and size known for this structure were also observed in our preparations (Figure. 16C). This confirmed that the isolation procedure has worked successfully. In addition, since we were aiming to use an antibody specific to aSyn in the next steps for pulldown assays, it was necessary to confirm the presence of aSyn in the synaptic vesicles for successful pulldown assays. aSyn was detected in synaptic vesicles obtained from WT and animals (Figure. 16).

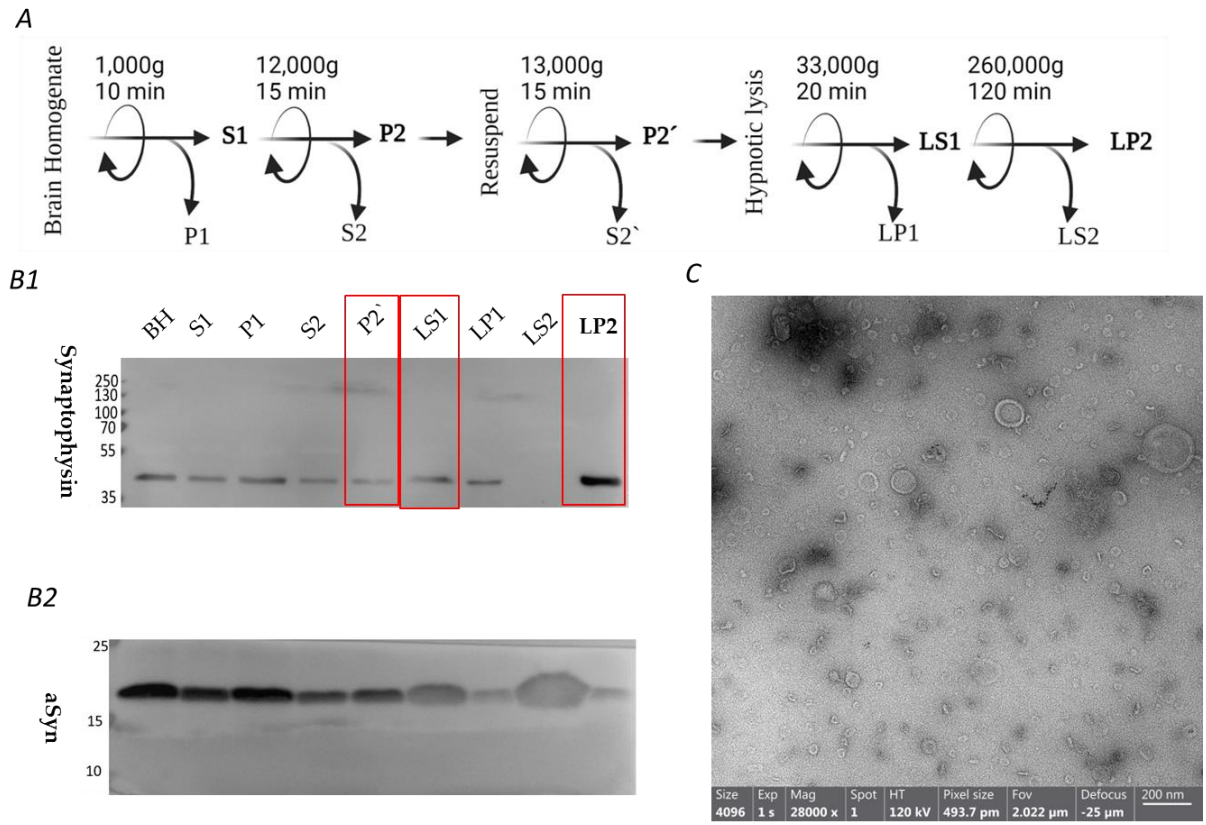

Figure 16. Preparation and characterization of synaptic vesicles. A. Scheme representing the differential centrifugation steps to prepare synaptic vesicles represented in the LP2 fraction. **B1.** Immunoblotting shows the enrichment of synaptic vesicles in the LP2 fraction from the LS1 fraction, as checked by the synaptophysin antibody. **B2.** The aSyn antibody was used to verify the presence of aSyn in synaptic vesicles LP2, as indicated by immunoblotting. **C.** Representative image for prepared synaptic vesicles. Scale bar = 200nm. Figure. 1A was created with Biorender.com.

3.4.2 Co-Immunoprecipitation of aSyn from synaptic vesicles

After the isolation of synaptic vesicles, we performed Co-IP experiments to pull down aSyn with its potential interacting partners. To do this, we used a mouse anti-aSyn antibody (SYN1) that was coupled to magnetic beads and ran the Co-IP experiments as described in the methodology part. In parallel, Co-IP assays were also done using mouse anti-Igg1 antibody as a negative control. At the end of the pulldowns, complexes were eluted from antibodies conjugated beads to be used for mass spectrometry analysis. Before sending samples for MS analysis, immunoblotting was conducted to validate the Co-IP protocol. As expected, aSyn was mainly detected

in eluted samples from beads conjugated to SYN1 antibody, and not the Igg1 control (Figure. 17).

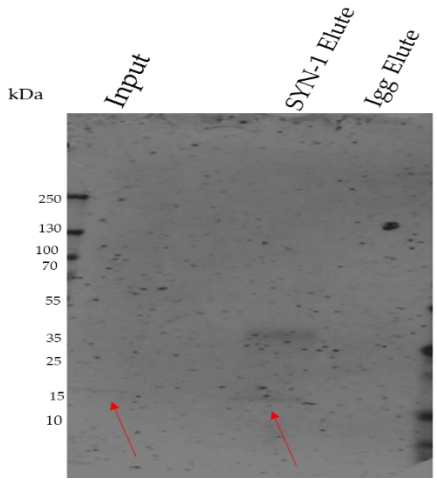

Figure 17. Validating aSyn pull-down assays. Immunoblot shows the coimmunoprecipitation of aSyn from synaptic vesicles**.** Pulldown of samples was performed using mouse aSyn antibody or mouse IGg antibody. aSyn was detected only from sample coimmunoprecipitated with aSyn antibody SYN-1.

3.4.3 Mass spectrometry analysis and Gene Ontology

To check if we could detect any novel aSyn interactions, we sent samples for MS analysis. MS analysis was performed in collaboration with Dr. Christof Lenz and Prof. Dr. Henning Urlaub from the Core Facility Proteomics of University Medical Center Göttingen. A list of proteins enriched in SYN1 elute was created by performing a student's T-test. These candidates represent the potential aSyn interacting partners. The main comparisons were between candidates in SYN1 and Igg1 Co-Ip samples. The initial list from mass spectrometry data included 126 potential candidates enriched in aSyn sample (Figure. 18). Since our focus was to first check the potential synaptic vesicle-associated proteins that are known to have a presynaptic function, I filtered the data based on this and checked which synaptic proteins could interact with aSyn. 15 synaptic proteins were identified. The proteins are listed in Table. 4 based on Q value significance. Among these candidates, we found some interacting partners that were already documented to interact with aSyn. These include CAMK2G and SV2c proteins, which support and validate our data.

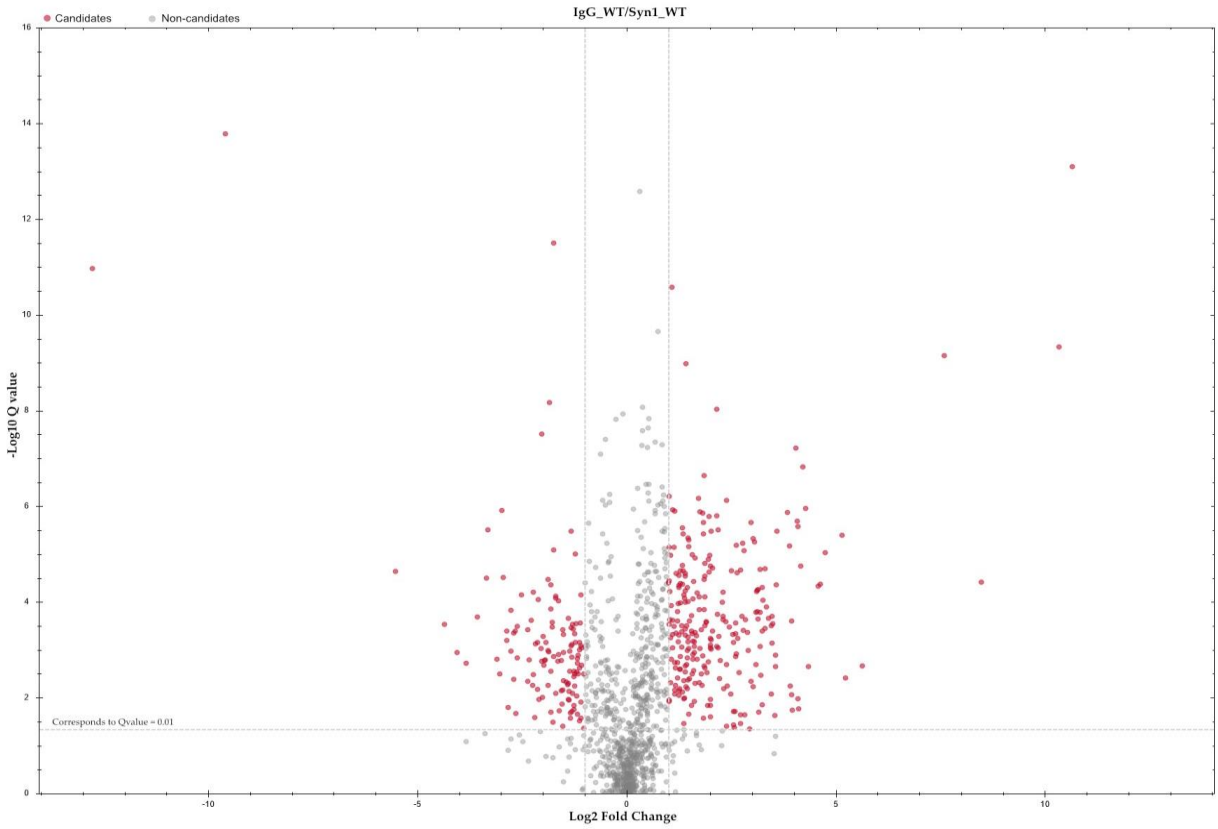

Figure 18. Several proteins were enriched in the aSyn pulldown samples. Volcano plot for mass spectrometry data for coimmunoprecipitation samples for synaptic vesicles obtained from WT mice. Data were plotted using log2Fold change of IgG over Syn1 pulldown samples on the X axis and -log Q value on the Y axis. Proteins enriched in Syn1 sample have negative log2 fold change values and proteins enriched in the IgG control have positive values. Proteins with values between -1 and 1 log fold change or that don't pass the Q value threshold 0.01 were considered insignificant.

Table 4. A list of potential aSyn interacting candidates based on association with synaptic vesicles.

Protein names	Gene Names	Log2 Ratio IgG/ WT	-log10(Q-value)
Alpha synuclein	SNCA	-1.74	10.83
Calcium/calmodulin dependent protein kinase II gamma	CAMK2G	-2.51	4.45
Syntaxin 12	STX12	-1.82	4.20
Protein MAL2	MAL2	-2.77	4.17
Synaptogyrin-3	SYNGR3	-1.30	3.56
Protein unc-13 homolog A	UNC13A	-1.09	3.54

Proline-rich transmembrane protein 2	PRRT2	-1.12	3.47
Secretory carrier-associated membrane protein 5	SCAMP5	-1.31	3.33
Secretory carrier-associated membrane protein 1	SCAMP1	-1.95	3.28
Synaptoporin	SYNPR	-3.84	3.23
Calcium/calmodulin dependent protein kinase II beta	Camk2b	-1.99	3.18
Syntaxin-binding protein 1	Stxbp1	-2.36	2.89
Ras-related protein Rab-33B	Rab33b	-1.38	2.70
Synaptic vesicle glycoprotein 2C	Sv2c	-2.01	2.60
Ras-related protein Rab-33A	Rab33a	-2.83	2.40
Syntaxin-7	Stx7	-2.20	2.22
Synaptobrevin homolog YKT6	Ykt6	-1.13	2.16

After the analysis of aSyn potential interaction with synaptic proteins, I performed a comprehensive analysis of the entire list of 126 candidates identified from mass spectrometry analysis. The analysis was based on conducting gene ontology (GO) enrichment analysis for the whole proteomic list. This would for sure result in a more comprehensive overview of the biological processes and molecular functions that aSyn is involved in. The enrichment analysis was performed using ToppGene Suite database (Chen et al., 2009). After entering the protein list into the database, proteins will be clustered and significantly enriched according to similar biological processes, molecular functions, and cellular compartments. The top 10 significant pathways were selected for each category based on the P value for enrichment analysis. Several clusters of interest were observed for each category.

When analyzing the enriched biological processes related to potential interacting partners for aSyn, aSyn is significantly associated with the enriched biological processes related to vesicle-mediated transport, exocytosis, and synaptic signaling (Figure. 19). Our data further support the involvement of aSyn in regulating synaptic vesicle release. In addition, aSyn is expected to have many interacting partners involved in these processes table. Interestingly, aSyn is involved in biological processes related to neuron development and neuronal projection development. These

represent extra roles beyond the traditional synaptic function for aSyn. Our data showed interesting findings that will need further investigation.

After analyzing biological processes, the next step was to look at the molecular functions that are connected with aSyn. Interestingly, I found protein domain-specific binding, SNARE binding, and syntaxin-1 binding to be among the most enriched molecular functions (Figure. 19). Synaptic vesicle-mediated transport and exocytosis require SNARE complex assembly and binding activity. This agrees with the enriched biological processes we mentioned before. Furthermore, syntaxin-1 is a crucial part of the SNARE complex required for synaptic vesicle docking and exocytosis. aSyn is well-established to play a role in SNARE complex assembly and is therefore expected to be enriched in molecular functions related to this. aSyn is also enriched in molecular functions associated with cytoskeletal protein binding, which is really interesting. That means aSyn functions are expanded to multiple roles, ranging from regulating synaptic vesicle release to binding and supporting the cytoskeleton structures that keep the synapse working. In other words, our study suggests that aSyn is involved in biological processes that are related to the synapse at the structural and functional levels. Given that aSyn has been documented to interact with cytoskeletal actin and tubulin, other potential interacting partners that were identified in our study and are involved in these enriched molecular functions need to be further investigated and validated.

Finally, looking at the cellular component category from GO, it appears that aSyn localizes to many subcellular components of the synapse machinery (Figure. 19). As we found from previous data that aSyn is active and associated with many biological processes and molecular functions that take place in different locations in the synapse, enriched cellular components support our previous findings. Among the top enriched cellular components aSyn is associated with are the exocytic vesicle membrane, synaptic vesicle membrane, cytoplasmic vesicle membrane, and synaptic vesicle. This is consistent with our previous data for enriched vesicle-mediated transport, exocytosis, and synaptic signaling biological processes. Furthermore, we also observed

before that aSyn is enriched in biological processes related to neuron development and neuronal projection development, and this matches our results for aSyn being localized in neuron projection and axons.

Taken together, our data support the important role aSyn plays in many biological processes and shed light on functions beyond known aSyn synaptic functions. The findings suggest that aSyn is not just involved in regulating the synaptic vesicle cycle, but also interacts with other proteins involved in other biological processes and molecular functions related to synapse architecture and neuron development. Further investigations are needed to fully understand the significance of these observed associations.

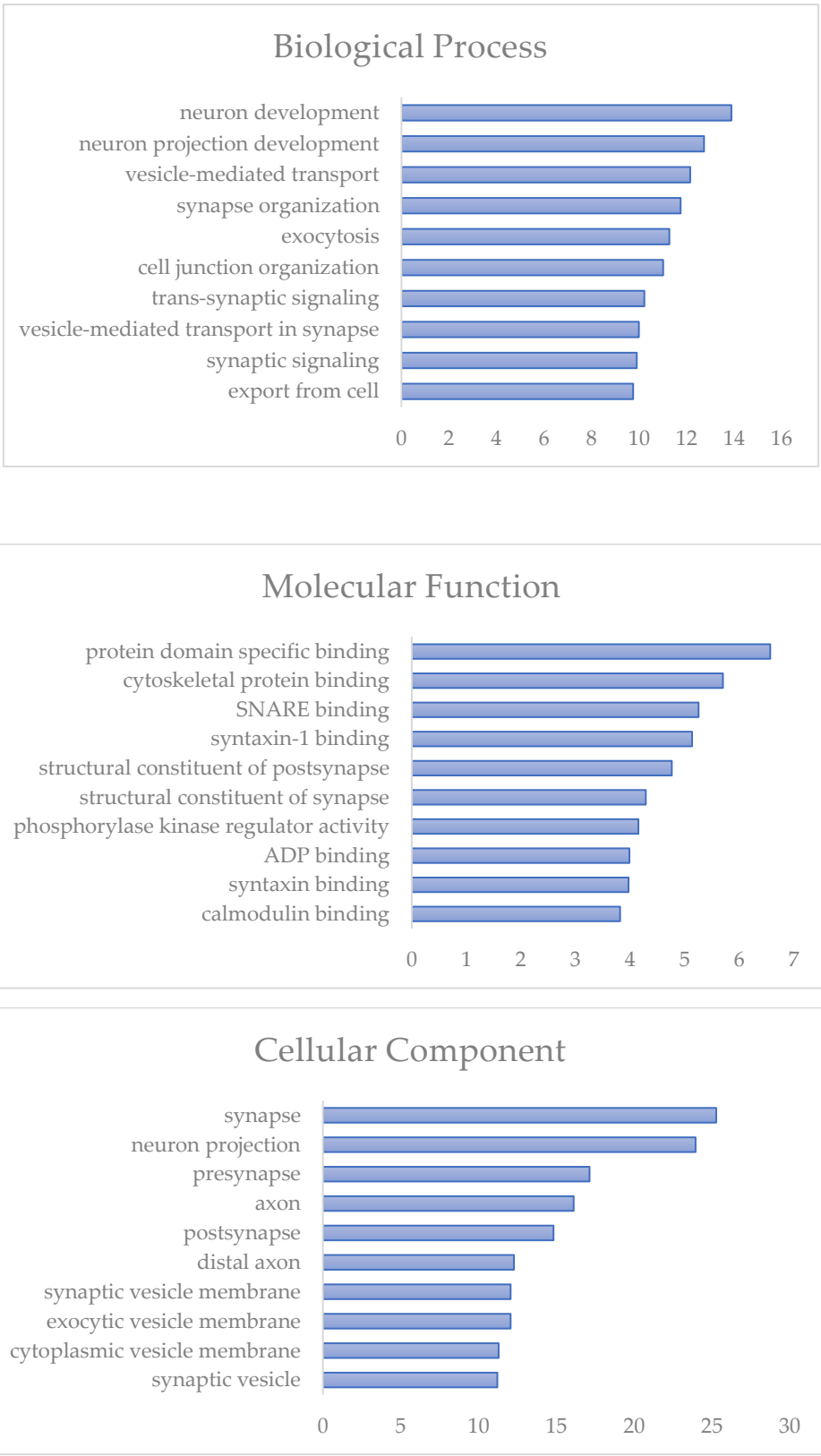

Figure 19. Gene ontology enrichment analysis of the top 10 biological processes, molecular functions, and cellular components for aSyn interacting partners. GO terms were plotted as -log10 of the p value.

3.5 Identification of general aSyn interacting partners using SILAC experiments

For the purpose of exploring the general interacting partners of aSyn, we utilized HEK293 cells. As stated previously, we conducted two biological replicates by switching the labeling scheme in order to mitigate any potential bias introduced by the SILAC labeling procedure. In what we refer to as the forward condition of the first SILAC experiment, we cultivated GFP-expressing cells in light (L) SILAC medium, cells expressing WT aSyn in medium (M) SILAC medium, and cells with A30P aSyn expression in heavy (H) SILAC medium. Conversely, in the reverse condition, we switched the order of labeling to A30P(L)-GFP(M)-WT(H). It is important to mention that GFP-expressing cells contain some endogenous levels of aSyn, while aSyn is overexpressed in other conditions. The idea was to investigate if endogenous aSyn interactome could differ when it is overexpressed, and what would be the impact of the A30P mutation.

Cells were grown in SILAC media for at least 5 passages, and then the cells were harvested for Co-IP experiments. aSyn pulldown assays were conducted using antibody targeting total aSyn. We checked first if aSyn pulldown had worked. Immunoblotting has revealed the presence of aSyn in all groups and in both forward and reverse replicates, with a relatively low amount in the GFP control cell line reflecting the endogenous levels of aSyn (Figure. 20). Furthermore, a dimeric band for aSyn was observed and was more pronounced in cells overexpressing WT aSyn compared to A30P aSyn when normalized to the corresponding monomeric band, suggesting a higher aggregation profile for WT aSyn (Figure. 20).

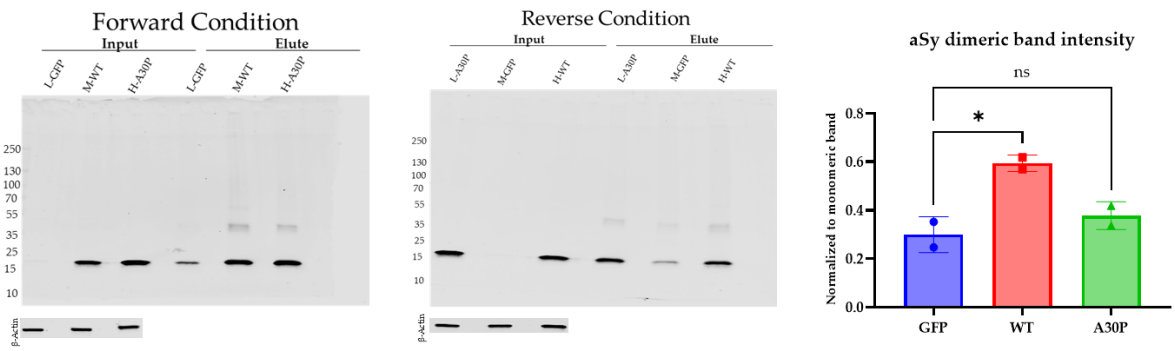

Figure 20. Immunoblotting of aSyn pulldown from SILAC-labeled cells. Co-IP experiments for the forward condition in which HEK293 control cells were labeled with light (L) SILAC isotopes, cells overexpressing WT aSyn were labeled with medium (M) SILAC isotopes, and A30P overexpressing cells were labeled with heavy (H) SILAC isotopes. For the reverse condition, labeling was swabbed as it appears in the second blot. Co-IP experiments were performed using aSyn antibody SYN211. Samples from input and Co-IP elutes were immunoblotted and detected using total aSyn antibodies.

Prior to SILAC proteomics, equal proportions of protein complex elutes derived from light, medium, and heavy preparations in the Co-IP experiments were mixed in a 1:1:1 ratio for every forward or reverse scenario. SILAC proteomics samples analysis was done in cooperation with Dr. Christof Lenz from Prof. Dr. Henning Urlaub laboratory. Statistical tests were performed based on Significance B, and log SILAC ratios of A30P to GFP or GFP to WT were used after sign correction. A number of aSyn interacting partners were identified. We decided to focus only on the candidates that were enriched in both replicates of the experiment to ensure the robustness of our results. Surprisingly, we found that the main aSyn interacting proteins were identified in the GFP control cells (Figure. 21 and 22). In cells expressing either WT or A30P aSyn, only aSyn was detected to be enriched in both replicates (Figure. 21 and 22) which is logical since these cell lines overexpress aSyn. Although no interacting partners were obtained under overexpression systems, our current explanation for such results would be that these potential interacting candidates for aSyn identified in the GFP control cell line, compared with cells overexpressing WT aSyn, could be physiological since HEK cells contain some endogenous aSyn. Under our experimental conditions,

it seems aSyn overexpression may lead to the conversion of aSyn into aggregates and therefore reducing its availability for interactions. Further investigations are necessary to fully understand these observations.

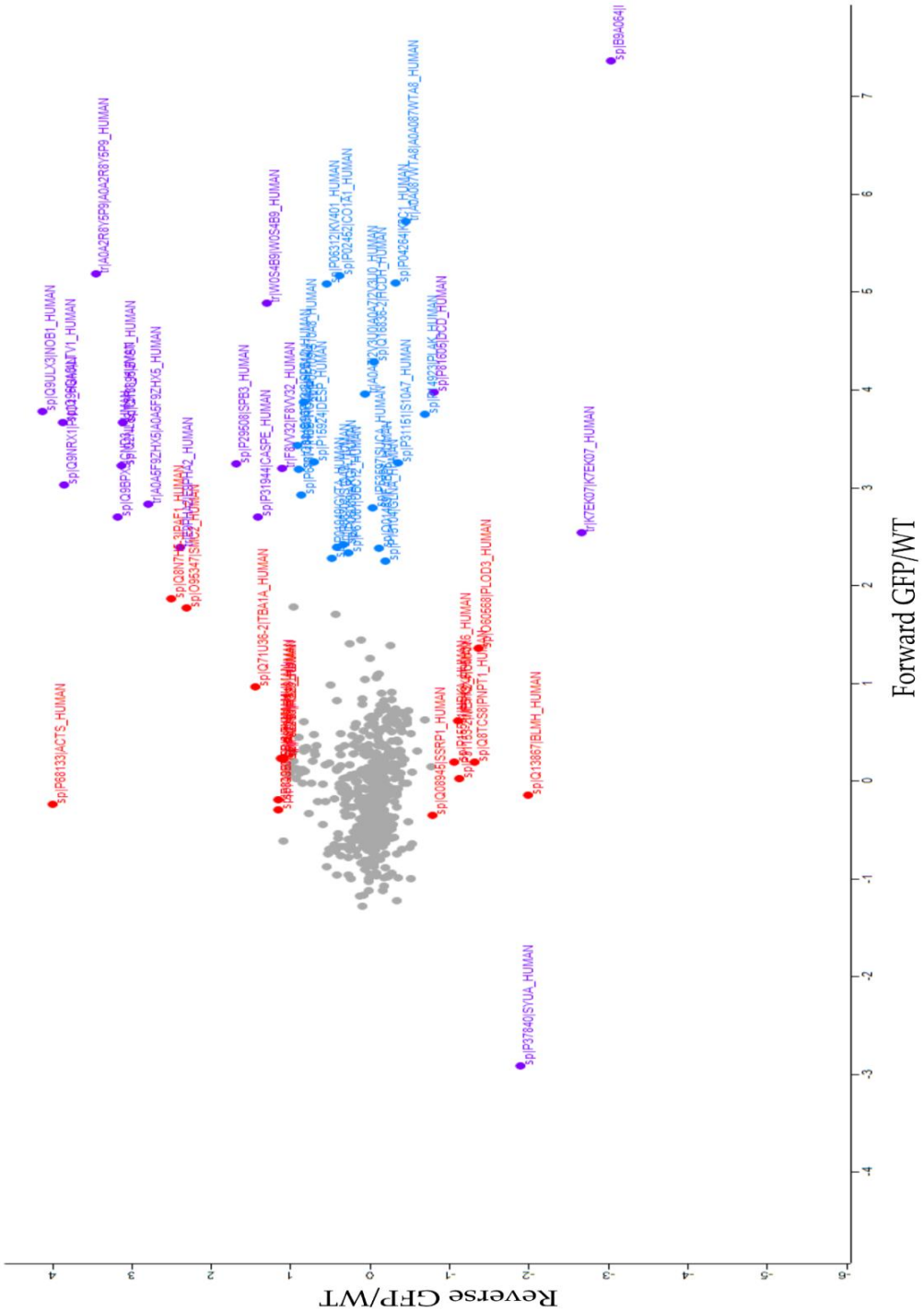

Figure 21. 2D scatter plot for GFP/WT SILAC proteomics data. The plot represents log2 SIALC ratios for proteins enriched in forward and reverse conditions. GFP

represents the control cell line expressing GFP, and WT represents cells overexpressing aSyn. The forward condition represents the first replicate, and in the reverse condition (second replicate) SIALC labeling was switched. Proteins enriched in forward condition are colored with blue dots, those enriched in the reverse condition are colored with red dots, and those enriched in both directions are colored with violet dots. Regardless of the direction, proteins higher in GFPs cells have positive Log2 SILAC ratios, while those higher in WT cells have negative ratios.

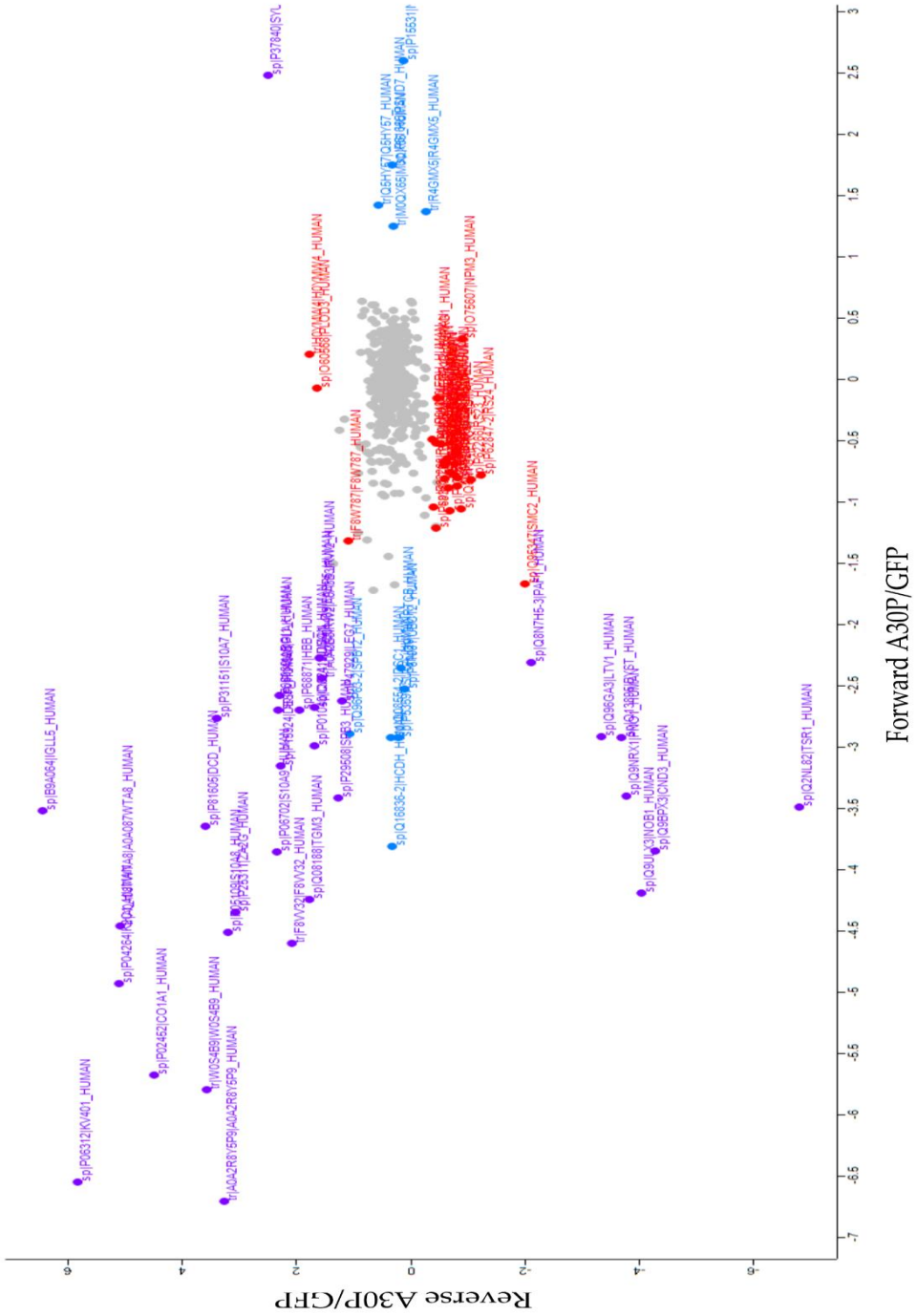

Figure 22. 2D scatter plot for A30P/GFP SILAC proteomics data. The plot represents log2 SIALC ratios for proteins enriched in forward and reverse conditions. GFP

represents the control cell line expressing GFP, and A30P represents cells overexpressing A30P aSyn. The forward condition represents the first replicate and in the reverse condition (second replicate) SIALC labeling was switched. Proteins enriched in the forward condition are colored with blue dots, those enriched in the reverse condition are colored with red dots, and those enriched in both directions are colored with violet dots. Regardless of the direction, proteins higher in GFPs cells have negative log2 SILAC ratios, while those higher in A30P cells have positive ratios.

The potential interacting candidates that were observed for aSyn at GFP cells compared to WT aSyn cells are summarized in Table 5. Interestingly, most of these proteins have nuclear localization, and five of them (PNO1, TSR1, LTV1, NOB1, BYSL) are involved in ribosome biogenesis and a major pathway of rRNA processing. NCAPH and NCAPG have regulatory roles in chromosome condensation. These data support the increasing role of aSyn at the nucleus. In addition, tyrosine-protein kinase Fer was one of the potential interacting candidates for aSyn. Fer kinase plays a role in the regulation of the actin cytoskeleton, microtubule assembly, and cell adhesion, and has been reported to be involved in synapses organization and function.

Interestingly, the 6 potential aSyn interacting partners in GFP-control cells over those expressing A30P aSyn are also enriched in GFP-control cells over those expressing WT aSyn as mentioned before. These include the proteins PNO1, TSR1, LTV1, NOB1, and BYSL which are important for ribosomal RNA processing. This further supports the idea that aSyn interactions are reduced under overexpression levels. Furthermore, it seems that the A30P mutation has a less pronounced effect on reducing aSyn interactions since only 6 potential interacting partners were identified in the case of GFP over A30P comparison. In conclusion, our data, although not conclusive, support nuclear roles for aSyn and suggest that the aSyn interactome is disrupted under overexpression systems. We believe that overexpression of aSyn in the cells expressing WT and A30P aSyn may have led to the sequestration of aSyn into protein aggregates, thus reducing its availability for interaction with other proteins.

Table 5. List of proteins enriched in GFP control cells over WT aSyn overexpressing cells.

Protein name	Gene Name	**log2 WT/GFP Forward**	**log2 WT/GFP Reverse**
Tyrosine-protein kinase Fer	FER	4.882	1.311
Serpin B3	SERPIN B3	3.236	1.701
Protein Shroom3	SHROOM3	5.187	3.462
Bystin	BYSL	3.664	3.119
Pre-rRNA-processing protein TSR1 homolog	TSR1	3.220	3.148
Protein LTV1 homolog	LTV1	3.665	3.884
Condensin complex subunit 3	NCAPG	2.700	3.191
RNA-binding protein PNO1 (Partner of NOB1)	PNO1	3.027	3.866
RNA-binding protein NOB1	NOB1	3.772	4.134
RNA polymerase II-associated factor 1 homolog (hPAF1)	PAF1	2.700	1.425
Caspase-14	CASP14	2.831	2.802
DNA helicase	CHD3	2.389	2.401
Condensin complex subunit 2	NCAPH	4.882	1.311

3.6 The effect of aSyn glycation at the synapse

aSyn undergoes several PTMs, and many of them were observed in PD patients and several models of PD. One of these PTMs is glycation, a non-enzymatic reaction between proteins and sugars, which has been reported to affect aSyn structure, aggregation, and functions. Previous studies from our group showed that glycation increases the oligomerization and toxicity of aSyn and increases neuronal loss in vitro and in vivo models. Given the central role of aSyn at the synapse, we wanted to further investigate how glycated aSyn can modulate synaptic activity. To do this, we first prepared glycated aSyn (aSynMGO) by incubating aSyn with the glycating agent MGO. Our controls were using unglycated aSyn or MGO alone, which were prepared in the same way as aSynMGO. Mouse hippocampal neurons were treated with 100 nM of different species at DIV 7 or DIV 14 for some assays, followed by different evaluative assays. Untreated cells (Q) were used as a control.

3.6.1 Cytotoxicity assays

The toxicity of Syn glycation in mouse hippocampal neuronal cells was first examined using the ToxiLight assay as previously described. The levels of AK released into the cells medium were significantly higher in cells exposed to glycated aSyn, corresponding to more cytotoxicity (Figure. 23).

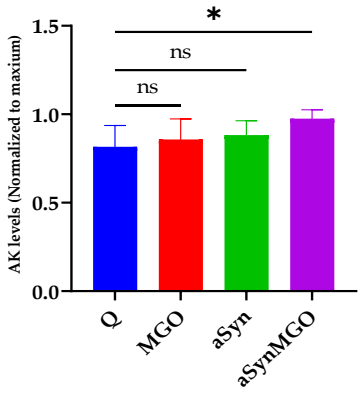

Figure 23. Glycated aSyn is more toxic to mouse hippocampal neurons. Toxlight cytotoxicity assay for treated cells with different species represented by the levels of adenylate kinase (AK). Cells were treated at DIV 7, and the assay was performed at DIV 26. AK levels were normalized to maximum value for each replicate. All data are expressed as mean ± SD. * p-value < 0.05, ** p-value < 0.01, *** p-value <0.001, **** p-value <0.0001.

3.6.2 Investigating the seeding capacity for glycated aSyn

The potential of some forms of aSyn to induce the aggregation of endogenous aSyn is known to be one of the pathological features in PD. Although previous studies have shown that glycation of aSyn enhances its oligomerization and toxicity, these studies were based primarily on treating cells with glycating agents like MGO in cell models expressing aSyn. In our study, we used glycated aSyn prepared in vitro, and a lower concentration (100 nM) was applied. We chose this concentration based on the concentration we used for the first part of this study regarding using different aSyn species, monomers, oligomers, and PFFs. Additionally, aSyn species prepared in vitro are normally used in the concentration range of 70–100 nM. Mouse hippocampal neurons were treated with aSynMGO, aSyn, or MGO at DIV 7, and the cells stayed in their culture medium until DIV 26. I then employed immunoblotting to check the

levels of high molecular-weight species formed endogenously as well as phosphorylation for aSyn at S129, which usually indicate seeding and aggregation of endogenous aSyn. Surprisingly, we could not detect any differences between glycated and unglycated aSyn species with regard to the formation of endogenous aggregated aSyn or detect pS129 in the blots (Figure. 24B). Also, pS129 was not observed in the blots or from immunocytochemistry data (Figure. 24A). Our data suggest the glycation of aSyn does not alter its seeding properties at the concentration used.

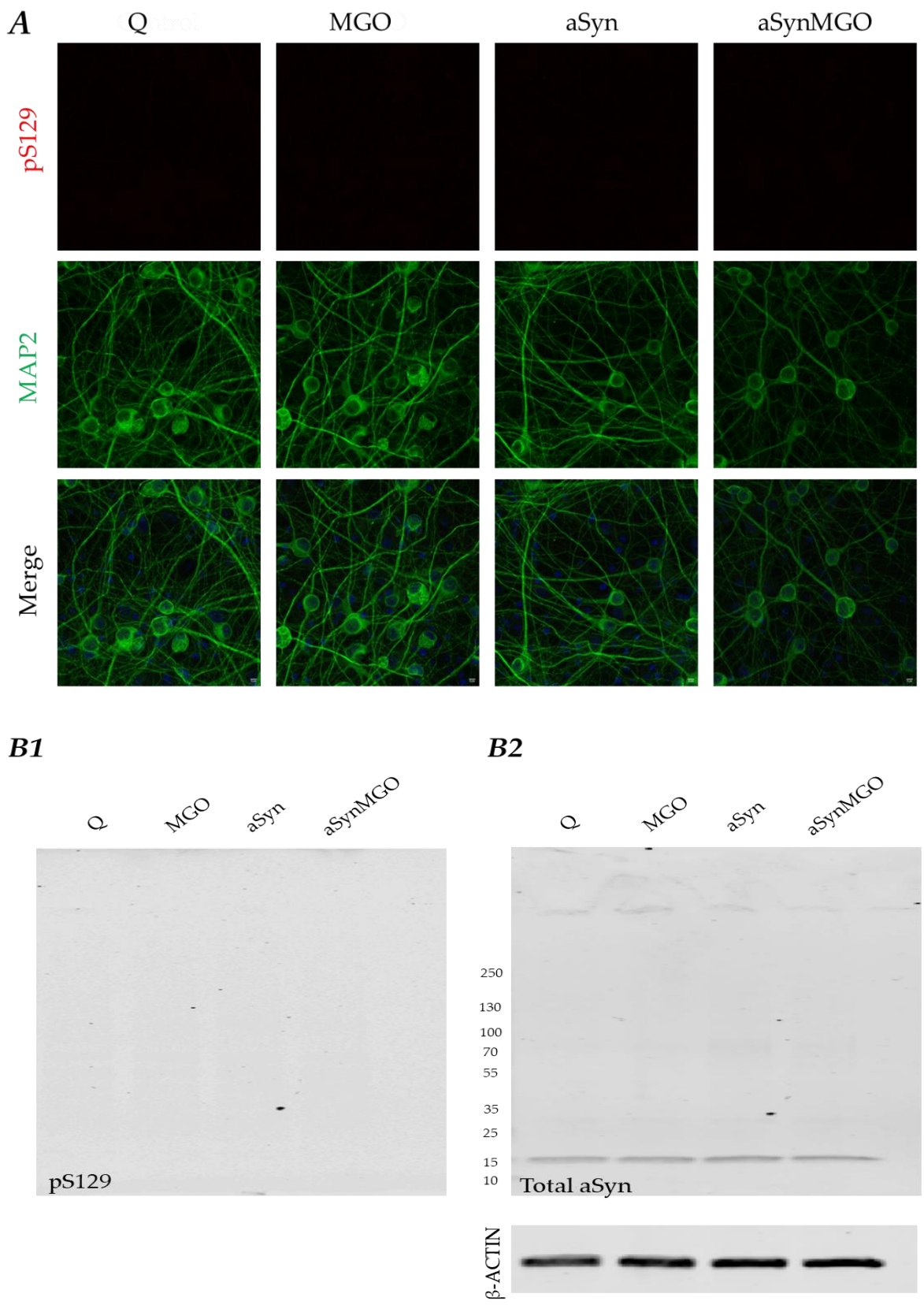

Figure 24. Glycated aSyn shows no difference in seeding capacity compared to unglycated species. A. Representative confocal images for mouse hippocampal neurons exposed to different aSyn species at DIV 7 and immunostained with MAP2,

and pS129 at DIV 26. Cells were counterstained with DAPI. Scale bar = 20 μm. **B.** Representative immunoblot probed with pS129 and total aSyn antibodies. β-actin was used as a loading control.

3.6.3 The impact of alpha-synuclein glycation on synaptic function

To study the effects of aSyn glycation on synaptic function, we performed two assays to check if there are biochemical or functional alterations. The levels of synaptic proteins VAMP2, SNAP25, SYTG1, and PSD 95 were checked post-treatment with glycated and unglycated aSyn. At DIV 26, immunoblotting data did not show any differences in the levels of these proteins (Figure. 25).

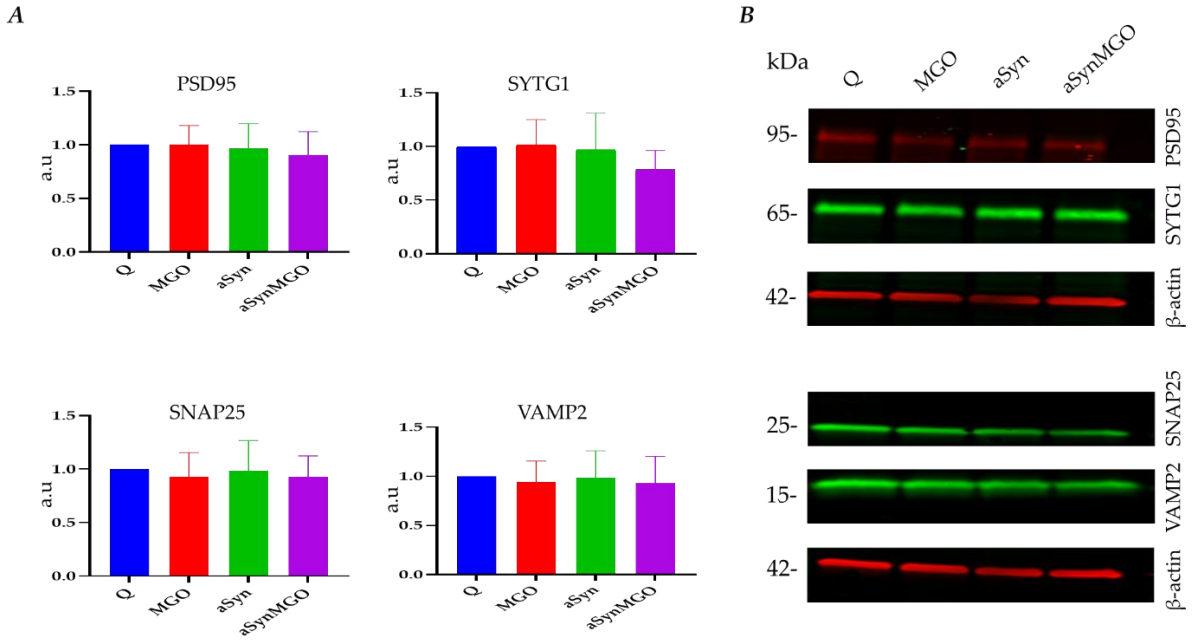

Figure 25. The levels of synaptic proteins are not affected by the use of glycated aSyn. A. Quantification of the biochemical levels different synaptic proteins. Mouse hippocampal neurons were treated at DIV7 and harvested at DIV 26. **B.** Representative immunoblots of the relevant proteins.

Finally, we wanted to check if there could be any functional alterations induced on synaptic neuronal activity after treatment with these species. For these experiments, neuronal cultures were treated at DIV 14, and neuronal activity was measured employing MEA recordings at DIV 20. In agreement with previous findings, no

significant alterations were documented for cells exposed to glycated species compared to unglycated species (Figure. 26).

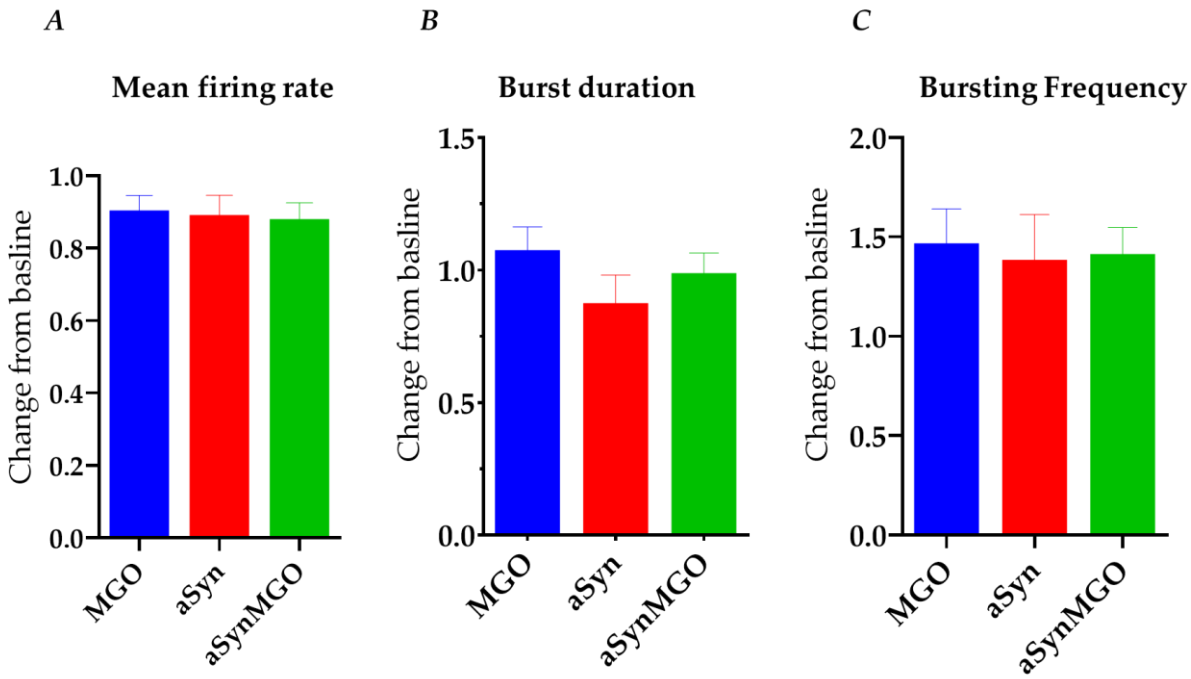

Figure 26. Comparable neuronal activity was observed in mouse hippocampal neurons exposed to glycated and unglycated aSyn. Data were obtained from recording spontaneous neuronal activity using MEA experiments. **A.** The Mean firing rate, **B.** Burst duration, and **C.** Bursting frequency for neuronal cultures exposed to different treatments at DIV 14. Bar graphs of values are represented by calculating changes from baseline DIV 14 values. N=3. All data are expressed as mean ± SEM.

In conclusion, our data under the experimental conditions employed suggest aSyn glycation does not appear to affect its seeding potential, accompanied by no alterations at the biochemical and functional aspects of synaptic function. However, glycated aSyn seems to be more toxic to cells.

4. Discussion

4.1 Synaptic alterations are more pronounced with exposure to aSyn PFFs.

Although there is clear evidence that aSyn aggregation has been implicated in the pathogenesis of PD, there is still ongoing debate about which species of aSyn have more toxic effects on neuronal cells and, more importantly, at the synapse.

There are different species of aSyn during the conversion of aSyn into LBs. In the simplest way, these include diffuse or soluble monomers, soluble oligomers, and fibrillar species. However, the range of species is more complex even within each aggregation state, and each species might behave differently with regard to cellular and neuronal dysfunctions (Hansen et al., 2011; Luk et al., 2009b; Volpicelli-Daley et al., 2014b). Some studies suggest aSyn fibrillar aggregates as the main culprits for causing neuronal toxicity (Hansen et al., 2011; Luk et al., 2009b; Luk, Kehm, Zhang, et al., 2012; Rey et al., 2013; Volpicelli-Daley et al., 2014b). On the other hand, others argue that oligomeric forms of aSyn might actually constitute proteotoxic agents (Cascella et al., 2021; Diógenes et al., 2012). Furthermore, the majority of studies checking the toxic potential of different species on neuronal function and at the synapse are either comparing PFFs with control or oligomers with control. Comprehensive studies that compare aSyn monomers, oligomers, and PFFs together are very limited. To our knowledge, two studies have tried to directly assess the differences in toxicity potential of all aSyn species within the same experimental setup (Diógenes et al., 2012). Therefore, our research seeks to fill this knowledge gap by performing a comparative evaluation of various aSyn species and studying their impact on synaptic function in order to shed light on the existing debate. Ultimately, we are trying to clarify the ongoing controversy and contribute to a better understanding of aSyn pathology in PD.

Our study conducted a comprehensive comparison of different aSyn species, namely monomers, oligomers, and PFFs. We first prepared and characterized these species. We then compared the direct cytotoxic effects of different species. The seeding potential of different species was also compared in order to explore if any subsequent

effects could be associated with them. We also checked the effect of different treatments on the biochemical levels of synaptic proteins at two different time points. We finally investigated if any functional alterations at the synapse could be induced by different species prior to possible changes in the biochemical levels of synaptic proteins and eventually cell death.

aSyn is a natively unfolded protein but aggregation-prone, and under certain conditions, it can aggregate, forming initially oligomeric species of different sizes and eventually fibrils (Paleologou & El-Agnaf, 2012; Srinivasan et al., 2021). The use of recombinant exogenous aSyn species in models of PD has become traditional since the observation that injecting aSyn PFFs into the animal brain seeded the aggregation of endogenous aSyn and resulted in the formation of inclusions and pathological changes similar to LBs observed in many synucleinopathies (Hansen et al., 2011; J. Y. Li et al., 2008). Prepared aSyn PFFs used in several cellular and animal models of PD typically consist of insoluble aggregated material, characterized by beta-sheet rich structures and a fibrillar morphology, and they represent the final product in the aggregation process for aSyn (Alam et al., 2019). Oligomers represent the intermediate transition species during aSyn aggregation. Several protocols are available in the literature, but oligomers are generally heterogeneous soluble structures that vary in size and morphology (Cappai et al., 2005; Lashuel et al., 2002b). In addition, they have variable beta-sheet content, usually less than PFFs (Vaikath et al., 2022). Our PFFs preparations exhibited structural features similar to those described in the literature. They are twisted and straight fibrillar structures rich in beta sheet, as confirmed by the ThT assay and EM images. We also found that oligomeric species were soluble containing high molecular weight species with a wide range of spherical, chain-like, or annular structures, as observed by EM imaging, which aligns with previous studies. The ThT fluorescence for our oligomers was almost twice that of monomers but much lower than that of PFFs, indicating too much beta-sheet content in PFFs, with a modest increase for oligomers compared with monomers. Such differences could have different impacts upon exposing cells to these species.

There is a substantial body of evidence indicating that the capacity of different aSyn strains to seed endogenous aSyn aggregation cannot be simply a passive property but can actively add to their toxicity (Tofaris, 2022). Several studies from cellular and in vivo models have checked the seeding potency of different exogenous aSyn species including, oligomers and PFFs. While different types of oligomeric preparations have been described in the literature, only some have been shown to have some seeding efficiency in a few studies (Danzer et al., 2007b, 2009). Unlike oligomers, the seeding capacity of PFFs is well established, and they are considered more potent seeding agents (Alam et al., 2019; Froula et al., 2019). In addition, when injected into mice brains, only PFFs seeded the aggregation of endogenous aSyn (Peelaerts et al., 2015). Our results are consistent with the preceding literature. We found that higher levels of aSyn pS129, which is a marker of LB pathology and endogenous aSyn aggregation, were obtained mainly in mouse hippocampal neurons exposed to PFFs compared with monomers and oligomers. Our study reinforces the current findings and offers further proof for PFFs as the main species triggering aSyn aggregation and propagation.

As mentioned before, exogenous aSyn species are frequently used in PD research. However, which species are more harmful in either causing cytotoxicity or causing synaptic function is still a matter of ongoing conflict and active research. In cellular models of LB-like pathology, the addition of exogenous PFFs to hippocampal neurons has resulted in the aggregation of endogenous aSyn associated with a reduction in levels of many synaptic proteins and eventually cell death (Volpicelli-Daley et al., 2011). Additionally, animal models based on the injection of PFFs showed increased neuronal loss (Luk, Kehm, Carroll, et al., 2012b; Luk, Kehm, Zhang, et al., 2012). On the other hand, the use of lentiviral vectors expressing mutant forms of aSyn, which have a higher propensity to form oligomers, resulted in marked toxicity and significant depletion of dopaminergic neurons in the brains of infected animals compared to mutants favoring fibril formation (Winner et al., 2011). After injection into rodents brains, PFFs rather than oligomers were the major toxic species to induce

significant loss of dopaminergic cells and projecting axons (Peelaerts et al., 2015). Two recent studies have demonstrated that increasing the dosage of aSyn PFFs can accelerate the cytotoxicity and subsequent neuronal loss in mouse hippocampal neurons. Comprehensive studies that compare the cytotoxic effects of different aSyn species are relatively sparse in the scientific literature, and many of these studies lack proper control. One study from our group has demonstrated that no significant differences in the cytotoxicity effects were observed in SH-SY5Y neuroblastoma cells exposed shortly to monomers, oligomers, and PFFs (Diógenes et al., 2012). In our work, we used all the different species in the lower concentration range that was reported to be less toxic in the short term (Volpicelli-Daley et al., 2014b). We observed mainly mouse hippocampal neurons treated with PFFs species to be the most affected by the neurotoxic effects of these species compared to cells treated with monomers and oligomers. The effects of different aSyn species treatments on the biochemical levels of pre- and post-synaptic proteins have been reported in two studies. However, these studies used aSyn PFFs as the experimental condition and PBS as the control. These studies have shown that exposure of hippocampal neuronal cultures to PFFs resulted in seeding the aggregation of endogenous aSyn associated with a reduction in synaptic protein levels including synaptic vesicle-associated SNARE proteins (Mahul-Mellier et al., 2020; Volpicelli-Daley et al., 2011). More importantly, the decrease in synaptic protein levels was reported to occur at later time points in parallel with the formation and maturation of LB-like pathology (Mahul-Mellier et al., 2020). In our study, we did a comprehensive comparison of all aSyn species. In agreement with the current findings, PFFs-treated neurons showed a higher aggregation for endogenous aSyn accompanied by a significant reduction in the levels of the presynaptic protein VAMP2, and the postsynaptic protein PSD95. This effect was observed only at DIV 26 but not DIV 21. However, exposure to oligomers and monomers did not show any differences in protein levels. Our study not only aligns with this established understanding but extends beyond just PFFs to provide new insights into the comparative effects of different aSyn species. This is of high importance since many

studies focus on one species over another. Furthermore, many studies do not check the levels of endotoxins when using just PFFs or oligomers and PBS as a control. Since these exogenous species are prepared from recombinant aSyn, it is expected that endotoxins levels differ from one preparation to another, and this issue needs to be taken into consideration. To make sure the observed effects are due entirely to one species without any confounding effects from potential endotoxins present, it is usually recommended to either use some kits to remove endotoxins to the minimum levels or at least use monomers from the same batch as a control.

We think that within the experimental setting and concentration used, PFFs are more damaging to the cells based on initial cytotoxicity assays.

Since synaptic alterations usually precede neuronal cell death and since aSyn pathology emerges first at the synaptic locations where aSyn exerts important physiological roles, several investigations have looked at the effects of different aSyn species with regard to synaptic homeostasis and synaptotoxicity. The functional alterations that take place at the synapse after exposure to different aSyn species have been studied by multiple research groups. Prior to neuronal cell death, early changes and events could take place at the synapse, and these changes can be tracked using several assays. Pathological changes that could take place include a reduction in synaptic transmission, changes in synaptic plasticity such as long-term potentiation (LTP) and long-term depression (LTD), changes in synaptic vesicle recycling and neurotransmitter release, and structural and morphological changes of synapses such as the number or size of dendritic spines. aSyn oligomers synaptotoxcity has been documented in several studies (B.-K. Choi et al., 2013; Trudler et al., 2021; Yoo et al., 2021). The impacts of aSyn oligomers have been manifested as reductions in neuron excitability, impaired LTP, decreased neuron firing, and increased membrane conductance. Moreover, in a human iPSC-based model, oligomerization of aSyn led to substantial degeneration of synaptic structures (Prots et al., 2018). Exposure to PFFs was also associated with disruption of neuronal excitability and network connectivity (Shrivastava et al., 2020; Volpicelli-Daley et al., 2011). A recently published study has

demonstrated that induction of endogenous aSyn aggregation after PFFs treatment resulted in a reduction in the synaptic activity of both excitatory glutamatergic and inhibitory GABAergic neurons, and this effect appears to be dose-dependent (Zhu et al., 2019). Again, comparative studies for all species regarding the effects on synaptic performance are lacking. To the best of our knowledge, one study has investigated the effects of different exogenous aSyn species on synaptic transmission. In this study, hippocampal slices were incubated with 500 nM aSyn monomers, oligomers, and PFFs for 90 minutes. Interestingly, impaired LTP was observed only in slices exposed to oligomeric species (Diógenes et al., 2012). In our work, we followed two approaches, measuring spontaneous neuronal activity using MEA experiments and quantifying synaptic vesicles recycling through measuring the fluorescence intensity of SYTG1. For MEA experiments, we treated hippocampal neurons at DIV 14 with different species and measured neuronal firing activity at DIV 20. We selected this day for this type of assay as neurons are already mature at this time point, and we wanted to check what would be the effect of different species when the neurons are already mature. Our findings showed notable effects on overall neuronal activity. PFFs exposure has resulted in a significantly lower mean firing rate one week after treatment. A reduction in the mean firing rate of neurons is consistent with several studies that found deleterious effects for PFFs on synaptic performance (Shrivastava et al., 2020). In contrast, no significant reductions in neuronal activity were observed in neurons exposed to monomers and oligomers. However, both PFFs and oligomeric species appeared to decrease synaptic vesicles recycling activity compared to monomeric aSyn, as evidenced by decreased fluorescence intensity of SYTG1. Our results showed that deleterious effects of aSyn oligomers and PFFs affect neuronal signaling and neurotransmitter release though disturbing synaptic vesicles recycling. Our results support the synaptotoxic effects of oligomers and PFFs on synaptic vesicles trafficking and that some synpatotoxcities are assay-dependent which could reflect different targeted mechanisms. In conclusion, our data suggest PFFs have more harmful effects at the synapses, but toxicity from oligomers has also been observed. Our data point to

seeding dependent and independent mechanisms attributed to synaptotoxcitits observed upon exposure to different species.

4.2 Recombinant aSyn: Extensively used in PD research with no standard purification protocol.

Several models of PD have been developed to recapitulate many of the clinical and pathological features observed in PD. Among these important models is one that relies on the use of exogenous aSyn PFFs and oligomers. The use of these exogenous species has contributed to a more comprehensive understanding of several pathological events and mechanisms behind PD. When injected into animals' brains, PFFs initiate neurodegeneration and cause behavioral impairments similar to those taking place in PD. Although multiple research groups have performed several studies in the PD field based on PFFs and oligomer models, consistency in the production of these species is a major challenge and varies among different labs. Since aSyn PFFs are being used heavily, a set of guidelines regarding the preparation and use of the PFFs model has been developed by the Michael J Fox Foundation in an attempt to increase the reducibility of such preparations. Although different conditions affecting aSyn transformations have extensively been studied, unexplained vitiations between experiments, batches, and laboratories concerning its aggregation propensity continue to pose challenges in the field.

aSyn used for the preparation of different oligomeric and PFFs species or for seeding assays is usually produced in *E. coli*. However, different production and purification protocols for aSyn in use are described in the literature (Al-Azzani et al., 2022). Upon reviewing all the protocols available in the literature, we observed that aSyn purification methods in use differ in many stages of its production, and sometimes it exists differences within one protocol from one research group to another. Although aSyn is considered an unfolded protein in solution, a dynamic ensemble of conformations coexists in equilibrium, and certain confirmations are more susceptible to aggregation than others (Stephens, Zacharopoulou, et al., 2020). In our

study, we hypothesized that any variations in the purification methods, even slight changes, can have an impact on the protein surrounding environment, thereby influencing the distribution of different conformations and ultimately resulting in different aggregation propensities. One of these differences that we found is that the composition of bacterial pellet extraction buffer varies widely among different protocols in salt concentration, where the NaCl concentration range in these buffers was 0-0.75 M. So, in our study, we decided to try to use either an extraction buffer containing ''No salt'' or ''0.75 M'' NaCl, and to see how aggregation properties could differ for aSyn extracted and purified under both conditions. We were interested in doing these since prepared aSyn is ultimately used for the preparation of oligomeric or PFFs species that will be used for downstream applications in several labs and studies. Surprisingly, we observed that differences in production protocols can affect the aggregation properties of purified aSyn which in turn impacts the interpretation of experimental data. ''No salt'' extracted aSyn exhibited a slower aggregation profile and a decreased overall ThT aggregation behavior compared to aSyn extracted in a ''High salt'' buffer. Furthermore, when loading aSyn samples purified from both conditions into the size exclusion column, a small second peak was observed at an elution volume of 19 mL in the chromatogram of the aSyn extracted from the "No salt" sample. Although samples from the second peak were loaded to SDS-PAGE and agarose gel stained with ethidium bromide in order to check if there is protein degradation and nucleic acids contamination, respectively, we cannot rule out that a degradation product of aSyn is present, and that this may affect the aggregation, or nucleic acid contamination, likely due to low abundance. If we interpret the second peak as a possible aSyn degradation product, this could signify that the presence of salt during aSyn extraction and purification helps maintain its stability. This might become more understandable upon detailed mass spectrometry analyses of the second peak.

Despite all of these issues, our study clearly highlights the importance of standardized purification protocols for aSyn research. Our findings support a recent

study that addressed a different aspect of aSyn purification protocols, where they found a difference in the aggregation kinetics when comparing different protocols (Stephens, Matak-Vinkovic, et al., 2020). Considering that aSyn produced through recombinant methods is frequently utilized to model the pathology of PD in cellular and animal models, it is crucial that monomeric aSyn is produced with rigorous attention, and under consistent conditions in an attempt to maintain aSyn purity and quality and to minimize inter-laboratory variations that make the interpretation of findings more complicated. Therefore, we propose that various laboratories should genuinely collaborate in order to first perform a systematical evaluation for the influence of crucial stages in the production and purification protocols used and second to design a more generalized protocol with slight differences, thus facilitating the study of aSyn physiological and pathological aspects among different research groups (Al-Azzani et al., 2022).

4.3 Identification of aSyn interactome in isolated synaptic vesicles

Certainly, aSyn has important roles in the synapse, as shown in several studies. The primary known function of aSyn is typically associated with its role in regulating synaptic vesicle trafficking and neurotransmitter release (Burré et al., 2010b; Gao et al., 2023). The process of synaptic vesicle docking and exocytosis require the assembly of several proteins from both the synaptic vesicle membrane and the plasma membrane (Sudhof & Rizo, 2011). aSyn has important roles in facilitating this process through interaction with proteins of this assembly, the so-called SNARE complex. However, it is thought that aSyn functions are not limited to this process but involve other processes that collectively enhance synaptic performance (Gao et al., 2023). Being enriched in synaptic vesicles, aSyn is expected to play several important synaptic roles through its interactome network. Indeed, although aSyn has been shown to interact with a number of synaptic proteins, the overall picture of its functions and of its interacting network remains largely unknown, and this gap in knowledge restricted our comprehension of the exact roles and mechanisms behind synaptic localization of

aSyn. To address this, we isolated synaptic vesicles from adult mice brains and followed pulldown and proteomic approaches to identify specific interacting partners of aSyn in isolated synaptic vesicles.

Some studies have reported interactors for aSyn at the synapse. The interaction with SNARE complex proteins is well established. Specifically, the direct interaction of aSyn with SNARE-protein VAMP2 from synaptic vesicles triggers SNARE complex assembly. Additionally, aSyn has been reported to contribute to the maintenance and reorganization of the SNARE complex, which ultimately affects exocytosis and neurotransmitter release (Yoo et al., 2023). The regulatory role of aSyn in exocytosis and neurotransmitter release is also supported by studies using knockout or overexpression models of the aSyn in mice (Murphy et al., 2000; Sun et al., 2019). aSyn has also been shown to interact with synaptic vesicle glycoprotein SV2C from WT mice (Dunn et al., 2017a). SV2 family proteins are present in synaptic vesicles and have been documented to enhance the exocytosis of synaptic vesicles by making them sensitive to calcium (Wan et al., 2010). Furthermore, SV2C was found to be highly expressed in dopaminergic neurons of SN, to modulate dopamine release, and its genetic deletion leads to a decrease in the synaptic release of dopamine (Dunn et al., 2017b). Calcium/calmodulin-dependent protein kinase II gamma CAMK2G, which plays important roles in synaptic plasticity and synaptic neurotransmission, has been reported to interact with aSyn oligomers in primary hippocampal neurons (Diggelen et al., 2020). In consistency with these findings, our data also revealed interactions for aSyn with SV2C and CAMK2G, indicating that aSyn, through its interactions with many synaptic proteins such as SV2C and CAMK2G, plays a crucial role in regulating various aspects of synaptic function. Other potential novel interactors for aSyn have been identified. Among these are syntaxin 12, syntaxin-binding protein 1, and syntaxin 7, all of which are considered parts of the SNARE complex that is crucial for synaptic vesicle docking (Südhof & Rizo, 2011). Such interactions strengthen the known roles of aSyn in modulating SNARE complex assembly. The presence of Ras-related proteins Rab-33B and Rab-33A among the potential interactors is interesting. These have been

associated with the vesicles trafficking and turnover of synaptic vehicles (Binotti et al., 2016). Secretory carrier-associated membrane proteins 1 and 5 (SCAMP1 and SCAMP5) are thought to play roles in exocytosis (U. Lee et al., 2021; Zhao et al., 2014). Additionally, synaptogyrin 3 was among the top potential interacting partners for aSyn in our study. This protein has been implicated in dopamine reuptake and recycling through interacting with dopamine transporter (DAT) (P. W. Ho et al., 2023). Interestingly, the levels of this protein were shown to be lower in the brains of PD patients and in the SN of toxin-induced PD mouse models (Miller et al., 2004; Palese et al., 2019; Simunovic et al., 2009). Our data suggest a potential mechanism by which aSyn can affect dopamine homeostasis in the context of PD. This interaction could be of significant importance since both dopamine and aSyn have been associated with the pathogenesis of PD. However, we first need to validate such interactions in order to address the context of these interactions under physiological and pathological conditions.

Furthermore, we performed GO enrichment analysis using the whole list of 126 proteins in order to concentrate on the enriched biological processes, molecular functions, and cellular components aSyn is potentially interacting with. GO enrichment analysis is an effective tool as it 1) provides a better interpretation of the biological meaning of a large set of data, 2) minimizes the complexity of proteomics data by grouping functionally related proteins together into clusters, facilitating data interpretation and management, and 3) helps us by selecting the most biologically significant enriched groups.

Our findings suggest that aSyn participates in several aspects with regard to synaptic function and regulation. We found aSyn to interact with enriched biological processes related to vesicle-mediated transport, exocytosis, and synaptic signaling. Furthermore, and in association with this, protein domain-specific binding, SNARE binding, and syntaxin-1 binding were among the top enriched molecular functions aSyn is associated with. Our data align with our current understanding of the integral roles for aSyn in regulating synaptic function. aSyn has been reported to mediate these

roles by working as a chaperone, interacting with SNARE complex proteins, and regulating synaptic vesicle pools (Burré et al., 2014).

Interestingly, we reported aSyn to be present in biological processes associated with neuron development and neuronal projection development. This suggests aSyn interacts with proteins that are important for neurogenesis and maturation of synapses, axonal and dendritic growth, and stabilizing the synaptic structures. We also noticed aSyn to be enriched in neuron projection and axons, which align with enriched biological processes. Furthermore, aSyn is also enriched in molecular functions associated with cytoskeletal protein binding. Our data suggest aSyn mediated synaptic function is broader and extends to include roles in modulating synapses architecture, playing roles at the structural and functional levels. Down-regulation of biological pathways associated with neuronal development has been observed in previous research from our group that conducted a transcriptional analysis using RNA sequencing on the midbrain of six-month-old A30P mice (Paiva et al., 2018b). In our case, we used WT mice, which could mean aSyn under physiological conditions is, in fact, interacting physiologically with proteins associated with biological processes related to neuronal development, and this interaction is lost under pathological conditions.

In conclusion, our findings suggest a number of interesting new potential interacting candidates for aSyn in synaptic vesicles emphasizing the key roles of aSyn in the modulation of synaptic functions. Due to time constraints and the unexpected difficulties, we faced in getting animals within the doctoral period, we could not do the further experiments needed to validate these interactions. We think our data are promising and would provide a strong basis for future experiments. Future experiments will not only be to validate such interactions but also explore the functional and pathological relevance of these interactions.

4.4 Identification of general aSyn interacting partners using SILAC experiments

aSyn is a key player not only in the pathogenesis of PD but has also been documented by several studies for some physiological roles, particularly in synapses.

However, aSyn is not present just at the synapse, it has multiple cellular localizations and has been detected in other non-neuronal tissues. Furthermore, little is known about aSyn overall biological roles; even its functions at the synapse are not fully understood. Despite its importance, aSyn precise interaction network has remained largely unexplored, and few interacting partners have been reported. Identification of aSyn interacting candidates will resolve its various roles in health and disease.

An increasing body of evidence supporting aSyn nuclear localization and functions has been reported. Although the functions of aSyn in the nucleus are not as well understood, aSyn has been reported to interact with histones, modulate gene expression, affect chromatin remodeling, and participate in DNA- and RNA-related biological processes (D. H. Ho et al., 2023a; Pavlou et al., 2017; Pinho et al., 2019; Surguchov, 2023). Furthermore, nuclear aSyn was recently documented to be present in healthy human brains, and its phosphorylation at S129 was higher in DLB patients (Koss et al., 2022). Additionally, the downregulation for transcription of DNA repair genes, and the increase in DNA damage by oxidative species have been suggested to play a role in the neurotoxicity observed under aSyn overexpression systems (Milanese et al., 2018; Paiva et al., 2017). However, how aSyn regulates all these suggested processes, and the pathological implications are still largely unknown. Furthermore, there is still no clear answer to why aSyn is present in many neuronal and non-neuronal cells. Therefore, in our study, we hypothesized that aSyn known and unknown roles are expected to be related to its interactome networks, which are largely unknown. In our study, we also looked not only for its interactions at the synapse, as discussed in the previous section, but also beyond that to investigate its general acting partners. By gaining insights into the interactome of aSyn, we could identify novel molecular mechanisms and pathways related to its physiological and pathological functions. For this purpose, we used HEK293 cells employing the SIALC approach. By using isotopically labeled cells, our SILAC proteomics data suggest many potential interacting partners for endogenous aSyn in GFP-expressing cells compared with cells overexpressing WT aSyn or A30P aSyn. It is noteworthy to

mention that naïve HEK293 cells express endogenous levels of aSyn (B. R. Lee & Kamitani, 2011). Under overexpression conditions, these interactions seem to be lost, as we detected only aSyn highly enriched in these conditions but no associated interacting partners in both replicates. Although these data seem unexpected, we think that the aSyn overexpression potentially resulted in the sequestration of aSyn into aggregates, and therefore making soluble aSyn unavailable for interaction with many proteins. Although this assumption needs to be validated, reductions in soluble somatic and nuclear aSyn are associated with aggregation of endogenous aSyn (Osterberg et al., 2015).

Interestingly, compared with cells overexpressing WT aSyn, we found many potential interacting candidates for aSyn in GFP control cell line, and most of these interacting partners have nuclear localization. Many of these proteins, including (PNO1, TSR1, LTV1, NOB1, BYSL) have roles in the biogenesis and processing of ribosomal RNA pathways. Our data support existing and increasing evidence for aSyn nuclear involvements. Furthermore, these potential interacting partners might provide a mechanistic explanation of how aSyn is related to some biological processes under physiological and pathological conditions. Interestingly, aSyn has been reported to be involved in RNA biogenesis, and its overexpression was associated with decreased ribosomal biogenesis and impairment of rRNA processing (D. H. Ho et al., 2021, 2023b; Popova et al., 2021). Our findings also point to the involvement of aSyn in chromosome stability and condensation processes through potential interactors NCAPH and NCAPG, which are essential components of the condensin complex that is important for chromatin condensation. Many studies have shown that aSyn interacts with histones and binds to DNA, suggesting nuclear function (Kontopoulos et al., 2006). A recent study found that aSyn knocking out leads to an increase in DNA double-strand break (DSB), suggesting a role for aSyn in DNA repair mechanisms (Schaser et al., 2019b). Our finding that NCAPH and NCAPG may interact with aSyn could provide a novel mechanism through which aSyn affects chromatin structure and function. In addition, since aSyn has been implicated in modulating gene expression, one possible

explanation for this could be through these potential interactors modulate the condensation status of chromatin and consequently affecting the accessibility of DNA for being available for transcription and translation processes.

Our data also suggest potential interaction for endogenous aSyn with the tyrosine-protein kinase Fer. This kinase is a non-transmembrane receptor tyrosine kinase that is involved in the regulation of the actin cytoskeleton, microtubule assembly, and cell adhesion and has been reported to be involved in synapses organization and function (S.-H. Lee et al., 2008). This potential interaction could provide extra information about how aSyn is involved in the cytoskeleton by modulating Fer activity. Furthermore, it could provide an additional mechanism for how aSyn regulates synaptic vesicle exocytosis. In the study mentioned above, it was noticed that depletion of FER in presynaptic neurons abolished excitatory synapse formation and synaptic transmission.

When comparing the GFP control cell line with the one that overexpresses A30P, we again found that PNO1, TSR1, LTV1, NOB1, and BYSL are potential interacting partners for endogenous aSyn. These findings further support the interactions that were observed when comparing the GFP control cell line with WT aSyn overexpressing cells. Our data also reinforce the hypothesis that overexpression conditions lead to a reduction in aSyn interactions.

Finally, our SILAC proteomics data suggest these novel and interesting interactions that could expand our knowledge about the biological roles of aSyn. They support the important roles for aSyn in the nucleus and its interactions with DNA and RNA related processes. However, we should mention that these data need further experimental validation. Despite the preliminary nature of our data, the suggested interactions have biological supporting relevance in the available literature, and these aSyn interacting proteins provide the background for future experiments.

4.5 The effect of aSyn glycation at the synapse

aSyn undergoes several PTM under physiological and pathological conditions. High levels of aSyn glycation end products AGEs have been reported in the brains of patients with synucleinopathies and are detected in LBs (Castellani et al., 1996; Choi & Lim, 2010; Dalfo et al., 2005; Munch et al., 2000). Furthermore, aSyn glycation has been implicated in neurodegeneration. Although aSyn glycation by MGO has not been extensively studied, the effects of MGO on aSyn aggregation are well documented. Using many physiologically relevant glycating agents, previous studies from our group indicated that glycation promotes aSyn oligomerization in vitro and modulates its aggregation in cellular models. In addition, aSyn glycation was not only causing cytotoxicity but also affecting many cellular pathways, including major protein clearance systems. MGO glycation was also associated with dopaminergic neuron loss, altered dopaminergic signaling, and impaired neuronal synaptic transmission (Vicente Miranda et al., 2017). A recently published study found that aSyn glycation by MGO accelerates sensorimotor and cognitive alterations similar to those observed in PD (Chegão et al., 2022). In most of these studies, the early pathological changes at the synapse were not well studied, and MGO was used directly, either injected into mice brains or added to cells in cellular models to glycate endogenous aSyn. In our study, we glycated recombinant aSyn in vitro and checked the effects of the glycated aSyn compared to controls on synaptic function. In alignment with the mentioned studies, we found higher cytotoxicity in neuronal cells exposed to glycated aSyn compared with unglycated aSyn. When checking the seeding capacity, we could not detect any significant differences between glycated and unglycated aSyn species concerning the aggregation of endogenous aSyn as reflected by pS129 levels. In a recent study, using aSyn seeding model in SH-SY5Y, no significant differences in pS129 levels were found when comparing the treatment between aSyn-MGO and unglycated aSyn (Farzadfard, König, et al., 2022). In our study, the levels of synaptic proteins were comparable in cells exposed to glycated and

unglycated aSyn. Furthermore, spontaneous neuronal activity was not affected by the glycation status of aSyn. This is in contrast to a previous study that showed that synaptic transmission is impaired in hippocampal slices exposed to aSyn-MGO (Vicente Miranda et al., 2017). However, this previous study used a higher concentration than what we used and different experimental setup. In the mentioned study, hippocampal slices were incubated for 90 minutes with the different species, followed by extracellular recordings of field excitatory post-synaptic potentials (fEPSPs). On the other hand, we used MEA system and checked spontaneous neuronal activity in mouse hippocampal neurons 7 days post-exposure to these species. We think the difference can be related to using different concentrations, different treatment approaches, and different parameters tested.

When comparing our results in general with studies that used MGO directly to glycate endogenous aSyn either in cellular or animal models, the fact that we could not observe significant effects when using in vitro prepared glycated aSyn by MGO can be attributed to several explanations. It is possible that glycated aSyn species prepared in solution are not similar to the species prepared under cellular context. Within cells, a totally different environment exists, and other interactions and modifications affect the formation of glycated products. The MGO concentration and the duration of the glycation reaction are different in both settings. Also, different cell types and experimental conditions represent another factor of variation . However, given the simplicity of neuronal culture models and their feasibility to use many assays and study several mechanisms, further investigation plans can include using higher concentrations of MGO-glycated aSyn, using other glycating agents to glycate aSyn, and also using MGO as an additional possible positive control in these assays.

5. Conclusions

synaptic alterations and dysfunction are among the initial pathological events that precede the loss of dopaminergic neurons and the appearance of motor symptoms. aSyn, which has important physiological roles at the synapse, aggregates under pathological conditions and accumulates inside neuronal cells, ultimately forming LB, a main pathological hallmark in PD and other synucleinopathies. This aggregation process has been associated with PD pathology and was reported to start at synapse and leads initially to synaptotoxicity. Therefore, multiple investigations are trying to study the effect of aSyn aggregation process at the synapse and because physiological roles are primarily related to the synapse. Despite several research efforts, it is still not clear when these pathological changes appear at the synapse, and which species are more implicated in the processes of synaptic dysfunction.

Our study provides further evidence of the toxic effects of some aSyn forms that take place in the synapse prior to the cytotoxicity, a fundamental feature known in PD. In our study, we found that most harmful effects on the synapse are associated with the exposure to aSyn PFFs species, as reflected by the increased cytotoxicity and the reduction in the levels of synaptic proteins. We think that the seeding potential of species plays an important role in their synaptotoxic effects, as the aggregation of endogenous aSyn was observed mainly neurons exposed to PFFs species. However, we found that oligomeric aSyn caused comparable functional synaptic alterations to PFFs with regard to synaptic vesicles recycling activity when measuring the uptake of SYTG1 antibody. Our data suggest different synaptic processes to be affected by different species, and toxic effects are not limited to the seeding potential of each species, but other mechanisms are involved.

As exogenous aSyn species are used heavily by many research groups in the field of PD, our studies highlighted the importance of standardizing the protocols used for the production and purification of monomeric aSyn. In our study, we found that changes in the composition of the buffer used for extracting aSyn from bacterial pellets affect its final aggregation propensity. Given that aSyn is used to prepare oligomeric

and PFFs species, we think that changes in the starting material can affect the quality of these prepared species, leading to inconsistencies in the findings of many studies and further complicating the interpretation of such data.

In our study, we found many potential and interesting interacting partners for aSyn in synaptic vesicles. Our data support many physiological processes aSyn is involved in. Furthermore, our data indicate potential interacting partners for aSyn that are beyond its traditional roles. We found that aSyn is possibly interacting with proteins important for neuron development and neuronal projection development. Although these interactions still need validation, we think that they are promising interacting candidates and suggest aSyn to not only be involved in synaptic vesicles exocytosis process but also in organizing synapse architecture and development.

Our data from SILAC experiments pointed to many nuclear roles for aSyn supporting increasing evidence for nuclear aSyn. Although the data are to be validated, we found a number of potential novel interacting candidates for aSyn with proteins involved in RNA and DNA processes. These proteins have biological relevance that supports our findings.

Finally, our data from glycated aSyn did not show significant differences on the synaptic function. However, we observed more cytotoxicity in neuronal cultures exposed to glycated species.

In conclusion, our study showed different synaptotoxicity profiles for aSyn PFFs and oligomers, highlighting the importance of studying more these species together, and analyzing why, in some assays, oligomers toxicity is more pronounced. It is also important for the PD scientific community to perform efforts to produce a standard protocol for producing aSyn monomers for better interpretation of data across different studies. Finally, we think that understanding aSyn interacting network would lead to a better understanding of its physiological and pathological roles.

6. References

Aarsland, D., Bronnick, K., Williams-Gray, C., Weintraub, D., Marder, K., Kulisevsky, J., Burn, D., Barone, P., Pagonabarraga, J., Allcock, L., Santangelo, G., Foltynie, T., Janvin, C., Larsen, J. P., Barker, R. A., & Emre, M. (2010). Mild cognitive impairment in Parkinson disease: A multicenter pooled analysis. *Neurology*, *75*(12), 1062–1069. https://doi.org/10.1212/WNL.0b013e3181f39d0e

Abdelmotilib, H., Maltbie, T., Delic, V., Liu, Z., Hu, X., Fraser, K. B., Moehle, M. S., Stoyka, L., Anabtawi, N., Krendelchtchikova, V., Volpicelli-Daley, L. A., & West, A. (2017). α-Synuclein fibril-induced inclusion spread in rats and mice correlates with dopaminergic Neurodegeneration. *Neurobiology of Disease*, *105*, 84–98. https://doi.org/10.1016/j.nbd.2017.05.014

Alam, P., Bousset, L., Melki, R., & Otzen, D. E. (2019). α-synuclein oligomers and fibrils: a spectrum of species, a spectrum of toxicities. In *Journal of Neurochemistry* (Vol. 150, Issue 5). https://doi.org/10.1111/jnc.14808

Al-Azzani, M., König, A., & Outeiro, T. F. (2022). Production of Recombinant Alpha-Synuclein: Still No Standardized Protocol in Sight. *Biomolecules*, *12*(2), 324. https://doi.org/10.3390/biom12020324

Anderson, J. P., Walker, D. E., Goldstein, J. M., de Laat, R., Banducci, K., Caccavello, R. J., Barbour, R., Huang, J., Kling, K., Lee, M., Diep, L., Keim, P. S., Shen, X., Chataway, T., Schlossmacher, M. G., Seubert, P., Schenk, D., Sinha, S., Gai, W. P., & Chilcote, T. J. (2006). Phosphorylation of Ser-129 Is the Dominant Pathological Modification of α-Synuclein in Familial and Sporadic Lewy Body Disease. *Journal of Biological Chemistry*, *281*(40), 29739–29752. https://doi.org/10.1074/jbc.M600933200

Atanassov, I., & Urlaub, H. (2013). Increased proteome coverage by combining PAGE and peptide isoelectric focusing: Comparative study of gel-based separation approaches. *Proteomics*, *13*(20). https://doi.org/10.1002/pmic.201300035

Atik, A., Stewart, T., & Zhang, J. (2016). Alpha-Synuclein as a Biomarker for Parkinson's Disease. *Brain Pathology*, *26*(3), 410–418. https://doi.org/10.1111/bpa.12370

Azeredo da Silveira, S., Schneider, B. L., Cifuentes-Diaz, C., Sage, D., Abbas-Terki, T., Iwatsubo, T., Unser, M., & Aebischer, P. (2008). Phosphorylation Does Not Prompt, Nor Prevent, the Formation of -synuclein Toxic Species in a Rat Model of Parkinson's Disease. *Human Molecular Genetics*. https://doi.org/10.1093/hmg/ddn417

Baltic, S., Perovic, M., Mladenovic, A., Raicevic, N., Ruzdijic, S., Rakic, L., & Kanazir, S. (2004). α-synuclein is expressed in different tissues during human fetal development. *Journal of Molecular Neuroscience*, *22*(3). https://doi.org/10.1385/JMN:22:3:199

Barker, R. A., & Björklund, A. (2020). Animal Models of Parkinson's Disease: Are They Useful or Not? *Journal of Parkinson's Disease*, *10*(4). https://doi.org/10.3233/JPD-202200

Bartels, T., Choi, J. G., & Selkoe, D. J. (2011). α-Synuclein occurs physiologically as a helically folded tetramer that resists aggregation. *Nature*, *477*(7362). https://doi.org/10.1038/nature10324

Bayer, T. A., Jäkälä, P., Hartmann, T., Egensperger, R., Buslei, R., Falkai, P., & Beyreuther, K. (1999). Neural expression profile of α-synuclein in developing human cortex. *NeuroReport*, *10*(13). https://doi.org/10.1097/00001756-199909090-00019

Bellucci, A., Navarria, L., Zaltieri, M., Falarti, E., Bodei, S., Sigala, S., Battistin, L., Spillantini, M., Missale, C., & Spano, P. (2011). Induction of the unfolded protein response by α-synuclein in experimental models of Parkinson's disease. *Journal of Neurochemistry*, *116*(4). https://doi.org/10.1111/j.1471-4159.2010.07143.x

Binotti, B., Jahn, R., & Chua, J. (2016). Functions of Rab Proteins at Presynaptic Sites. *Cells*, *5*(1), 7. https://doi.org/10.3390/cells5010007

Blesa, J., & Przedborski, S. (2014). Parkinson's disease: Animal models and dopaminergic cell vulnerability. *Frontiers in Neuroanatomy*, *8*(DEC). https://doi.org/10.3389/fnana.2014.00155

Bohnen, N. I., Albin, R. L., Koeppe, R. A., Wernette, K. A., Kilbourn, M. R., Minoshima, S., & Frey, K. A. (2006). Positron emission tomography of monoaminergic vesicular binding in aging and Parkinson disease. *Journal of Cerebral Blood Flow and Metabolism*, *26*(9). https://doi.org/10.1038/sj.jcbfm.9600276

Bonifati, V., Rizzu, P., Van Baren, M. J., Schaap, O., Breedveld, G. J., Krieger, E., Dekker, M. C. J., Squitieri, F., Ibanez, P., Joosse, M., Van Dongen, J. W., Vanacore, N., Van Swieten, J. C., Brice, A., Meco, G., Van Duijn, C. M., Oostra, B. A., & Heutink, P. (2003). Mutations in the DJ-1 gene associated with autosomal recessive early-onset parkinsonism. *Science*, *299*(5604). https://doi.org/10.1126/science.1077209

Braak, H., Del Tredici, K., Rüb, U., De Vos, R. A. I., Jansen Steur, E. N. H., & Braak, E. (2003). Staging of brain pathology related to sporadic Parkinson's disease. *Neurobiology of Aging*, *24*(2). https://doi.org/10.1016/S0197-4580(02)00065-9

Braak, H., Rüb, U., Gai, W. P., & Del Tredici, K. (2003). Idiopathic Parkinson's disease: Possible routes by which vulnerable neuronal types may be subject to neuroinvasion by an unknown pathogen. *Journal of Neural Transmission*, *110*(5). https://doi.org/10.1007/s00702-002-0808-2

Brás, I. C., Xylaki, M., & Outeiro, T. F. (2020). Mechanisms of alpha-synuclein toxicity: An update and outlook. In *Progress in Brain Research* (Vol. 252). https://doi.org/10.1016/bs.pbr.2019.10.005

Bruderer, R., Bernhardt, O. M., Gandhi, T., Miladinović, S. M., Cheng, L. Y., Messner, S., Ehrenberger, T., Zanotelli, V., Butscheid, Y., Escher, C., Vitek, O., Rinner, O., & Reiter, L. (2015). Extending the limits of quantitative proteome profiling with data-independent acquisition and application to acetaminophen-treated three-dimensional liver microtissues. *Molecular and Cellular Proteomics*, *14*(5). https://doi.org/10.1074/mcp.M114.044305

Burré, J., Sharma, M., & Südhof, T. C. (2014). α-Synuclein assembles into higher-order multimers upon membrane binding to promote SNARE complex formation. *Proceedings of the National Academy of Sciences*, *111*(40). https://doi.org/10.1073/pnas.1416598111

Burré, J., Sharma, M., Tsetsenis, T., Buchman, V., Etherton, M. R., & Südhof, T. C. (2010a). α-Synuclein Promotes SNARE-Complex Assembly in Vivo and in Vitro. *Science*, *329*(5999), 1663–1667. https://doi.org/10.1126/science.1195227

Burré, J., Sharma, M., Tsetsenis, T., Buchman, V., Etherton, M. R., & Südhof, T. C. (2010b). α-Synuclein Promotes SNARE-Complex Assembly in Vivo and in Vitro. *Science*, *329*(5999), 1663–1667. https://doi.org/10.1126/science.1195227

Campioni, S., Carret, G., Jordens, S., Nicoud, L., Mezzenga, R., & Riek, R. (2014). The presence of an air-water interface affects formation and elongation of α-synuclein fibrils. *Journal of the American Chemical Society*, *136*(7). https://doi.org/10.1021/ja412105t

Cappai, R., Leck, S., Tew, D. J., Williamson, N. A., Smith, D. P., Galatis, D., Sharpies, R. A., Curtain, C. C., Ali, F. E., Cherny, R. A., Culvenor, J. G., Bottomley, S. P., Masters, C. L., Barnham, K. J., & Hill, A. F. (2005). Dopamine promotes α-synuclein aggregation into SDS-resistant soluble oligomers via a distinct folding pathway. *The FASEB Journal*, *19*(10). https://doi.org/10.1096/fj.04-3437fje

Cascella, R., Chen, S. W., Bigi, A., Camino, J. D., Xu, C. K., Dobson, C. M., Chiti, F., Cremades, N., & Cecchi, C. (2021). The release of toxic oligomers from α-synuclein fibrils induces dysfunction in neuronal cells. *Nature Communications*, *12*(1). https://doi.org/10.1038/s41467-021-21937-3

Chandra, S., Gallardo, G., Fernández-Chacón, R., Schlüter, O. M., & Südhof, T. C. (2005). α-Synuclein cooperates with CSPα in preventing neurodegeneration. *Cell*, *123*(3). https://doi.org/10.1016/j.cell.2005.09.028

Chartier-Harlin, M. C., Kachergus, J., Roumier, C., Mouroux, V., Douay, X., Lincoln, S., Levecque, C., Larvor, L., Andrieux, J., Hulihan, M., Waucquier, N., Defebvre, L., Amouyel, P., Farrer, M., & Destée, A. (2004). α-synuclein locus duplication as a cause of familial Parkinson's disease. *Lancet*, *364*(9440). https://doi.org/10.1016/S0140-6736(04)17103-1

Chegão, A., Guarda, M., Alexandre, B. M., Shvachiy, L., Temido-Ferreira, M., Marques-Morgado, I., Fernandes Gomes, B., Matthiesen, R., Lopes, L. V., Florindo, P. R., Gomes, R. A., Gomes-Alves, P., Coelho, J. E., Outeiro, T. F., & Vicente Miranda, H. (2022). Glycation modulates glutamatergic signaling and exacerbates Parkinson's disease-like phenotypes. *Npj Parkinson's Disease*, *8*(1), 51. https://doi.org/10.1038/s41531-022-00314-x

Chen, J., Aronow, B. J., & Jegga, A. G. (2009). Disease candidate gene identification and prioritization using protein interaction networks. *BMC Bioinformatics*, *10*(1), 73. https://doi.org/10.1186/1471-2105-10-73

Cheng, H. C., Ulane, C. M., & Burke, R. E. (2010). Clinical progression in Parkinson disease and the neurobiology of axons. In *Annals of Neurology* (Vol. 67, Issue 6). https://doi.org/10.1002/ana.21995

Chinta, S. J., Mallajosyula, J. K., Rane, A., & Andersen, J. K. (2010). Mitochondrial alpha-synuclein accumulation impairs complex I function in dopaminergic neurons and results in increased mitophagy in vivo. *Neuroscience Letters*, *486*(3). https://doi.org/10.1016/j.neulet.2010.09.061

Choi, B. K., Choi, M. G., Kim, J. Y., Yang, Y., Lai, Y., Kweon, D. H., Lee, N. K., & Shin, Y. K. (2013). Large α-synuclein oligomers inhibit neuronal SNARE-mediated vesicle docking. *Proceedings of the National Academy of Sciences of the United States of America*, *110*(10). https://doi.org/10.1073/pnas.1218424110

Choi, B.-K., Choi, M.-G., Kim, J.-Y., Yang, Y., Lai, Y., Kweon, D.-H., Lee, N. K., & Shin, Y.-K. (2013). Large α-synuclein oligomers inhibit neuronal SNARE-mediated vesicle docking. *Proceedings of the National Academy of Sciences*, *110*(10), 4087–4092. https://doi.org/10.1073/pnas.1218424110

Colla, E., Jensen, P. H., Pletnikova, O., Troncoso, J. C., Glabe, C., & Lee, M. K. (2012). Accumulation of toxic α-synuclein oligomer within endoplasmic reticulum occurs in α-synucleinopathy in vivo. *Journal of Neuroscience*, *32*(10). https://doi.org/10.1523/JNEUROSCI.5368-11.2012

Conway, K. A., Harper, J. D., & Lansbury, P. T. (1998). Accelerated in vitro fibril formation by a mutant α-synuclein linked to early-onset Parkinson disease. *Nature Medicine*, *4*(11). https://doi.org/10.1038/3311

Cooper, A. A., Gitler, A. D., Cashikar, A., Haynes, C. M., Hill, K. J., Bhullar, B., Liu, K., Xu, K., Strathearn, K. E., Liu, F., Cao, S., Caldwell, K. A., Caldwell, G. A., Marsischky, G., Kolodner, R. D., LaBaer, J., Rochet, J. C., Bonini, N. M., & Lindquist, S. (2006). α-synuclein blocks ER-Golgi traffic and Rab1 rescues neuron loss in Parkinson's models. *Science*, *313*(5785). https://doi.org/10.1126/science.1129462

Cox, J., & Mann, M. (2008). MaxQuant enables high peptide identification rates, individualized p.p.b.-range mass accuracies and proteome-wide protein quantification. *Nature Biotechnology*, *26*(12). https://doi.org/10.1038/nbt.1511

Danielson, S. R., Held, J. M., Schilling, B., Oo, M., Gibson, B. W., & Andersen, J. K. (2009). Preferentially increased nitration of α-synuclein at tyrosine-39 in a cellular oxidative model of Parkinson's disease. *Analytical Chemistry*, *81*(18). https://doi.org/10.1021/ac901176t

Danzer, K. M., Haasen, D., Karow, A. R., Moussaud, S., Habeck, M., Giese, A., Kretzschmar, H., Hengerer, B., & Kostka, M. (2007a). Different Species of α-Synuclein Oligomers Induce Calcium Influx and Seeding. *The Journal of Neuroscience*, *27*(34), 9220–9232. https://doi.org/10.1523/JNEUROSCI.2617-07.2007

Danzer, K. M., Haasen, D., Karow, A. R., Moussaud, S., Habeck, M., Giese, A., Kretzschmar, H., Hengerer, B., & Kostka, M. (2007b). Different Species of α-Synuclein Oligomers Induce Calcium Influx and Seeding. *The Journal of Neuroscience*, *27*(34), 9220–9232. https://doi.org/10.1523/JNEUROSCI.2617-07.2007

Danzer, K. M., Krebs, S. K., Wolff, M., Birk, G., & Hengerer, B. (2009). Seeding induced by α-synuclein oligomers provides evidence for spreading of α-synuclein pathology. *Journal of Neurochemistry*, *111*(1), 192–203. https://doi.org/10.1111/j.1471-4159.2009.06324.x

Delic, V., Chandra, S., Abdelmotilib, H., Maltbie, T., Wang, S., Kem, D., Scott, H. J., Underwood, R. N., Liu, Z., Volpicelli-Daley, L. A., & West, A. B. (2018). Sensitivity and specificity of phospho-Ser129 α-synuclein monoclonal antibodies. *Journal of Comparative Neurology*, *526*(12). https://doi.org/10.1002/cne.24468

Der-Sarkissiant, A., Jao, C. C., Chen, J., & Langen, R. (2003). Structural organization of α-synuclein fibrils studied by site-directed spin labeling. *Journal of Biological Chemistry*, *278*(39). https://doi.org/10.1074/jbc.M305266200

Devi, L., Raghavendran, V., Prabhu, B. M., Avadhani, N. G., & Anandatheerthavarada, H. K. (2008). Mitochondrial import and accumulation of α-synuclein impair complex I in human dopaminergic neuronal cultures and Parkinson disease brain. *Journal of Biological Chemistry*, *283*(14). https://doi.org/10.1074/jbc.M710012200

Diao, J., Burré, J., Vivona, S., Cipriano, D. J., Sharma, M., Kyoung, M., Südhof, T. C., & Brunger, A. T. (2013). Native α-synuclein induces clustering of synaptic-vesicle mimics via binding to phospholipids and synaptobrevin-2/VAMP2. *ELife*, *2*. https://doi.org/10.7554/eLife.00592

Dickson, D. W., Uchikado, H., Fujishiro, H., & Tsuboi, Y. (2010). Evidence in favor of Braak staging of Parkinson's disease. *Movement Disorders*, *25*(SUPPL. 1). https://doi.org/10.1002/mds.22637

Diggelen, F., Frank, S. A., Somavarapu, A. K., Scavenius, C., Apetri, M. M., Nielsen, J., Tepper, A. W. J. W., Enghild, J. J., & Otzen, D. E. (2020). The interactome of stabilized α-synuclein oligomers and neuronal proteins. *The FEBS Journal*, *287*(10), 2037–2054. https://doi.org/10.1111/febs.15124

Diógenes, M. J., Dias, R. B., Rombo, D. M., Vicente Miranda, H., Maiolino, F., Guerreiro, P., Näsström, T., Franquelim, H. G., Oliveira, L. M. A., Castanho, M. A. R. B., Lannfelt, L., Bergström, J., Ingelsson, M., Quintas, A., Sebastião, A. M., Lopes, L. V., & Outeiro, T. F. (2012). Extracellular Alpha-Synuclein Oligomers Modulate Synaptic Transmission and Impair LTP Via NMDA-Receptor Activation. *The Journal of Neuroscience*, *32*(34), 11750–11762. https://doi.org/10.1523/JNEUROSCI.0234-12.2012

Dunn, A. R., Stout, K. A., Ozawa, M., Lohr, K. M., Hoffman, C. A., Bernstein, A. I., Li, Y., Wang, M., Sgobio, C., Sastry, N., Cai, H., Caudle, W. M., & Miller, G. W. (2017a). Synaptic vesicle glycoprotein 2C (SV2C) modulates dopamine release and is disrupted in Parkinson disease. *Proceedings of the National Academy of Sciences*, *114*(11). https://doi.org/10.1073/pnas.1616892114

Dunn, A. R., Stout, K. A., Ozawa, M., Lohr, K. M., Hoffman, C. A., Bernstein, A. I., Li, Y., Wang, M., Sgobio, C., Sastry, N., Cai, H., Caudle, W. M., & Miller, G. W. (2017b). Synaptic vesicle glycoprotein 2C (SV2C) modulates dopamine release and is disrupted in Parkinson disease. *Proceedings of the National Academy of Sciences*, *114*(11). https://doi.org/10.1073/pnas.1616892114

El-Agnaf, O. M. A., Jakes, R., Curran, M. D., & Wallace, A. (1998). Effects of the mutations Ala30 to Pro and Ala53 to Thr on the physical and morphological properties of α-synuclein protein implicated in Parkinson's disease. *FEBS Letters*, *440*(1–2). https://doi.org/10.1016/S0014-5793(98)01419-7

Eliezer, D., Kutluay, E., Bussell, R., & Browne, G. (2001a). Conformational properties of α-synuclein in its free and lipid-associated states. *Journal of Molecular Biology*, *307*(4). https://doi.org/10.1006/jmbi.2001.4538

Eliezer, D., Kutluay, E., Bussell, R., & Browne, G. (2001b). Conformational properties of α-synuclein in its free and lipid-associated states 1 1Edited by P. E. Wright. *Journal of Molecular Biology*, *307*(4), 1061–1073. https://doi.org/10.1006/jmbi.2001.4538

Emamzadeh, F. N. (2016). Alpha-synuclein structure, functions, and interactions. In *Journal of Research in Medical Sciences* (Vol. 21, Issue 2). https://doi.org/10.4103/1735-1995.181989

Fares, M. B., Ait-Bouziad, N., Dikiy, I., Mbefo, M. K., Jovičić, A., Kiely, A., Holton, J. L., Lee, S. J., Gitler, A. D., Eliezer, D., & Lashuel, H. A. (2014). The novel Parkinson's disease linked mutation G51D attenuates in vitro aggregation and membrane binding of α-synuclein, and enhances its secretion and nuclear localization in cells. *Human Molecular Genetics*, *23*(17). https://doi.org/10.1093/hmg/ddu165

Fares, M. B., Maco, B., Oueslati, A., Rockenstein, E., Ninkina, N., Buchman, V. L., Masliah, E., & Lashuel, H. A. (2016). Induction of de novo a-synuclein fibrillization in a neuronal model for Parkinson's disease. *Proceedings of the National Academy of Sciences of the United States of America*, *113*(7). https://doi.org/10.1073/pnas.1512876113

Farzadfard, A., König, A., Petersen, S. V., Nielsen, J., Vasili, E., Dominguez-Meijide, A., Buell, A. K., Outeiro, T. F., & Otzen, D. E. (2022). Glycation modulates alpha-synuclein fibrillization kinetics: A sweet spot for inhibition. *Journal of Biological Chemistry*, *298*(5), 101848. https://doi.org/10.1016/j.jbc.2022.101848

Farzadfard, A., Pedersen, J. N., Meisl, G., Somavarapu, A. K., Alam, P., Goksøyr, L., Nielsen, M. A., Sander, A. F., Knowles, T. P. J., Pedersen, J. S., & Otzen, D. E. (2022). The C-terminal tail of α-synuclein protects against aggregate replication but is critical for oligomerization. *Communications Biology*, *5*(1), 123. https://doi.org/10.1038/s42003-022-03059-8

Fauvet, B., Mbefo, M. K., Fares, M. B., Desobry, C., Michael, S., Ardah, M. T., Tsika, E., Coune, P., Prudent, M., Lion, N., Eliezer, D., Moore, D. J., Schneider, B., Aebischer, P., El-Agnaf, O. M., Masliah, E., & Lashuel, H. A. (2012). α-Synuclein in central nervous system and from erythrocytes, mammalian cells, and Escherichia coli exists predominantly as disordered monomer. *Journal of Biological Chemistry*, *287*(19). https://doi.org/10.1074/jbc.M111.318949

Fayyad, M., Majbour, N. K., Vaikath, N. N., Erskine, D., El-Tarawneh, H., Sudhakaran, I. P., Abdesselem, H., & El-Agnaf, O. M. A. (2020). Generation of monoclonal antibodies against phosphorylated α-Synuclein at serine 129: Research tools for synucleinopathies. *Neuroscience Letters*, *725*. https://doi.org/10.1016/j.neulet.2020.134899

Fearnley, J. M., & Lees, A. J. (1991). Ageing and parkinson's disease: Substantia nigra regional selectivity. *Brain*, *114*(5). https://doi.org/10.1093/brain/114.5.2283

Flagmeier, P., Meisl, G., Vendruscolo, M., Knowles, T. P. J., Dobson, C. M., Buell, A. K., & Galvagnion, C. (2016). Mutations associated with familial Parkinson's disease alter the initiation and amplification steps of α-synuclein aggregation. *Proceedings of the National Academy of Sciences of the United States of America*, *113*(37). https://doi.org/10.1073/pnas.1604645113

Froula, J. M., Castellana-Cruz, M., Anabtawi, N. M., Camino, J. D., Chen, S. W., Thrasher, D. R., Freire, J., Yazdi, A. A., Fleming, S., Dobson, C. M., Kumita, J. R., Cremades, N., & Volpicelli-Daley, L. A. (2019). Defining α-synuclein species responsible for Parkinson's disease phenotypes in mice. *Journal of Biological Chemistry*, *294*(27), 10392–10406. https://doi.org/10.1074/jbc.RA119.007743

Fujita, Y., Ohama, E., Takatama, M., Al-Sarraj, S., & Okamoto, K. (2006). Fragmentation of Golgi apparatus of nigral neurons with α-synuclein-positive inclusions in patients with Parkinson's disease. *Acta Neuropathologica*, *112*(3). https://doi.org/10.1007/s00401-006-0114-4

Fujiwara, H., Hasegawa, M., Dohmae, N., Kawashima, A., Masliah, E., Goldberg, M. S., Shen, J., Takio, K., & Iwatsubo, T. (2002a). α-synuclein is phosphorylated in synucleinopathy lesions. *Nature Cell Biology*, *4*(2). https://doi.org/10.1038/ncb748

Fujiwara, H., Hasegawa, M., Dohmae, N., Kawashima, A., Masliah, E., Goldberg, M. S., Shen, J., Takio, K., & Iwatsubo, T. (2002b). α-Synuclein is phosphorylated in synucleinopathy lesions. *Nature Cell Biology*, *4*(2), 160–164. https://doi.org/10.1038/ncb748

Galesic, A., Rakshit, A., Cutolo, G., Pacheco, R. P., Balana, A. T., Moon, S. P., & Pratt, M. R. (2021). Comparison of N-Acetyl-Glucosamine to Other Monosaccharides Reveals Structural Differences for the Inhibition of α-Synuclein Aggregation. *ACS Chemical Biology*, *16*(1). https://doi.org/10.1021/acschembio.0c00716

Galvin, J. E., Schuck, T. M., Lee, V. M. Y., & Trojanowski, J. Q. (2001). Differential expression and distribution of α-, β-, and γ-synuclein in the developing human substantia nigra. *Experimental Neurology*, *168*(2). https://doi.org/10.1006/exnr.2000.7615

Gao, V., Briano, J. A., Komer, L. E., & Burré, J. (2023). Functional and Pathological Effects of α-Synuclein on Synaptic SNARE Complexes. *Journal of Molecular Biology*, *435*(1), 167714. https://doi.org/10.1016/j.jmb.2022.167714

Garcia-Esparcia, P., Hernández-Ortega, K., Koneti, A., Gil, L., Delgado-Morales, R., Castaño, E., Carmona, M., & Ferrer, I. (2015). Altered machinery of protein synthesis is region- and stage-dependent and is associated with α-synuclein oligomers in Parkinson's disease. *Acta Neuropathologica Communications*, *3*(1), 76. https://doi.org/10.1186/s40478-015-0257-4

Garcia-Reitböck, P., Anichtchik, O., Bellucci, A., Iovino, M., Ballini, C., Fineberg, E., Ghetti, B., Della Corte, L., Spano, P., Tofaris, G. K., Goedert, M., & Spillantini, M. G. (2010). SNARE protein redistribution and synaptic failure in a transgenic mouse model of Parkinson's disease. *Brain*, *133*(7). https://doi.org/10.1093/brain/awq132

Gelpi, E., Navarro-Otano, J., Tolosa, E., Gaig, C., Compta, Y., Rey, M. J., Martí, M. J., Hernández, I., Valldeoriola, F., Reñé, R., & Ribalta, T. (2014). Multiple organ involvement by alpha-synuclein pathology in lewy body disorders. *Movement Disorders*, *29*(8). https://doi.org/10.1002/mds.25776

Ghanem, S. S., Majbour, N. K., Vaikath, N. N., Ardah, M. T., Erskine, D., Jensen, N. M., Fayyad, M., Sudhakaran, I. P., Vasili, E., Melachroinou, K., Abdi, I. Y., Poggiolini, I., Santos, P., Dorn, A., Carloni, P., Vekrellis, K., Attems, J., McKeith, I., Outeiro, T. F., … El-Agnaf, O. M. A. (2022). α-Synuclein phosphorylation at serine 129 occurs after initial protein deposition and inhibits seeded fibril formation and toxicity. *Proceedings of the National Academy of Sciences of the United States of America*, *119*(15). https://doi.org/10.1073/pnas.2109617119

Ghee, M., Melki, R., Michot, N., & Mallet, J. (2005). PA700, the regulatory complex of the 26S proteasome, interferes with α-synuclein assembly. *FEBS Journal*, *272*(16). https://doi.org/10.1111/j.1742-4658.2005.04776.x

Giasson, B. I., Murray, I. V. J., Trojanowski, J. Q., & Lee, V. M.-Y. (2001). A Hydrophobic Stretch of 12 Amino Acid Residues in the Middle of α-Synuclein Is Essential for Filament Assembly. *Journal of Biological Chemistry*, *276*(4), 2380–2386. https://doi.org/10.1074/jbc.M008919200

Goedert, M. (2001). Alpha-synuclein and neurodegenerative diseases. In *Nature Reviews Neuroscience* (Vol. 2, Issue 7). https://doi.org/10.1038/35081564

Gombash, S. E., Manfredsson, F. P., Kemp, C. J., Kuhn, N. C., Fleming, S. M., Egan, A. E., Grant, L. M., Ciucci, M. R., MacKeigan, J. P., & Sortwell, C. E. (2013). Morphological and behavioral impact of AAV2/5-mediated overexpression of

human wildtype alpha-synuclein in the rat nigrostriatal system. *PLoS ONE*, *8*(11). https://doi.org/10.1371/journal.pone.0081426

Gómez-Tortosa, E., Newell, K., Irizarry, M. C., Sanders, J. L., & Hyman, B. T. (2000). α-synuclein immunoreactivity in dementia with Lewy bodies: Morphological staging and comparison with ubiquitin immunostaining. *Acta Neuropathologica*, *99*(4). https://doi.org/10.1007/s004010051135

Gonera, E. G., Van't Hof, M., Berger, H. J. C., Van Weel, C., & Horstink, M. W. I. M. (1997). Symptoms and duration of the prodromal phase in Parkinson's disease. *Movement Disorders*, *12*(6). https://doi.org/10.1002/mds.870120607

Gorbatyuk, O. S., Li, S., Sullivan, L. F., Chen, W., Kondrikova, G., Manfredsson, F. P., Mandel, R. J., & Muzyczka, N. (2008). The phosphorylation state of Ser-129 in human α-synuclein determines neurodegeneration in a rat model of Parkinson disease. *Proceedings of the National Academy of Sciences*, *105*(2), 763–768. https://doi.org/10.1073/pnas.0711053105

Gosavi, N., Lee, H. J., Lee, J. S., Patel, S., & Lee, S. J. (2002). Golgi fragmentation occurs in the cells with prefibrillar α-synuclein aggregates and precedes the formation of fibrillar inclusion. *Journal of Biological Chemistry*, *277*(50). https://doi.org/10.1074/jbc.M208194200

Grazia Spillantini, M., Anthony Crowther, R., Jakes, R., Cairns, N. J., Lantos, P. L., & Goedert, M. (1998). Filamentous α-synuclein inclusions link multiple system atrophy with Parkinson's disease and dementia with Lewy bodies. *Neuroscience Letters*, *251*(3), 205–208. https://doi.org/10.1016/S0304-3940(98)00504-7

Hansen, C., Angot, E., Bergström, A. L., Steiner, J. A., Pieri, L., Paul, G., Outeiro, T. F., Melki, R., Kallunki, P., Fog, K., Li, J. Y., & Brundin, P. (2011). α-Synuclein propagates from mouse brain to grafted dopaminergic neurons and seeds aggregation in cultured human cells. *Journal of Clinical Investigation*, *121*(2). https://doi.org/10.1172/JCI43366

Harper, J. D., & Lansbury, P. T. (1997). MODELS OF AMYLOID SEEDING IN ALZHEIMER'S DISEASE AND SCRAPIE: Mechanistic Truths and Physiological Consequences of the Time-Dependent Solubility of Amyloid Proteins. *Annual Review of Biochemistry*, *66*(1), 385–407. https://doi.org/10.1146/annurev.biochem.66.1.385

Hattori, N., Tanaka, M., Ozawa, T., & Mizuno, Y. (1991). Immunohistochemical studies on complexes I, II, III, and IV of mitochondria in parkinson's disease. *Annals of Neurology*, *30*(4). https://doi.org/10.1002/ana.410300409

Hell, J. W., & Jahn, R. (2006). Chapter 12 - Preparation of Synaptic Vesicles from Mammalian Brain A2 - Celis, Julio E. In *Cell Biology (Third Edition)*.

Heman-Ackah, S. M., Manzano, R., Hoozemans, J. J. M., Scheper, W., Flynn, R., Haerty, W., Cowley, S. A., Bassett, A. R., & Wood, M. J. A. (2017). Alpha-synuclein induces the unfolded protein response in Parkinson's disease SNCA triplication iPSC-derived neurons. *Human Molecular Genetics*, *26*(22). https://doi.org/10.1093/hmg/ddx331

Ho, D. H., Kim, H., Nam, D., Heo, J., & Son, I. (2023a). Nuclear α-Synuclein-Derived Cytotoxic Effect via Altered Ribosomal RNA Processing in Primary Mouse Embryonic Fibroblasts. *International Journal of Molecular Sciences*, *24*(3), 2132. https://doi.org/10.3390/ijms24032132

Ho, D. H., Kim, H., Nam, D., Heo, J., & Son, I. (2023b). Nuclear α-Synuclein-Derived Cytotoxic Effect via Altered Ribosomal RNA Processing in Primary Mouse Embryonic Fibroblasts. *International Journal of Molecular Sciences*, *24*(3), 2132. https://doi.org/10.3390/ijms24032132

Ho, D. H., Nam, D., Jeong, S., Seo, M. K., Park, S. W., Seol, W., & Son, I. (2021). Expression of transduced nucleolin promotes the clearance of accumulated α-synuclein in rodent cells and animal model. *Neurobiology of Disease*, *154*, 105349. https://doi.org/10.1016/j.nbd.2021.105349

Ho, P. W., Li, L., Liu, H., Choi, Z. Y., Chang, E. E. S., Pang, S. Y., Malki, Y., Leung, C., Kung, M. H., Ramsden, D. B., & Ho, S. (2023). In vivo overexpression of synaptogyrin-3 promotes striatal synaptic dopamine uptake in LRRK2 ^{R1441G} mutant mouse model of Parkinson's disease. *Brain and Behavior*, *13*(2). https://doi.org/10.1002/brb3.2886

Hodara, R., Norris, E. H., Giasson, B. I., Mishizen-Eberz, A. J., Lynch, D. R., Lee, V. M.-Y., & Ischiropoulos, H. (2004). Functional Consequences of α-Synuclein Tyrosine Nitration. *Journal of Biological Chemistry*, *279*(46), 47746–47753. https://doi.org/10.1074/jbc.M408906200

Holtz, W. A., & O'Malley, K. L. (2003). Parkinsonian mimetics induce aspects of unfolded protein response in death of dopaminergic neurons. *Journal of Biological Chemistry*, *278*(21). https://doi.org/10.1074/jbc.M211821200

Hoyer, W., Antony, T., Cherny, D., Heim, G., Jovin, T. M., & Subramaniam, V. (2002). Dependence of α-synuclein aggregate morphology on solution conditions. *Journal of Molecular Biology*, *322*(2). https://doi.org/10.1016/S0022-2836(02)00775-1

Hoyer, W., Cherny, D., Subramaniam, V., & Jovin, T. M. (2004). Impact of the Acidic C-Terminal Region Comprising Amino Acids 109−140 on α-Synuclein

Aggregation in Vitro. *Biochemistry*, *43*(51), 16233–16242. https://doi.org/10.1021/bi048453u

Hsu, L. J., Mallory, M., Xia, Y., Veinbergs, I., Hashimoto, M., Yoshimoto, M., Thal, L. J., Saitoh, T., & Masliah, E. (1998). Expression pattern of synucleins (non-Aβ component of Alzheimer's disease amyloid precursor protein/α-synuclein) during murine brain development. *Journal of Neurochemistry*, *71*(1). https://doi.org/10.1046/j.1471-4159.1998.71010338.x

Huang, C., Ren, G., Zhou, H., & Wang, C. C. (2005). A new method for purification of recombinant human α-synuclein in Escherichia coli. *Protein Expression and Purification*, *42*(1). https://doi.org/10.1016/j.pep.2005.02.014

Huang, Z., Xu, Z., Wu, Y., & Zhou, Y. (2011). Determining nuclear localization of alpha-synuclein in mouse brains. *Neuroscience*, *199*. https://doi.org/10.1016/j.neuroscience.2011.10.016

Ibáñez, P., Bonnet, A. M., Débarges, B., Lohmann, E., Tison, F., Pollak, P., Agid, Y., Dürr, A., & Brice, P. A. (2004). Causal relation between α-synuclein gene duplication and familial Parkinson's disease. *Lancet*, *364*(9440). https://doi.org/10.1016/S0140-6736(04)17104-3

Ikenaka, K., Suzuki, M., Mochizuki, H., & Nagai, Y. (2019). Lipids as trans-acting effectors for α-synuclein in the pathogenesis of Parkinson's disease. In *Frontiers in Neuroscience* (Vol. 13, Issue JUL). https://doi.org/10.3389/fnins.2019.00693

Iwai, A., Masliah, E., Yoshimoto, M., Ge, N., Flanagan, L., Rohan de Silva, H. A., Kittel, A., & Saitoh, T. (1995). The precursor protein of non-Aβ component of Alzheimer's disease amyloid is a presynaptic protein of the central nervous system. *Neuron*, *14*(2). https://doi.org/10.1016/0896-6273(95)90302-X

Jackson-Lewis, V., Blesa, J., & Przedborski, S. (2012). Animal models of Parkinson's disease. *Parkinsonism & Related Disorders*, *18*, S183–S185. https://doi.org/10.1016/S1353-8020(11)70057-8

Janezic, S., Threlfell, S., Dodson, P. D., Dowie, M. J., Taylor, T. N., Potgieter, D., Parkkinen, L., Senior, S. L., Anwar, S., Ryan, B., Deltheil, T., Kosillo, P., Cioroch, M., Wagner, K., Ansorge, O., Bannerman, D. M., Bolam, J. P., Magill, P. J., Cragg, S. J., & Wade-Martins, R. (2013). Deficits in dopaminergic transmission precede neuron loss and dysfunction in a new Parkinson model. *Proceedings of the National Academy of Sciences of the United States of America*, *110*(42). https://doi.org/10.1073/pnas.1309143110

Kapasi, A., Brosch, J. R., Nudelman, K. N., Agrawal, S., Foroud, T. M., & Schneider, J. A. (2020). A novel SNCA E83Q mutation in a case of dementia with Lewy bodies

and atypical frontotemporal lobar degeneration. *Neuropathology*, *40*(6). https://doi.org/10.1111/neup.12687

Karampetsou, M., Ardah, M. T., Semitekolou, M., Polissidis, A., Samiotaki, M., Kalomoiri, M., Majbour, N., Xanthou, G., El-Agnaf, O. M. A., & Vekrellis, K. (2017). Phosphorylated exogenous alpha-synuclein fibrils exacerbate pathology and induce neuronal dysfunction in mice. *Scientific Reports*, *7*(1), 16533. https://doi.org/10.1038/s41598-017-15813-8

Keeney, P. M., Xie, J., Capaldi, R. A., & Bennett, J. P. (2006). Parkinson's disease brain mitochondrial complex I has oxidatively damaged subunits and is functionally impaired and misassembled. *Journal of Neuroscience*, *26*(19). https://doi.org/10.1523/JNEUROSCI.0984-06.2006

Kirik, D., Rosenblad, C., Burger, C., Lundberg, C., Johansen, T. E., Muzyczka, N., Mandel, R. J., & Björklund, A. (2002). Parkinson-Like Neurodegeneration Induced by Targeted Overexpression of α-Synuclein in the Nigrostriatal System. *Journal of Neuroscience*, *22*(7). https://doi.org/10.1523/jneurosci.22-07-02780.2002

Kline, E. M., Houser, M. C., Herrick, M. K., Seibler, P., Klein, C., West, A., & Tansey, M. G. (2021). Genetic and Environmental Factors in Parkinson's Disease Converge on Immune Function and Inflammation. In *Movement Disorders* (Vol. 36, Issue 1). https://doi.org/10.1002/mds.28411

Koga, S., Sekiya, H., Kondru, N., Ross, O. A., & Dickson, D. W. (2021). Neuropathology and molecular diagnosis of Synucleinopathies. In *Molecular Neurodegeneration* (Vol. 16, Issue 1). https://doi.org/10.1186/s13024-021-00501-z

Kontopoulos, E., Parvin, J. D., & Feany, M. B. (2006). α-synuclein acts in the nucleus to inhibit histone acetylation and promote neurotoxicity. *Human Molecular Genetics*, *15*(20), 3012–3023. https://doi.org/10.1093/hmg/ddl243

Kordower, J. H., Chu, Y., Hauser, R. A., Freeman, T. B., & Olanow, C. W. (2008). Lewy body-like pathology in long-term embryonic nigral transplants in Parkinson's disease. *Nature Medicine*, *14*(5). https://doi.org/10.1038/nm1747

Kordower, J. H., Olanow, C. W., Dodiya, H. B., Chu, Y., Beach, T. G., Adler, C. H., Halliday, G. M., & Bartus, R. T. (2013). Disease duration and the integrity of the nigrostriatal system in Parkinson's disease. *Brain*, *136*(8). https://doi.org/10.1093/brain/awt192

Koss, D. J., Erskine, D., Porter, A., Palmoski, P., Menon, H., Todd, O. G. J., Leite, M., Attems, J., & Outeiro, T. F. (2022). Nuclear alpha-synuclein is present in the human brain and is modified in dementia with Lewy bodies. *Acta Neuropathologica Communications*, *10*(1). https://doi.org/10.1186/s40478-022-01403-x

Kramer, M. L., & Schulz-Schaeffer, W. J. (2007). Presynaptic α-Synuclein Aggregates, Not Lewy Bodies, Cause Neurodegeneration in Dementia with Lewy Bodies. *The Journal of Neuroscience*, *27*(6), 1405–1410. https://doi.org/10.1523/JNEUROSCI.4564-06.2007

Krüger, R., Kuhn, W., Müller, T., Woitalla, D., Graeber, M., Kösel, S., Przuntek, H., Epplen, J. T., Schöls, L., & Riess, O. (1998). Ala30Pro mutation in the gene encoding α-synuclein in Parkinson's disease. *Nature Genetics*, *18*(2). https://doi.org/10.1038/ng0298-106

Kumar, S. T., Jagannath, S., Francois, C., Vanderstichele, H., Stoops, E., & Lashuel, H. A. (2020). How specific are the conformation-specific α-synuclein antibodies? Characterization and validation of 16 α-synuclein conformation-specific antibodies using well-characterized preparations of α-synuclein monomers, fibrils and oligomers with distinct structures and morphology. *Neurobiology of Disease*, *146*. https://doi.org/10.1016/j.nbd.2020.105086

Laemmli, U. K. (1970). Cleavage of structural proteins during the assembly of the head of bacteriophage T4. *Nature*, *227*(5259). https://doi.org/10.1038/227680a0

Lagundžin, D., Krieger, K. L., Law, H. C. H., & Woods, N. T. (2022). An optimized co-immunoprecipitation protocol for the analysis of endogenous protein-protein interactions in cell lines using mass spectrometry. *STAR Protocols*, *3*(1). https://doi.org/10.1016/j.xpro.2022.101234

Lang, T., Bruns, D., Wenzel, D., Riedel, D., Holroyd, P., Thiele, C., & Jahn, R. (2001). SNAREs are concentrated in cholesterol-dependent clusters that define docking and fusion sites for exocytosis. *EMBO Journal*, *20*(9). https://doi.org/10.1093/emboj/20.9.2202

Larsen, K. E., Schmitz, Y., Troyer, M. D., Mosharov, E., Dietrich, P., Quazi, A. Z., Savalle, M., Nemani, V., Chaudhry, F. A., Edwards, R. H., Stefanis, L., & Sulzer, D. (2006). α-Synuclein Overexpression in PC12 and Chromaffin Cells Impairs Catecholamine Release by Interfering with a Late Step in Exocytosis. *The Journal of Neuroscience*, *26*(46), 11915–11922. https://doi.org/10.1523/JNEUROSCI.3821-06.2006

Lashuel, H. A., & Grillo-Bosch, D. (2005). In Vitro Preparation of Prefibrillar Intermediates of Amyloid-β and α-Synuclein. In *Amyloid Proteins* (pp. 019–034). Humana Press. https://doi.org/10.1385/1-59259-874-9:019

Lashuel, H. A., Petre, B. M., Wall, J., Simon, M., Nowak, R. J., Walz, T., & Lansbury, P. T. (2002a). α-Synuclein, Especially the Parkinson's Disease-associated Mutants,

Forms Pore-like Annular and Tubular Protofibrils. *Journal of Molecular Biology*, *322*(5), 1089–1102. https://doi.org/10.1016/S0022-2836(02)00735-0

Lashuel, H. A., Petre, B. M., Wall, J., Simon, M., Nowak, R. J., Walz, T., & Lansbury, P. T. (2002b). α-Synuclein, Especially the Parkinson's Disease-associated Mutants, Forms Pore-like Annular and Tubular Protofibrils. *Journal of Molecular Biology*, *322*(5), 1089–1102. https://doi.org/10.1016/S0022-2836(02)00735-0

Lauwers, E., Debyser, Z., Van Dorpe, J., De Strooper, B., Nuttin, B., & Baekelandt, V. (2003). Neuropathology and neurodegeneration in rodent brain induced by lentiviral vector-mediated overexpression of α-synuclein. *Brain Pathology*, *13*(3). https://doi.org/10.1111/j.1750-3639.2003.tb00035.x

Lázaro, D. F., Rodrigues, E. F., Langohr, R., Shahpasandzadeh, H., Ribeiro, T., Guerreiro, P., Gerhardt, E., Kröhnert, K., Klucken, J., Pereira, M. D., Popova, B., Kruse, N., Mollenhauer, B., Rizzoli, S. O., Braus, G. H., Danzer, K. M., & Outeiro, T. F. (2014a). Systematic Comparison of the Effects of Alpha-synuclein Mutations on Its Oligomerization and Aggregation. *PLoS Genetics*, *10*(11), e1004741. https://doi.org/10.1371/journal.pgen.1004741

Lázaro, D. F., Rodrigues, E. F., Langohr, R., Shahpasandzadeh, H., Ribeiro, T., Guerreiro, P., Gerhardt, E., Kröhnert, K., Klucken, J., Pereira, M. D., Popova, B., Kruse, N., Mollenhauer, B., Rizzoli, S. O., Braus, G. H., Danzer, K. M., & Outeiro, T. F. (2014b). Systematic Comparison of the Effects of Alpha-synuclein Mutations on Its Oligomerization and Aggregation. *PLoS Genetics*, *10*(11). https://doi.org/10.1371/journal.pgen.1004741

Lee, A., Hirabayashi, Y., Kwon, S. K., Lewis, T. L., & Polleux, F. (2018). Emerging roles of mitochondria in synaptic transmission and neurodegeneration. In *Current Opinion in Physiology* (Vol. 3). https://doi.org/10.1016/j.cophys.2018.03.009

Lee, B. R., & Kamitani, T. (2011). Improved Immunodetection of Endogenous α-Synuclein. *PLoS ONE*, *6*(8), e23939. https://doi.org/10.1371/journal.pone.0023939

Lee, S.-H., Peng, I.-F., Ng, Y. G., Yanagisawa, M., Bamji, S. X., Elia, L. P., Balsamo, J., Lilien, J., Anastasiadis, P. Z., Ullian, E. M., & Reichardt, L. F. (2008). Synapses are regulated by the cytoplasmic tyrosine kinase Fer in a pathway mediated by p120catenin, Fer, SHP-2, and β-catenin. *Journal of Cell Biology*, *183*(5), 893–908. https://doi.org/10.1083/jcb.200807188

Lee, U., Choi, C., Ryu, S. H., Park, D., Lee, S.-E., Kim, K., Kim, Y., & Chang, S. (2021). SCAMP5 plays a critical role in axonal trafficking and synaptic localization of NHE6 to adjust quantal size at glutamatergic synapses. *Proceedings of the National Academy of Sciences*, *118*(2). https://doi.org/10.1073/pnas.2011371118

Lee, Y., Dawson, V. L., & Dawson, T. M. (2012). Animal models of Parkinson's disease: Vertebrate genetics. *Cold Spring Harbor Perspectives in Medicine*, *2*(10). https://doi.org/10.1101/cshperspect.a009324

Lesage, S., Anheim, M., Letournel, F., Bousset, L., Honoré, A., Rozas, N., Pieri, L., Madiona, K., Dürr, A., Melki, R., Verny, C., & Brice, A. (2013). G51D α-synuclein mutation causes a novel Parkinsonian-pyramidal syndrome. *Annals of Neurology*, *73*(4). https://doi.org/10.1002/ana.23894

Lewis, K. A., Su, Y., Jou, O., Ritchie, C., Foong, C., Hynan, L. S., White, C. L., Thomas, P. J., & Hatanpaa, K. J. (2010). Abnormal neurites containing C-terminally truncated α-synuclein are present in Alzheimer's disease without conventional lewy body pathology. *American Journal of Pathology*, *177*(6). https://doi.org/10.2353/ajpath.2010.100552

Lewy FH. (1912). *Paralysis agitans. 1. Pathologische Anatomie.* (Lewandowsky M, Ed.). Julius Springer.

Li, H. T., Du, H. N., Tang, L., Hu, J., & Hu, H. Y. (2002). Structural transformation and aggregation of human α-synuclein in trifluoroethanol: Non-amyloid component sequence is essential and β-sheet formation is prerequisite to aggregation. *Biopolymers*, *64*(4). https://doi.org/10.1002/bip.10179

Li, J. Y., Englund, E., Holton, J. L., Soulet, D., Hagell, P., Lees, A. J., Lashley, T., Quinn, N. P., Rehncrona, S., Björklund, A., Widner, H., Revesz, T., Lindvall, O., & Brundin, P. (2008). Lewy bodies in grafted neurons in subjects with Parkinson's disease suggest host-to-graft disease propagation. *Nature Medicine*, *14*(5). https://doi.org/10.1038/nm1746

Li, W. W., Yang, R., Guo, J. C., Ren, H. M., Zha, X. L., Cheng, J. S., & Cai, D. F. (2007). Localization of α-synuclein to mitochondria within midbrain of mice. *NeuroReport*, *18*(15). https://doi.org/10.1097/WNR.0b013e3282f03db4

Li, W., West, N., Colla, E., Pletnikova, O., Troncoso, J. C., Marsh, L., Dawson, T. M., Jäkälä, P., Hartmann, T., Price, D. L., & Lee, M. K. (2005). Aggregation promoting C-terminal truncation of α-synuclein is a normal cellular process and is enhanced by the familial Parkinson's disease-linked mutations. *Proceedings of the National Academy of Sciences of the United States of America*, *102*(6). https://doi.org/10.1073/pnas.0406976102

Loeb, V., Yakunin, E., Saada, A., & Sharon, R. (2010). The transgenic overexpression of α-synuclein and not its related pathology associates with complex I inhibition. *Journal of Biological Chemistry*, *285*(10). https://doi.org/10.1074/jbc.M109.061051

Löw, K., & Aebischer, P. (2012). Use of viral vectors to create animal models for Parkinson's disease. In *Neurobiology of Disease* (Vol. 48, Issue 2). https://doi.org/10.1016/j.nbd.2011.12.038

Lücking, C. B., Dürr, A., Bonifati, V., Vaughan, J., De Michele, G., Gasser, T., Harhangi, B. S., Meco, G., Denèfle, P., Wood, N. W., Agid, Y., Nicholl, D., Breteler, M. M. B., Oostra, B. A., De Mari, M., Marconi, R., Filla, A., Bonnet, A.-M., Broussolle, E., … Brice, A. (2000). Association between Early-Onset Parkinson's Disease and Mutations in the Parkin Gene . *New England Journal of Medicine*, *342*(21). https://doi.org/10.1056/nejm200005253422103

Luk, K. C., Kehm, V., Carroll, J., Zhang, B., O'Brien, P., Trojanowski, J. Q., & Lee, V. M.-Y. (2012a). Pathological α-Synuclein Transmission Initiates Parkinson-like Neurodegeneration in Nontransgenic Mice. *Science*, *338*(6109), 949–953. https://doi.org/10.1126/science.1227157

Luk, K. C., Kehm, V., Carroll, J., Zhang, B., O'Brien, P., Trojanowski, J. Q., & Lee, V. M.-Y. (2012b). Pathological α-Synuclein Transmission Initiates Parkinson-like Neurodegeneration in Nontransgenic Mice. *Science*, *338*(6109), 949–953. https://doi.org/10.1126/science.1227157

Luk, K. C., Kehm, V. M., Zhang, B., O'Brien, P., Trojanowski, J. Q., & Lee, V. M. Y. (2012). Intracerebral inoculation of pathological α-synuclein initiates a rapidly progressive neurodegenerative α-synucleinopathy in mice. *Journal of Experimental Medicine*, *209*(5), 975–986. https://doi.org/10.1084/jem.20112457

Luk, K. C., Song, C., O'Brien, P., Stieber, A., Branch, J. R., Brunden, K. R., Trojanowski, J. Q., & Lee, V. M. Y. (2009a). Exogenous α-synuclein fibrils seed the formation of Lewy body-like intracellular inclusions in cultured cells. *Proceedings of the National Academy of Sciences of the United States of America*, *106*(47). https://doi.org/10.1073/pnas.0908005106

Luk, K. C., Song, C., O'Brien, P., Stieber, A., Branch, J. R., Brunden, K. R., Trojanowski, J. Q., & Lee, V. M.-Y. (2009b). Exogenous α-synuclein fibrils seed the formation of Lewy body-like intracellular inclusions in cultured cells. *Proceedings of the National Academy of Sciences*, *106*(47), 20051–20056. https://doi.org/10.1073/pnas.0908005106

Mahul-Mellier, A. L., Burtscher, J., Maharjan, N., Weerens, L., Croisier, M., Kuttler, F., Leleu, M., Knott, G. W., & Lashuel, H. A. (2020). The process of Lewy body formation, rather than simply α-synuclein fibrillization, is one of the major drivers of neurodegeneration. *Proceedings of the National Academy of Sciences of the United States of America*, *117*(9). https://doi.org/10.1073/pnas.1913904117

Manzanza, N. de O., Sedlackova, L., & Kalaria, R. N. (2021). Alpha-Synuclein Post-translational Modifications: Implications for Pathogenesis of Lewy Body Disorders. *Frontiers in Aging Neuroscience*, *13*. https://doi.org/10.3389/fnagi.2021.690293

Maroteaux, L., Campanelli, J., & Scheller, R. (1988a). Synuclein: a neuron-specific protein localized to the nucleus and presynaptic nerve terminal. *The Journal of Neuroscience*, *8*(8), 2804–2815. https://doi.org/10.1523/JNEUROSCI.08-08-02804.1988

Maroteaux, L., Campanelli, J. T., & Scheller, R. H. (1988b). Synuclein: A neuron-specific protein localized to the nucleus and presynaptic nerve terminal. *Journal of Neuroscience*, *8*(8). https://doi.org/10.1523/jneurosci.08-08-02804.1988

Maroteaux, L., & Scheller, R. H. (1991). The rat brain synucleins; family of proteins transiently associated with neuronal membrane. *Molecular Brain Research*, *11*(3–4). https://doi.org/10.1016/0169-328X(91)90043-W

Marui, W., Iseki, E., Nakai, T., Miura, S., Kato, M., Uéda, K., & Kosaka, K. (2002). Progression and staging of Lewy pathology in brains from patients with dementia with Lewy bodies. *Journal of the Neurological Sciences*, *195*(2). https://doi.org/10.1016/S0022-510X(02)00006-0

Mayo, M., & Bordelon, Y. (2014). Dementia with Lewy Bodies. *Seminars in Neurology*, *34*(02), 182–188. https://doi.org/10.1055/s-0034-1381741

McFarland, N. R., Fan, Z., Xu, K., Schwarzschild, M. A., Feany, M. B., Hyman, B. T., & McLean, P. J. (2009). α-Synuclein S129 Phosphorylation Mutants Do Not Alter Nigrostriatal Toxicity in a Rat Model of Parkinson Disease. *Journal of Neuropathology & Experimental Neurology*, *68*(5), 515–524. https://doi.org/10.1097/NEN.0b013e3181a24b53

Milanese, C., Cerri, S., Ulusoy, A., Gornati, S. V., Plat, A., Gabriels, S., Blandini, F., Di Monte, D. A., Hoeijmakers, J. H., & Mastroberardino, P. G. (2018). Activation of the DNA damage response in vivo in synucleinopathy models of Parkinson's disease. *Cell Death and Disease*, *9*(8). https://doi.org/10.1038/s41419-018-0848-7

Milber, J. M., Noorigian, J. V., Morley, J. F., Petrovitch, H., White, L., Ross, G. W., & Duda, J. E. (2012). Lewy pathology is not the first sign of degeneration in vulnerable neurons in parkinson disease. *Neurology*, *79*(24). https://doi.org/10.1212/WNL.0b013e318278fe32

Miller, R. M., Callahan, L. M., Casaceli, C., Chen, L., Kiser, G. L., Chui, B., Kaysser-Kranich, T. M., Sendera, T. J., Palaniappan, C., & Federoff, H. J. (2004). Dysregulation of Gene Expression in the 1-Methyl-4-Phenyl-1,2,3,6-

Tetrahydropyridine-Lesioned Mouse Substantia Nigra. *The Journal of Neuroscience*, *24*(34), 7445–7454. https://doi.org/10.1523/JNEUROSCI.4204-03.2004

Mor, D. E., Tsika, E., Mazzulli, J. R., Gould, N. S., Kim, H., Daniels, M. J., Doshi, S., Gupta, P., Grossman, J. L., Tan, V. X., Kalb, R. G., Caldwell, K. A., Caldwell, G. A., Wolfe, J. H., & Ischiropoulos, H. (2017). Dopamine induces soluble α-synuclein oligomers and nigrostriatal degeneration. *Nature Neuroscience*, *20*(11), 1560–1568. https://doi.org/10.1038/nn.4641

Mosharov, E. V., Staal, R. G. W., Bové, J., Prou, D., Hananiya, A., Markov, D., Poulsen, N., Larsen, K. E., Moore, C. M. H., Troyer, M. D., Edwards, R. H., Przedborski, S., & Sulzer, D. (2006). α-Synuclein Overexpression Increases Cytosolic Catecholamine Concentration. *The Journal of Neuroscience*, *26*(36), 9304–9311. https://doi.org/10.1523/JNEUROSCI.0519-06.2006

Muntané, G., Ferrer, I., & Martinez-Vicente, M. (2012). α-synuclein phosphorylation and truncation are normal events in the adult human brain. *Neuroscience*, *200*. https://doi.org/10.1016/j.neuroscience.2011.10.042

Muntel, J., Gandhi, T., Verbeke, L., Bernhardt, O. M., Treiber, T., Bruderer, R., & Reiter, L. (2019). Surpassing 10 000 identified and quantified proteins in a single run by optimizing current LC-MS instrumentation and data analysis strategy. *Molecular Omics*, *15*(5). https://doi.org/10.1039/c9mo00082h

Murphy, D. D., Rueter, S. M., Trojanowski, J. Q., & Lee, V. M. Y. (2000). Synucleins are developmentally expressed, and α-synuclein regulates the size of the presynaptic vesicular pool in primary hippocampal neurons. *Journal of Neuroscience*, *20*(9). https://doi.org/10.1523/jneurosci.20-09-03214.2000

Murray, I. V. J., Giasson, B. I., Quinn, S. M., Koppaka, V., Axelsen, P. H., Ischiropoulos, H., Trojanowski, J. Q., & Lee, V. M. Y. (2003). Role of α-synuclein carboxy-terminus on fibril formation in vitro. *Biochemistry*, *42*(28). https://doi.org/10.1021/bi027363r

Nakamura, K., Nemani, V. M., Wallender, E. K., Kaehlcke, K., Ott, M., & Edwards, R. H. (2008). Optical reporters for the conformation of α-synuclein reveal a specific interaction with mitochondria. *Journal of Neuroscience*, *28*(47). https://doi.org/10.1523/JNEUROSCI.3088-08.2008

Narhi, L., Wood, S. J., Steavenson, S., Jiang, Y., Wu, G. M., Anafi, D., Kaufman, S. A., Martin, F., Sitney, K., Denis, P., Louis, J. C., Wypych, J., Biere, A. L., & Citron, M. (1999). Both familial Parkinson's disease mutations accelerate alpha-synuclein aggregation [published erratum appears in J Biol Chem 1999 May 7;274(19):13728]. *J Biol Chem*, *274*(14).

Nemani, V. M., Lu, W., Berge, V., Nakamura, K., Onoa, B., Lee, M. K., Chaudhry, F. A., Nicoll, R. A., & Edwards, R. H. (2010). Increased Expression of α-Synuclein Reduces Neurotransmitter Release by Inhibiting Synaptic Vesicle Reclustering after Endocytosis. *Neuron*, *65*(1). https://doi.org/10.1016/j.neuron.2009.12.023

Neumann, M., Kahle, P. J., Giasson, B. I., Ozmen, L., Borroni, E., Spooren, W., Müller, V., Odoy, S., Fujiwara, H., Hasegawa, M., Iwatsubo, T., Trojanowski, J. Q., Kretzschmar, H. A., & Haass, C. (2002). Misfolded proteinase K-resistant hyperphosphorylated α-synuclein in aged transgenic mice with locomotor deterioration and in human α-synucleinopathies. *Journal of Clinical Investigation*, *110*(10). https://doi.org/10.1172/JCI200215777

Norris, E. H., Giasson, B. I., Ischiropoulos, H., & Lee, V. M.-Y. (2003). Effects of Oxidative and Nitrative Challenges on α-Synuclein Fibrillogenesis Involve Distinct Mechanisms of Protein Modifications. *Journal of Biological Chemistry*, *278*(29), 27230–27240. https://doi.org/10.1074/jbc.M212436200

Osterberg, V. R., Spinelli, K. J., Weston, L. J., Luk, K. C., Woltjer, R. L., & Unni, V. K. (2015). Progressive Aggregation of Alpha-Synuclein and Selective Degeneration of Lewy Inclusion-Bearing Neurons in a Mouse Model of Parkinsonism. *Cell Reports*, *10*(8), 1252–1260. https://doi.org/10.1016/j.celrep.2015.01.060

Osterhaus, A., Groen, J., Bildt, M. Van De, Martina, B., Vos, J., & Egmond, H. Van. (1997). a -Synuclein in Lewy bodies. *Nature*, *388*.

Oueslati, A., Fournier, M., & Lashuel, H. A. (2010). Role of post-translational modifications in modulating the structure, function and toxicity of α-synuclein. Implications for Parkinson's disease pathogenesis and therapies. In *Progress in Brain Research* (Vol. 183, Issue C). https://doi.org/10.1016/S0079-6123(10)83007-9

Outeiro, T. F., Kontopoulos, E., Altmann, S. M., Kufareva, I., Strathearn, K. E., Amore, A. M., Volk, C. B., Maxwell, M. M., Rochet, J. C., McLean, P. J., Young, A. B., Abagyan, R., Feany, M. B., Hyman, B. T., & Kazantsev, A. G. (2007). Sirtuin 2 inhibitors rescue α-synuclein-mediated toxicity in models of Parkinson's disease. *Science*, *317*(5837). https://doi.org/10.1126/science.1143780

Outeiro, T. F., Koss, D. J., Erskine, D., Walker, L., Kurzawa-Akanbi, M., Burn, D., Donaghy, P., Morris, C., Taylor, J. P., Thomas, A., Attems, J., & McKeith, I. (2019). Dementia with Lewy bodies: An update and outlook. In *Molecular Neurodegeneration* (Vol. 14, Issue 1). https://doi.org/10.1186/s13024-019-0306-8

Outeiro, T. F., Putcha, P., Tetzlaff, J. E., Spoelgen, R., Koker, M., Carvalho, F., Hyman, B. T., & McLean, P. J. (2008). Formation of Toxic Oligomeric α-Synuclein Species

in Living Cells. *PLoS ONE*, *3*(4), e1867. https://doi.org/10.1371/journal.pone.0001867

Outerio, T. F., Klucken, J., Bercury, K., Tetzlaff, J., Putcha, P., Oliveira, L. M. A., Quintas, A., McLean, P. J., & Hyman, B. T. (2009). Dopamine-induced conformational changes in alpha-synuclein. *PLoS ONE*, *4*(9). https://doi.org/10.1371/journal.pone.0006906

Paiva, I., Jain, G., Lázaro, D. F., Jerčić, K. G., Hentrich, T., Kerimoglu, C., Pinho, R., Szegő, È. M., Burkhardt, S., Capece, V., Halder, R., Islam, R., Xylaki, M., Caldi Gomes, L. A., Roser, A. E., Lingor, P., Schulze-Hentrich, J. M., Borovečki, F., Fischer, A., & Outeiro, T. F. (2018a). Alpha-synuclein deregulates the expression of COL4A2 and impairs ER-Golgi function. *Neurobiology of Disease*, *119*. https://doi.org/10.1016/j.nbd.2018.08.001

Paiva, I., Jain, G., Lázaro, D. F., Jerčić, K. G., Hentrich, T., Kerimoglu, C., Pinho, R., Szegő, È. M., Burkhardt, S., Capece, V., Halder, R., Islam, R., Xylaki, M., Caldi Gomes, L. A., Roser, A.-E., Lingor, P., Schulze-Hentrich, J. M., Borovečki, F., Fischer, A., & Outeiro, T. F. (2018b). Alpha-synuclein deregulates the expression of COL4A2 and impairs ER-Golgi function. *Neurobiology of Disease*, *119*, 121–135. https://doi.org/10.1016/j.nbd.2018.08.001

Paiva, I., Pinho, R., Pavlou, M. A., Hennion, M., Wales, P., Schütz, A. L., Rajput, A., Szego, É. M., Kerimoglu, C., Gerhardt, E., Rego, A. C., Fischer, A., Bonn, S., & Outeiro, T. F. (2017). Sodium butyrate rescues dopaminergic cells from alpha-synuclein-induced transcriptional deregulation and DNA damage. *Human Molecular Genetics*, *26*(12). https://doi.org/10.1093/hmg/ddx114

Paleologou, K. E., & El-Agnaf, O. M. A. (2012). *α-Synuclein Aggregation and Modulating Factors* (pp. 109–164). https://doi.org/10.1007/978-94-007-5416-4_6

Palese, F., Pontis, S., Realini, N., & Piomelli, D. (2019). A protective role for N-acylphosphatidylethanolamine phospholipase D in 6-OHDA-induced neurodegeneration. *Scientific Reports*, *9*(1), 15927. https://doi.org/10.1038/s41598-019-51799-1

Parker, W. D., Boyson, S. J., & Parks, J. K. (1989). Abnormalities of the electron transport chain in idiopathic parkinson's disease. *Annals of Neurology*, *26*(6). https://doi.org/10.1002/ana.410260606

Parra-rivas, L. A., Madhivanan, K., Wang, L., Boyer, N. P., Dheeraj, D., Aulston, B. D., Pizzo, D. P., Branes-guerrero, K., Tang, Y., Das, U., Scott, D. A., Rangamani, P., Roy, S., Diego, S., Jolla, L., Diego, S., Jolla, L., Diego, S., & Jolla, L. (2022). Serine-

129 phosphorylation of α -synuclein is a trigger for physiologic protein-protein interactions and synaptic function. *BioRxiv*.

Pasanen, P., Myllykangas, L., Siitonen, M., Raunio, A., Kaakkola, S., Lyytinen, J., Tienari, P. J., Pöyhönen, M., & Paetau, A. (2014). A novel α-synuclein mutation A53E associated with atypical multiple system atrophy and Parkinson's disease-type pathology. *Neurobiology of Aging*, *35*(9). https://doi.org/10.1016/j.neurobiolaging.2014.03.024

Paslawski, W., Lorenzen, N., & Otzen, D. E. (2016). *Formation and Characterization of α-Synuclein Oligomers* (pp. 133–150). https://doi.org/10.1007/978-1-4939-2978-8_9

Paumier, K. L., Luk, K. C., Manfredsson, F. P., Kanaan, N. M., Lipton, J. W., Collier, T. J., Steece-Collier, K., Kemp, C. J., Celano, S., Schulz, E., Sandoval, I. M., Fleming, S., Dirr, E., Polinski, N. K., Trojanowski, J. Q., Lee, V. M., & Sortwell, C. E. (2015). Intrastriatal injection of pre-formed mouse α-synuclein fibrils into rats triggers α-synuclein pathology and bilateral nigrostriatal degeneration. *Neurobiology of Disease*, *82*. https://doi.org/10.1016/j.nbd.2015.06.003

Pavlou, M. A. S., Pinho, R., Paiva, I., & Outeiro, T. F. (2017). The yin and yang of α-synuclein-associated epigenetics in Parkinson's disease. *Brain*, *140*(4). https://doi.org/10.1093/brain/aww227

Paxinou, E., Chen, Q., Weisse, M., Giasson, B. I., Norris, E. H., Rueter, S. M., Trojanowski, J. Q., Lee, V. M.-Y., & Ischiropoulos, H. (2001). Induction of α-Synuclein Aggregation by Intracellular Nitrative Insult. *The Journal of Neuroscience*, *21*(20), 8053–8061. https://doi.org/10.1523/JNEUROSCI.21-20-08053.2001

Peelaerts, W., Bousset, L., Van Der Perren, A., Moskalyuk, A., Pulizzi, R., Giugliano, M., Van Den Haute, C., Melki, R., & Baekelandt, V. (2015). α-Synuclein strains cause distinct synucleinopathies after local and systemic administration. *Nature*, *522*(7556). https://doi.org/10.1038/nature14547

Perez, R. G., Waymire, J. C., Lin, E., Liu, J. J., Guo, F., & Zigmond, M. J. (2002). A Role for α-Synuclein in the Regulation of Dopamine Biosynthesis. *The Journal of Neuroscience*, *22*(8), 3090–3099. https://doi.org/10.1523/JNEUROSCI.22-08-03090.2002

Pingale, T., & Gupta, G. L. (2020). Classic and evolving animal models in Parkinson's disease. *Pharmacology Biochemistry and Behavior*, *199*, 173060. https://doi.org/10.1016/j.pbb.2020.173060

Pinho, R., Paiva, I., Jerčić, K. G., Fonseca-Ornelas, L., Gerhardt, E., Fahlbusch, C., Garcia-Esparcia, P., Kerimoglu, C., Pavlou, M. A. S., Villar-Piqué, A., Szego, É.,

Lopes Da Fonseca, T., Odoardi, F., Soeroes, S., Rego, A. C., Fischle, W., Schwamborn, J. C., Meyer, T., Kügler, S., … Outeiro, T. F. (2019). Nuclear localization and phosphorylation modulate pathological effects of alpha-synuclein. *Human Molecular Genetics*, *28*(1). https://doi.org/10.1093/hmg/ddy326

Poewe, W., Seppi, K., Tanner, C. M., Halliday, G. M., Brundin, P., Volkmann, J., Schrag, A.-E., & Lang, A. E. (2017a). Parkinson disease. *Nature Reviews Disease Primers*, *3*(1), 17013. https://doi.org/10.1038/nrdp.2017.13

Poewe, W., Seppi, K., Tanner, C. M., Halliday, G. M., Brundin, P., Volkmann, J., Schrag, A.-E., & Lang, A. E. (2017b). Parkinson disease. *Nature Reviews Disease Primers*, *3*(1), 17013. https://doi.org/10.1038/nrdp.2017.13

Polinski, N. K., Volpicelli-Daley, L. A., Sortwell, C. E., Luk, K. C., Cremades, N., Gottler, L. M., Froula, J., Duffy, M. F., Lee, V. M. Y., Martinez, T. N., & Dave, K. D. (2018). Best practices for generating and using alpha-synuclein pre-formed fibrils to model Parkinson's disease in rodents. *Journal of Parkinson's Disease*, *8*(2). https://doi.org/10.3233/JPD-171248

Polymeropoulos, M. H., Lavedan, C., Leroy, E., Ide, S. E., Dehejia, A., Dutra, A., Pike, B., Root, H., Rubenstein, J., Boyer, R., Stenroos, E. S., Chandrasekharappa, S., Athanassiadou, A., Papapetropoulos, T., Johnson, W. G., Lazzarini, A. M., Duvoisin, R. C., Di Iorio, G., Golbe, L. I., & Nussbaum, R. L. (1997). Mutation in the α-synuclein gene identified in families with Parkinson's disease. *Science*, *276*(5321). https://doi.org/10.1126/science.276.5321.2045

Popova, B., Wang, D., Pätz, C., Akkermann, D., Lázaro, D. F., Galka, D., Kolog Gulko, M., Bohnsack, M. T., Möbius, W., Bohnsack, K. E., Outeiro, T. F., & Braus, G. H. (2021). DEAD-box RNA helicase Dbp4/DDX10 is an enhancer of α-synuclein toxicity and oligomerization. *PLOS Genetics*, *17*(3), e1009407. https://doi.org/10.1371/journal.pgen.1009407

Prots, I., Grosch, J., Brazdis, R.-M., Simmnacher, K., Veber, V., Havlicek, S., Hannappel, C., Krach, F., Krumbiegel, M., Schütz, O., Reis, A., Wrasidlo, W., Galasko, D. R., Groemer, T. W., Masliah, E., Schlötzer-Schrehardt, U., Xiang, W., Winkler, J., & Winner, B. (2018). α-Synuclein oligomers induce early axonal dysfunction in human iPSC-based models of synucleinopathies. *Proceedings of the National Academy of Sciences*, *115*(30), 7813–7818. https://doi.org/10.1073/pnas.1713129115

Proukakis, C., Dudzik, C. G., Brier, T., MacKay, D. S., Cooper, J. M., Millhauser, G. L., Houlden, H., & Schapira, A. H. (2013). A novel α-synuclein missense mutation in Parkinson disease. In *Neurology* (Vol. 80, Issue 11). https://doi.org/10.1212/WNL.0b013e31828727ba

Qin, Z., Hu, D., Han, S., Hong, D. P., & Fink, A. L. (2007). Role of different regions of α-synuclein in the assembly of fibrils. *Biochemistry*, *46*(46). https://doi.org/10.1021/bi7014053

Ramalingam, N., Jin, S.-X., Moors, T. E., Fonseca-Ornelas, L., Shimanaka, K., Lei, S., Cam, H. P., Watson, A. H., Brontesi, L., Ding, L., Hacibaloglu, D. Y., Jiang, H., Choi, S. J., Kanter, E., Liu, L., Bartels, T., Nuber, S., Sulzer, D., Mosharov, E. V., … Dettmer, U. (2023). Dynamic physiological α-synuclein S129 phosphorylation is driven by neuronal activity. *Npj Parkinson's Disease*, *9*(1), 4. https://doi.org/10.1038/s41531-023-00444-w

Rendón, W. O., Martínez-Alonso, E., Tomás, M., Martínez-Martínez, N., & Martínez-Menárguez, J. A. (2013). Golgi fragmentation is Rab and SNARE dependent in cellular models of Parkinson's disease. *Histochemistry and Cell Biology*, *139*(5). https://doi.org/10.1007/s00418-012-1059-4

Rey, N. L., Petit, G. H., Bousset, L., Melki, R., & Brundin, P. (2013). Transfer of human α-synuclein from the olfactory bulb to interconnected brain regions in mice. *Acta Neuropathologica*, *126*(4). https://doi.org/10.1007/s00401-013-1160-3

Rey, N. L., Wesson, D. W., & Brundin, P. (2018a). The olfactory bulb as the entry site for prion-like propagation in neurodegenerative diseases. *Neurobiology of Disease*, *109*. https://doi.org/10.1016/j.nbd.2016.12.013

Rey, N. L., Wesson, D. W., & Brundin, P. (2018b). The olfactory bulb as the entry site for prion-like propagation in neurodegenerative diseases. *Neurobiology of Disease*, *109*, 226–248. https://doi.org/10.1016/j.nbd.2016.12.013

Rizo, J., & Südhof, T. C. (2002). Snares and munc18 in synaptic vesicle fusion. In *Nature Reviews Neuroscience* (Vol. 3, Issue 8). https://doi.org/10.1038/nrn898

Rizo, J., & Südhof, T. C. (2012). The membrane fusion enigma: SNAREs, Sec1/Munc18 proteins, and their accomplices guilty as charged? *Annual Review of Cell and Developmental Biology*, *28*. https://doi.org/10.1146/annurev-cellbio-101011-155818

Roos, D. S., Klein, M., Deeg, D. J. H., Doty, R. L., & Berendse, H. W. (2022). Prevalence of Prodromal Symptoms of Parkinson's Disease in the Late Middle-Aged Population. *Journal of Parkinson's Disease*, *12*(3), 967–974. https://doi.org/10.3233/JPD-213007

Rott, R., Szargel, R., Haskin, J., Shani, V., Shainskaya, A., Manov, I., Liani, E., Avraham, E., & Engelender, S. (2008). Monoubiquitylation of α-Synuclein by seven in absentia homolog (SIAH) promotes its aggregation in dopaminergic cells. *Journal of Biological Chemistry*, *283*(6). https://doi.org/10.1074/jbc.M704809200

Rott, R., Szargel, R., Shani, V., Hamza, H., Savyon, M., Abd Elghani, F., Bandopadhyay, R., & Engelender, S. (2017). SUMOylation and ubiquitination reciprocally regulate α-synuclein degradation and pathological aggregation. *Proceedings of the National Academy of Sciences*, *114*(50), 13176–13181. https://doi.org/10.1073/pnas.1704351114

Rovere, M., Sanderson, J. B., Fonseca-Ornelas, L., Patel, D. S., & Bartels, T. (2018). Refolding of helical soluble α-synuclein through transient interaction with lipid interfaces. *FEBS Letters*, *592*(9), 1464–1472. https://doi.org/10.1002/1873-3468.13047

Ryu, E. J., Harding, H. P., Angelastro, J. M., Vitolo, O. V., Ron, D., & Greene, L. A. (2002). Endoplasmic reticulum stress and the unfolded protein response in cellular models of Parkinson's disease. *Journal of Neuroscience*, *22*(24). https://doi.org/10.1523/jneurosci.22-24-10690.2002

Sakurai, A., Okamoto, K., Yaguchi, M., Fujita, Y., Mizuno, Y., Nakazato, Y., & Gonatas, N. K. (2002). Pathology of the inferior olivary nucleus in patients with multiple system atrophy. *Acta Neuropathologica*, *103*(6). https://doi.org/10.1007/s00401-001-0500-x

Salat, D., Noyce, A. J., Schrag, A., & Tolosa, E. (2016). Challenges of modifying disease progression in prediagnostic Parkinson's disease. In *The Lancet Neurology* (Vol. 15, Issue 6). https://doi.org/10.1016/S1474-4422(16)00060-0

Santos, A. L., & Lindner, A. B. (2017). Protein Posttranslational Modifications: Roles in Aging and Age-Related Disease. *Oxidative Medicine and Cellular Longevity*, *2017*, 1–19. https://doi.org/10.1155/2017/5716409

Schaser, A. J., Osterberg, V. R., Dent, S. E., Stackhouse, T. L., Wakeham, C. M., Boutros, S. W., Weston, L. J., Owen, N., Weissman, T. A., Luna, E., Raber, J., Luk, K. C., McCullough, A. K., Woltjer, R. L., & Unni, V. K. (2019a). Alpha-synuclein is a DNA binding protein that modulates DNA repair with implications for Lewy body disorders. *Scientific Reports*, *9*(1). https://doi.org/10.1038/s41598-019-47227-z

Schaser, A. J., Osterberg, V. R., Dent, S. E., Stackhouse, T. L., Wakeham, C. M., Boutros, S. W., Weston, L. J., Owen, N., Weissman, T. A., Luna, E., Raber, J., Luk, K. C., McCullough, A. K., Woltjer, R. L., & Unni, V. K. (2019b). Alpha-synuclein is a DNA binding protein that modulates DNA repair with implications for Lewy body disorders. *Scientific Reports*, *9*(1), 10919. https://doi.org/10.1038/s41598-019-47227-z

Schober, A. (2004). Classic toxin-induced animal models of Parkinson's disease: 6-OHDA and MPTP. In *Cell and Tissue Research* (Vol. 318, Issue 1). https://doi.org/10.1007/s00441-004-0938-y

Schulz-Schaeffer, W. J. (2010). The synaptic pathology of α-synuclein aggregation in dementia with Lewy bodies, Parkinson's disease and Parkinson's disease dementia. In *Acta Neuropathologica* (Vol. 120, Issue 2). https://doi.org/10.1007/s00401-010-0711-0

Scott, D. A., Tabarean, I., Tang, Y., Cartier, A., Masliah, E., & Roy, S. (2010). A Pathologic Cascade Leading to Synaptic Dysfunction in -Synuclein-Induced Neurodegeneration. *Journal of Neuroscience*, *30*(24), 8083–8095. https://doi.org/10.1523/JNEUROSCI.1091-10.2010

Shahmoradian, S. H., Lewis, A. J., Genoud, C., Hench, J., Moors, T. E., Navarro, P. P., Castaño-Díez, D., Schweighauser, G., Graff-Meyer, A., Goldie, K. N., Sütterlin, R., Huisman, E., Ingrassia, A., Gier, Y. de, Rozemuller, A. J. M., Wang, J., Paepe, A. De, Erny, J., Staempfli, A., … Lauer, M. E. (2019). Lewy pathology in Parkinson's disease consists of crowded organelles and lipid membranes. *Nature Neuroscience*, *22*(7). https://doi.org/10.1038/s41593-019-0423-2

Shrivastava, A. N., Bousset, L., Renner, M., Redeker, V., Savistchenko, J., Triller, A., & Melki, R. (2020). Differential Membrane Binding and Seeding of Distinct α-Synuclein Fibrillar Polymorphs. *Biophysical Journal*, *118*(6). https://doi.org/10.1016/j.bpj.2020.01.022

Siddiqui, A., Chinta, S. J., Mallajosyula, J. K., Rajagopolan, S., Hanson, I., Rane, A., Melov, S., & Andersen, J. K. (2012). Selective binding of nuclear alpha-synuclein to the PGC1alpha promoter under conditions of oxidative stress may contribute to losses in mitochondrial function: Implications for Parkinson's disease. *Free Radical Biology and Medicine*, *53*(4), 993–1003. https://doi.org/10.1016/j.freeradbiomed.2012.05.024

Simon, D. K., Tanner, C. M., & Brundin, P. (2020a). Parkinson Disease Epidemiology, Pathology, Genetics, and Pathophysiology. In *Clinics in Geriatric Medicine* (Vol. 36, Issue 1). https://doi.org/10.1016/j.cger.2019.08.002

Simon, D. K., Tanner, C. M., & Brundin, P. (2020b). Parkinson Disease Epidemiology, Pathology, Genetics, and Pathophysiology. *Clinics in Geriatric Medicine*, *36*(1), 1–12. https://doi.org/10.1016/j.cger.2019.08.002

Simunovic, F., Yi, M., Wang, Y., Macey, L., Brown, L. T., Krichevsky, A. M., Andersen, S. L., Stephens, R. M., Benes, F. M., & Sonntag, K. C. (2009). Gene expression profiling of substantia nigra dopamine neurons: further insights into Parkinson's disease pathology. *Brain*, *132*(7), 1795–1809. https://doi.org/10.1093/brain/awn323

Singleton, A. B., Farrer, M., Johnson, J., Singleton, A., Hague, S., Kachergus, J., Hulihan, M., Peuralinna, T., Dutra, A., Nussbaum, R., Lincoln, S., Crawley, A., Hanson, M.,

Maraganore, D., Adler, C., Cookson, M. R., Muenter, M., Baptista, M., Miller, D., … Gwinn-Hardy, K. (2003). α-Synuclein Locus Triplication Causes Parkinson's Disease. *Science*, *302*(5646). https://doi.org/10.1126/science.1090278

Spillantini, M. G., Crowther, R. A., Jakes, R., Hasegawa, M., & Goedert, M. (1998). α-Synuclein in filamentous inclusions of Lewy bodies from Parkinson's disease and dementia with Lewy bodies. *Proceedings of the National Academy of Sciences of the United States of America*, *95*(11). https://doi.org/10.1073/pnas.95.11.6469

Spillantini, M. G., & Goedert, M. (2000). The α-synucleinopathies: Parkinson's disease, dementia with Lewy bodies, and multiple system atrophy. *Annals of the New York Academy of Sciences*, *920*. https://doi.org/10.1111/j.1749-6632.2000.tb06900.x

Spillantini, M. G., Schmidt, M. L., Lee, V. M. Y., Trojanowski, J. Q., Jakes, R., & Goedert, M. (1997). α-synuclein in Lewy bodies [8]. In *Nature* (Vol. 388, Issue 6645). https://doi.org/10.1038/42166

Srinivasan, E., Chandrasekhar, G., Chandrasekar, P., Anbarasu, K., Vickram, A. S., Karunakaran, R., Rajasekaran, R., & Srikumar, P. S. (2021). Alpha-Synuclein Aggregation in Parkinson's Disease. *Frontiers in Medicine*, *8*. https://doi.org/10.3389/fmed.2021.736978

Stephens, A. D., Matak-Vinkovic, D., Fernandez-Villegas, A., & Kaminski Schierle, G. S. (2020). Purification of Recombinant α-synuclein: A Comparison of Commonly Used Protocols. *Biochemistry*, *59*(48), 4563–4572. https://doi.org/10.1021/acs.biochem.0c00725

Stephens, A. D., Zacharopoulou, M., Moons, R., Fusco, G., Seetaloo, N., Chiki, A., Woodhams, P. J., Mela, I., Lashuel, H. A., Phillips, J. J., De Simone, A., Sobott, F., & Schierle, G. S. K. (2020). Extent of N-terminus exposure of monomeric alpha-synuclein determines its aggregation propensity. *Nature Communications*, *11*(1). https://doi.org/10.1038/s41467-020-16564-3

Strohäker, T., Jung, B. C., Liou, S. H., Fernandez, C. O., Riedel, D., Becker, S., Halliday, G. M., Bennati, M., Kim, W. S., Lee, S. J., & Zweckstetter, M. (2019). Structural heterogeneity of α-synuclein fibrils amplified from patient brain extracts. *Nature Communications*, *10*(1). https://doi.org/10.1038/s41467-019-13564-w

Sudhof, T. C., & Rizo, J. (2011). Synaptic Vesicle Exocytosis. *Cold Spring Harbor Perspectives in Biology*, *3*(12), a005637–a005637. https://doi.org/10.1101/cshperspect.a005637

Südhof, T. C., & Rothman, J. E. (2009). Membrane fusion: Grappling with SNARE and SM proteins. In *Science* (Vol. 323, Issue 5913). https://doi.org/10.1126/science.1161748

Sugeno, N., Takeda, A., Hasegawa, T., Kobayashi, M., Kikuchi, A., Mori, F., Wakabayashi, K., & Itoyama, Y. (2008). Serine 129 Phosphorylation of α-Synuclein Induces Unfolded Protein Response-mediated Cell Death. *Journal of Biological Chemistry*, *283*(34), 23179–23188. https://doi.org/10.1074/jbc.M802223200

Sun, J., Wang, L., Bao, H., Premi, S., Das, U., Chapman, E. R., & Roy, S. (2019). Functional cooperation of α-synuclein and VAMP2 in synaptic vesicle recycling. *Proceedings of the National Academy of Sciences of the United States of America*, *166*(23). https://doi.org/10.1073/pnas.1903049116

Surguchov, A. (2023). α-Synuclein and Mechanisms of Epigenetic Regulation. *Brain Sciences*, *13*(1), 150. https://doi.org/10.3390/brainsci13010150

Takahashi, T., Yamashita, H., Nakamura, T., Nagano, Y., & Nakamura, S. (2002). Tyrosine 125 of α-synuclein plays a critical role for dimerization following nitrative stress. *Brain Research*, *938*(1–2). https://doi.org/10.1016/S0006-8993(02)02498-8

Tarutani, A., Suzuki, G., Shimozawa, A., Nonaka, T., Akiyama, H., Hisanaga, S. I., & Hasegawa, M. (2016). The effect of fragmented pathogenic α-synuclein seeds on prion-like propagation. *Journal of Biological Chemistry*, *291*(36). https://doi.org/10.1074/jbc.M116.734707

Tenreiro, S., Reimão-Pinto, M. M., Antas, P., Rino, J., Wawrzycka, D., Macedo, D., Rosado-Ramos, R., Amen, T., Waiss, M., Magalhães, F., Gomes, A., Santos, C. N., Kaganovich, D., & Outeiro, T. F. (2014). Phosphorylation Modulates Clearance of Alpha-Synuclein Inclusions in a Yeast Model of Parkinson's Disease. *PLoS Genetics*, *10*(5), e1004302. https://doi.org/10.1371/journal.pgen.1004302

Tiscornia, G., Singer, O., & Verma, I. M. (2006). Production and purification of lentiviral vectors. *Nature Protocols*, *1*(1), 241–245. https://doi.org/10.1038/nprot.2006.37

Tofaris, G. K. (2022). Initiation and progression of α-synuclein pathology in Parkinson's disease. *Cellular and Molecular Life Sciences*, *79*(4), 210. https://doi.org/10.1007/s00018-022-04240-2

Tofaris, G. K., Kim, H. T., Hourez, R., Jung, J.-W., Kim, K. P., & Goldberg, A. L. (2011). Ubiquitin ligase Nedd4 promotes α-synuclein degradation by the endosomal–lysosomal pathway. *Proceedings of the National Academy of Sciences*, *108*(41), 17004–17009. https://doi.org/10.1073/pnas.1109356108

Trexler, A. J., & Rhoades, E. (2012). N-terminal acetylation is critical for forming α-helical oligomer of α-synuclein. *Protein Science*, *21*(5). https://doi.org/10.1002/pro.2056

Truckenbrodt, S., Viplav, A., Jähne, S., Vogts, A., Denker, A., Wildhagen, H., Fornasiero, E. F., & Rizzoli, S. O. (2018). Newly produced synaptic vesicle proteins are preferentially used in synaptic transmission. *The EMBO Journal*, *37*(15). https://doi.org/10.15252/embj.201798044

Trudler, D., Sanz-Blasco, S., Eisele, Y. S., Ghatak, S., Bodhinathan, K., Akhtar, M. W., Lynch, W. P., Piña-Crespo, J. C., Talantova, M., Kelly, J. W., & Lipton, S. A. (2021). α-Synuclein Oligomers Induce Glutamate Release from Astrocytes and Excessive Extrasynaptic NMDAR Activity in Neurons, Thus Contributing to Synapse Loss. *The Journal of Neuroscience*, *41*(10), 2264–2273. https://doi.org/10.1523/JNEUROSCI.1871-20.2020

Tu, P., Galvin, J. E., Baba, M., Giasson, B., Tomita, T., Leight, S., Nakajo, S., Iwatsubo, T., Trojanowski, J. Q., & Lee, V. M.-Y. (1998). Glial cytoplasmic inclusions in white matter oligodendrocytes of multiple system atrophy brains contain insoluble ?-synuclein. *Annals of Neurology*, *44*(3), 415–422. https://doi.org/10.1002/ana.410440324

Tysnes, O. B., & Storstein, A. (2017). Epidemiology of Parkinson's disease. In *Journal of Neural Transmission* (Vol. 124, Issue 8). https://doi.org/10.1007/s00702-017-1686-y

Ueda, K., Fukushima, H., Masliah, E., Xia, Y., Iwai, A., Yoshimoto, M., Otero, D. A. C., Kondo, J., Ihara, Y., & Saitoh, T. (1993). Molecular cloning of cDNA encoding an unrecognized component of amyloid in Alzheimer disease. *Proceedings of the National Academy of Sciences of the United States of America*, *90*(23). https://doi.org/10.1073/pnas.90.23.11282

Uéda, K., Saitoh, T., & Mori, H. (1994). Tissue-dependent alternative splicing of mRNA for NACP, the precursor of non-Aβ component of alzheimer's disease amyloid. *Biochemical and Biophysical Research Communications*, *205*(2). https://doi.org/10.1006/bbrc.1994.2816

Ulmer, T. S., Bax, A., Cole, N. B., & Nussbaum, R. L. (2005). Structure and Dynamics of Micelle-bound Human α-Synuclein. *Journal of Biological Chemistry*, *280*(10), 9595–9603. https://doi.org/10.1074/jbc.M411805200

Vaikath, N., Sudhakaran, I., Abdi, I., Gupta, V., Majbour, N., Ghanem, S., Abdesselem, H., Vekrellis, K., & El-Agnaf, O. (2022). Structural and Biophysical Characterization of Stable Alpha-Synuclein Oligomers. *International Journal of Molecular Sciences*, *23*(23), 14630. https://doi.org/10.3390/ijms232314630

Valente, E. M., Abou-Sleiman, P. M., Caputo, V., Muqit, M. M. K., Harvey, K., Gispert, S., Ali, Z., Del Turco, D., Bentivoglio, A. R., Healy, D. G., Albanese, A., Nussbaum, R., González-Maldonado, R., Deller, T., Salvi, S., Cortelli, P., Gilks, W. P.,

Latchman, D. S., Harvey, R. J., … Wood, N. W. (2004). Hereditary early-onset Parkinson's disease caused by mutations in PINK1. *Science*, *304*(5674). https://doi.org/10.1126/science.1096284

Van der Perren, A., Van den Haute, C., & Baekelandt, V. (2014). *Viral Vector-Based Models of Parkinson's Disease* (pp. 271–301). https://doi.org/10.1007/7854_2014_310

Visanji, N. P., Brotchie, J. M., Kalia, L. V., Koprich, J. B., Tandon, A., Watts, J. C., & Lang, A. E. (2016). α-Synuclein-Based Animal Models of Parkinson's Disease: Challenges and Opportunities in a New Era. In *Trends in Neurosciences* (Vol. 39, Issue 11). https://doi.org/10.1016/j.tins.2016.09.003

Volles, M. J., Lee, S. J., Rochet, J. C., Shtilerman, M. D., Ding, T. T., Kessler, J. C., & Lansbury, P. T. (2001). Vesicle permeabilization by protofibrillar α-synuclein: Implications for the pathogenesis and treatment of Parkinson's disease. *Biochemistry*, *40*(26). https://doi.org/10.1021/bi0102398

Volpicelli-Daley, L. A., Kirik, D., Stoyka, L. E., Standaert, D. G., & Harms, A. S. (2016). How can rAAV-α-synuclein and the fibril α-synuclein models advance our understanding of Parkinson's disease? *Journal of Neurochemistry*, *139*, 131–155. https://doi.org/10.1111/jnc.13627

Volpicelli-Daley, L. A., Luk, K. C., & Lee, V. M. Y. (2014a). Addition of exogenous α-synuclein preformed fibrils to primary neuronal cultures to seed recruitment of endogenous α-synuclein to Lewy body and Lewy neurite-like aggregates. In *Nature Protocols* (Vol. 9, Issue 9). https://doi.org/10.1038/nprot.2014.143

Volpicelli-Daley, L. A., Luk, K. C., & Lee, V. M.-Y. (2014b). Addition of exogenous α-synuclein preformed fibrils to primary neuronal cultures to seed recruitment of endogenous α-synuclein to Lewy body and Lewy neurite–like aggregates. *Nature Protocols*, *9*(9), 2135–2146. https://doi.org/10.1038/nprot.2014.143

Volpicelli-Daley, L. A., Luk, K. C., Patel, T. P., Tanik, S. A., Riddle, D. M., Stieber, A., Meaney, D. F., Trojanowski, J. Q., & Lee, V. M. Y. (2011). Exogenous α-Synuclein Fibrils Induce Lewy Body Pathology Leading to Synaptic Dysfunction and Neuron Death. *Neuron*, *72*(1). https://doi.org/10.1016/j.neuron.2011.08.033

Wakabayashi, K. (2020). Where and how alpha-synuclein pathology spreads in Parkinson's disease: *Neuropathology*, *40*(5). https://doi.org/10.1111/neup.12691

Wakabayashi, K., Yoshimoto, M., Tsuji, S., & Takahashi, H. (1998). α-synuclein immunoreactivity in glial cytoplasmic inclusions in multiple system atrophy. *Neuroscience Letters*, *249*(2–3). https://doi.org/10.1016/S0304-3940(98)00407-8

Wales, P., Lázaro, D. F., Pinho, R., & Outeiro, T. F. (2013). Limelight on alpha-synuclein: Pathological and mechanistic implications in neurodegeneration. In *Journal of Parkinson's Disease* (Vol. 3, Issue 4). https://doi.org/10.3233/JPD-130216

Wales, P., Pinho, R., Lázaro, D. F., & Outeiro, T. F. (2013). Limelight on Alpha-Synuclein: Pathological and Mechanistic Implications in Neurodegeneration. *Journal of Parkinson's Disease*, *3*(4), 415–459. https://doi.org/10.3233/JPD-130216

Wan, Q.-F., Zhou, Z.-Y., Thakur, P., Vila, A., Sherry, D. M., Janz, R., & Heidelberger, R. (2010). SV2 Acts via Presynaptic Calcium to Regulate Neurotransmitter Release. *Neuron*, *66*(6), 884–895. https://doi.org/10.1016/j.neuron.2010.05.010

Wang, L., Das, U., Scott, D. A., Tang, Y., McLean, P. J., & Roy, S. (2014). α-Synuclein multimers cluster synaptic vesicles and attenuate recycling. *Current Biology*, *24*(19). https://doi.org/10.1016/j.cub.2014.08.027

Wang, Y., Wang, C., Ranefall, P., Broussard, G. J., Wang, Y., Shi, G., Lyu, B., Wu, C. T., Wang, Y., Tian, L., & Yu, G. (2020). SynQuant: An automatic tool to quantify synapses from microscopy images. *Bioinformatics*, *36*(5). https://doi.org/10.1093/bioinformatics/btz760

Wersinger, C., & Sidhu, A. (2003). Attenuation of dopamine transporter activity by α-synuclein. *Neuroscience Letters*, *340*(3). https://doi.org/10.1016/S0304-3940(03)00097-1

Winner, B., Jappelli, R., Maji, S. K., Desplats, P. A., Boyer, L., Aigner, S., Hetzer, C., Loher, T., Vilar, M., Campioni, S., Tzitzilonis, C., Soragni, A., Jessberger, S., Mira, H., Consiglio, A., Pham, E., Masliah, E., Gage, F. H., & Riek, R. (2011). In vivo demonstration that α-synuclein oligomers are toxic. *Proceedings of the National Academy of Sciences*, *108*(10), 4194–4199. https://doi.org/10.1073/pnas.1100976108

Withers, G. S., George, J. M., Banker, G. A., & Clayton, D. F. (1997). Delayed localization of synelfin (synuclein, NACP) to presynaptic terminals in cultured rat hippocampal neurons. *Developmental Brain Research*, *99*(1). https://doi.org/10.1016/S0165-3806(96)00210-6

Wood, S. J., Wypych, J., Steavenson, S., Louis, J.-C., Citron, M., & Biere, A. L. (1999). α-Synuclein Fibrillogenesis Is Nucleation-dependent. *Journal of Biological Chemistry*, *274*(28). https://doi.org/10.1074/jbc.274.28.19509

Wu, Q., Takano, H., Riddle, D. M., Trojanowski, J. Q., Coulter, D. A., & Lee, V. M. Y. (2019). α-Synuclein (αsyn) preformed fibrils induce endogenous αsyn aggregation, compromise synaptic activity and enhance synapse loss in cultured excitatory hippocampal neurons. *Journal of Neuroscience*, *39*(26). https://doi.org/10.1523/JNEUROSCI.0060-19.2019

Xu, Y., & Chou, K.-C. (2015). Recent Progress in Predicting Posttranslational Modification Sites in Proteins. *Current Topics in Medicinal Chemistry*, *16*(6). https://doi.org/10.2174/1568026615666150819110421

Yamin, G., Uversky, V. N., & Fink, A. L. (2003). Nitration inhibits fibrillation of human α-synuclein in vitro by formation of soluble oligomers. *FEBS Letters*, *542*(1–3). https://doi.org/10.1016/S0014-5793(03)00367-3

Yoo, G., Shin, Y.-K., & Lee, N. K. (2023). The Role of α-Synuclein in SNARE-mediated Synaptic Vesicle Fusion. *Journal of Molecular Biology*, *435*(1), 167775. https://doi.org/10.1016/j.jmb.2022.167775

Yoo, G., Yeou, S., Son, J. B., Shin, Y.-K., & Lee, N. K. (2021). Cooperative inhibition of SNARE-mediated vesicle fusion by α-synuclein monomers and oligomers. *Scientific Reports*, *11*(1), 10955. https://doi.org/10.1038/s41598-021-90503-0

Yoshino, H., Hirano, M., Stoessl, A. J., Imamichi, Y., Ikeda, A., Li, Y., Funayama, M., Yamada, I., Nakamura, Y., Sossi, V., Farrer, M. J., Nishioka, K., & Hattori, N. (2017). Homozygous alpha-synuclein p.A53V in familial Parkinson's disease. *Neurobiology of Aging*, *57*. https://doi.org/10.1016/j.neurobiolaging.2017.05.022

Zarranz, J. J., Alegre, J., Gómez-Esteban, J. C., Lezcano, E., Ros, R., Ampuero, I., Vidal, L., Hoenicka, J., Rodriguez, O., Atarés, B., Llorens, V., Gomez Tortosa, E., Del Ser, T., Muñoz, D. G., & De Yebenes, J. G. (2004). The New Mutation, E46K, of α-Synuclein Causes Parkinson and Lewy Body Dementia. *Annals of Neurology*, *55*(2). https://doi.org/10.1002/ana.10795

Zhao, H., Kim, Y., Park, J., Park, D., Lee, S.-E., Chang, I., & Chang, S. (2014). SCAMP5 Plays a Critical Role in Synaptic Vesicle Endocytosis during High Neuronal Activity. *Journal of Neuroscience*, *34*(30), 10085–10095. https://doi.org/10.1523/JNEUROSCI.2156-14.2014

Zhong, S., Luo, X., Chen, X., Cai, Q., Liu, J., Chen, X., & Yao, Z. (2010). Expression and Subcellular Location of Alpha-Synuclein During Mouse-Embryonic Development. *Cellular and Molecular Neurobiology*, *30*(3), 469–482. https://doi.org/10.1007/s10571-009-9473-4

Zhu, H., Xiang, H.-C., Li, H.-P., Lin, L.-X., Hu, X.-F., Zhang, H., Meng, W.-Y., Liu, L., Chen, C., Shu, Y., Zhang, R.-Y., Zhang, P., Si, J.-Q., & Li, M. (2019). Inhibition of GABAergic Neurons and Excitation of Glutamatergic Neurons in the Ventrolateral Periaqueductal Gray Participate in Electroacupuncture Analgesia Mediated by Cannabinoid Receptor. *Frontiers in Neuroscience*, *13*. https://doi.org/10.3389/fnins.2019.00484

Zigoneanu, I. G., Yang, Y. J., Krois, A. S., Haque, M. E., & Pielak, G. J. (2012). Interaction of α-synuclein with vesicles that mimic mitochondrial membranes. *Biochimica et Biophysica Acta - Biomembranes*, *1818*(3). https://doi.org/10.1016/j.bbamem.2011.11.024

Zimprich, A., Biskup, S., Leitner, P., Lichtner, P., Farrer, M., Lincoln, S., Kachergus, J., Hulihan, M., Uitti, R. J., Calne, D. B., Stoessl, A. J., Pfeiffer, R. F., Patenge, N., Carbajal, I. C., Vieregge, P., Asmus, F., Müller-Myhsok, B., Dickson, D. W., Meitinger, T., … Gasser, T. (2004). Mutations in LRRK2 cause autosomal-dominant parkinsonism with pleomorphic pathology. *Neuron*, *44*(4). https://doi.org/10.1016/j.neuron.2004.11.005

Zucker, R. S., Kullmann, D. M., & Kaeser, P. S. (2014). *Chapter 15 – Release of Neurotransmitters*.